

**Geochemical characteristics and structural features
of the LCT pegmatites in Potoskavaara,
Kitee-Tohmajärvi pegmatite province**

Kirsi Pääkkönen

Geology
Master's thesis
Credits: 30 ECTS

Supervisors:
Esa Heilimo
Jaro Kuikka

25.02.2025
Turku

The originality of this thesis has been checked in accordance with the University of Turku quality assurance system using the Turnitin OriginalityCheck service.

Master's thesis

Subject: Bedrock Geology

Author: Kirsi Pääkkönen

Title: Geochemical characteristics and structural features of the LCT-pegmatites in Potoskavaara, Kitee-Tohmajärvi pegmatite province

Supervisors: Esa Heilimo, Jaro Kuikka

Number of pages: 80 pages + 3 appendixes

Date: 25.02.2025

The demand for battery materials such as lithium, cobalt and graphite are increasing with the green transition towards more sustainable energy sources. Lithium plays a particularly important role in the development of energy storage, electric vehicles, with LCT (Lithium-Cesium-Tantalum) pegmatite deposits being an important source for these critical metals. Several heterogeneous and Svecofennian LCT pegmatite dykes have been discovered in the 200 km² wide area of the Kitee-Tohmajärvi pegmatite province, with the most prominent Li-dykes located in the northern parts of the Potoskavaara area. The aim of this study is to find the compositional differences and variations in fertility of the pegmatite dykes in the Potoskavaara. The study additionally provides regional information to better understand the formation of the pegmatite dykes in the area.

The elemental results indicate that the Potoskavaara dykes represent peraluminous S-type fertile pegmatites, which are characterized by elevated concentrations of rare metals, along with $A/CNK > 1.1$, $Mg/Li < 10$, and $Nb/Ta < 8$ ratios. Furthermore, they display high Al, low Ca, Fe, and Mg concentrations, and varying K and Na contents. The pegmatite dykes exhibit both geochemical and mineralogical compositional differences, with enrichment in rare elements such as $Be > Cs > Rb > Nb \geq Ta > Li > Sn$ as fractionation progresses. Elemental enrichment supports the hypothesis of regional zonation, which enables the classification of the area's pegmatites into four fertile rock types: the most evolved RE-pegmatites, potassic pegmatites, sodic aplites, and the most common pegmatitic leucogranites. Signs of hydrothermal events are evident in pegmatite dykes, as mineral inclusions, compositional, and textural changes. In conjunction with the geochemical results, these observations suggest that the enrichment of the pegmatites with rare metals is a result of both magmatic and hydrothermal processes. Alongside fractional crystallization, the partial melting of surrounding rocks may have affected the formation.

The most evolved pegmatites are found in the northern parts of the Potoskavaara area approximately 10 km from the so-called Kitee granite intrusion. The source of the Li-pegmatites is likely the Kitee granite, although further relative age dating is needed to confirm this. The multiple deformation phases of different ages have occurred in the area, which complicates the interpretation of the original source of the pegmatite dykes. The enrichment of rare elements in the surrounding rock could potentially lead to the discovery of undiscovered Li-pegmatite dykes in the area and guiding future mineral exploration efforts.

Key words: LCT-pegmatite, lithium, fertility, source, zonation, exploration

Pro gradu -tutkielma

Pääaine: Kallioperägeologia

Tekijä: Kirsi Pääkkönen

Otsikko: Potoskavaaran LCT-pegmatiittijuonien geokemialliset ominaisuudet ja rakennepiirteet, Kiteen-Tohmajärven pegmatiittiprovinssissa

Ohjaajat: Esa Heilimo, Jaro Kuikka

Sivumäärä: 80 sivua + 3 liitettä

Päivämäärä: 25.02.2025

Akkumateriaalien, kuten litiumin, koboltin ja grafiitin kysyntä kasvaa vihreän siirtymän myötä kohti kestävämpiä energialähteitä. Erityisesti litiumilla on merkittävä rooli energian varastoinnin ja sähköajoneuvojen kehittämisessä. Näiden kasvavien tarpeiden vuoksi LCT (Litium-Cesium-Tantaali) -pegmatiittiesiintymät ovat tärkeitä lähteitä kriittisille metalleille. Kiteen-Tohmajärven 200 km² laajuiselta pegmatiittiprovinssin alueelta on löydetty useita heterogeenisiä ja Svekofennisiä LCT-pegmatiittijuonia, joista Li-rikkaimmat juonet sijaitsevat Potoskavaaran alueella. Tämän tutkimuksen tavoitteena on osoittaa Potoskavaaran alueen pegmatiittijuonten koostumuserot ja vaihtelut niiden fertiilisydessä. Lisäksi tutkimus laajentaa ymmärrystä alueen pegmatiittien muodostumisesta ja lähdegranitoidista.

Tulokset osoittavat, että Potoskavaaran juonet edustavat peralumiinisia S-tyyppin fertiilejä pegmatiittijuonia, joille on tyypillistä kohonnut harvinaisten metallien pitoisuudet sekä $A/CNK > 1.1$, $Mg/Li < 10$ ja $Nb/Ta < 8$. Lisäksi niille on ominaista korkea Al-pitoisuus, matalat Ca-, Fe- ja Mg-pitoisuudet, sekä vaihtelevat K- ja Na-pitoisuudet. Pegmatiittijuonissa on sekä geokemiallisia että mineralogisia koostumuseroja, jotka ilmenevät harvinaisten alkuaineiden $Be > Cs > Rb > Nb \geq Ta > Li > Sn$ rikastumisella fraktioitumisen kehittyessä. Alkuaineiden rikastumistrendit tukevat hypoteesia alueellisesta vyöhykkeellisyydestä, joka mahdollistaa alueen pegmatiittien luokittelun neljään kivilajiryhmään: kehittyneimpiin RE-pegmatiitteihin, kalipegmatiitteihin, natriumapliitteihin sekä kaikista yleisimpiin pegmatiittisiin leukograniteihin. Pegmatiittijuonissa on hydrotermisten tapahtumien merkkejä, kuten mineraalisulkeumia, koostumus- sekä tekstuuri muutoksia. Geokemiallisten tulosten kanssa nämä havainnot viittaavat siihen, että pegmatiittijuonten rikastuminen harvinaisilla metalleilla on seurausta sekä magmaattisista että hydrotermisistä prosesseista. Fraktioitumisen kiteytymisen lisäksi muodostumiseen on saattanut vaikuttaa ympäröivän isäntäkiven osittaissulamisen.

Kaikista kehittyneimmät pegmatiitit sijoittuvat Potoskavaaran alueen pohjoisosiin rakenteellisesti monimutkaistelle ja litologisesti vaihtelevalle alueelle, noin 10 km päähän Kiteen graniitista. Tuloksien perusteella Li-pegmatiittien lähde on Kiteen graniitti, mutta tarkempia iänmäärytyksiä tarvitaan tämän varmistamiseksi. Tutkimusalueen rakenteelliset piirteet viittaavat kuitenkin siihen, että alueella on vaikuttanut useita eri-ikäisiä deformaatiovaiheita, jotka vaikeuttavat pegmatiittien alkuperäisen lähteen tulkintaa. Harvinaisten alkuaineiden mahdollinen rikastuminen ympäröivään isäntäkiveen voisi mahdollisesti ohjata malminetsintää alueen vielä paljastumattomien Li-pegmatiittijuonien löytämiseksi.

Avainsanat: LCT-pegmatiitti, litium, fertiilisyys, lähde, vyöhykkeellisyys, malminetsintä

Content

1	Introduction	7
2	Pegmatites	8
2.1	Petrogenesis of pegmatites	9
2.1.1	Fertile granites	10
2.1.2	Regional zonation	11
2.2	Internal zonation	13
2.3	Pegmatite classification	14
2.3.1	Granitic pegmatites classification	14
2.3.2	Pegmatites petrologic classification	16
2.4	LCT pegmatites mineralogy and geochemistry	17
2.5	Potential of RE-pegmatites in Finland	18
3	Regional geology	20
3.1	Karelia province	20
3.2	Karelian schist belt	21
3.3	Puruvesi granite	21
3.4	Kitee-Tohmajärvi pegmatite province	23
3.4.1	Evolution and structural evolution	23
3.4.2	Earlier pegmatite studies	25
4	Materials & methods	26
4.1	Bedrock observations	26
4.2	Petrography	26
4.3	Geochemical analyses	26
4.4	Lineament interpretation	27
5	Results	28
5.1	Bedrock observations	28
5.1.1	RE-enriched pegmatites	29
5.1.2	Potassic pegmatites	32
5.1.3	Sodic aplite pegmatites	36
5.1.4	Pegmatitic leucogranites	37
5.2	Petrography	40
5.2.1	Mineralogical and textural features	40
5.2.2	Deformation and metamorphic features	44
5.3	Geochemical analyses	47
5.3.1	Major elements	47
5.3.2	Trace elements	51
5.3.3	Fractionation indicators	54
5.4	Structural interpretation	59

6	Discussion	61
6.1	Classifications	61
6.2	Fertility and fractionation	62
6.2.1	Determination of the fertile pegmatites	62
6.2.2	Geochemical fertility and fractionation variations	62
6.2.3	Field observation and petrography studies	67
6.2.4	Uncertainties in sampling	68
6.3	Regional origins and structural controls	69
6.3.1	Source of the pegmatite dykes	69
6.3.2	Regional structure and impact on formation	70
6.4	Comparison to LCT-pegmatites in Finland	71
6.5	Economic Li-potential	72
7	Conclusions	74
	Acknowledgements	75
	References	76
	Appendixes	81
	Appendix 1. Coordinates of the observations	81
	Appendix 2. Geochemical analysis results	82

1 Introduction

Critical Raw Materials (CRMs) are essential for today's economy, but their availability is limited, and supply risk has increased (European Commission 2023). The European Union (EU) has published a list of CRMs from 2023, which includes 34 identified raw materials. They are widely used in the production of industry, technology, renewable energy and electric vehicles as part of the green transition towards more sustainable and environmentally friendly energy sources. According to the European Commission (2023), lithium plays a key role in the green transition and a low-carbon society. This is primarily due to its use in lithium-ion batteries, which are widely used in electric vehicles and renewable energy.

Geological Survey of Finland (GTK) executed a four-year Battery mineral project in 2019–2022, with the purpose of assessing the potential of cobalt, lithium and graphite metals and minerals in Finland (eg. Nygård *et al.* 2023,2024; Kuikka *et al.* 2023). Research on Li-Cs-Ta deposits was focused on the Central and South Ostrobothnia as well as the Kitee-Tohmajärvi region, North Karelia. The project investigated several potential lithium areas and found that the lithium potential in the Kitee-Tohmajärvi pegmatite province is higher than previously estimated (Kuikka *et al.* 2023). The first lithium-rich pegmatite studies in the area were carried out by GTK during 1970 (Alviola 1974 a,b; Nykänen 1975, 1983). According to the Kuikka *et al.* (2023), there are indications of undiscovered Li-pegmatites in Kitee-Tohmajärvi pegmatite province. It is known that the LCT pegmatites in the area represent different pegmatite types by their geochemical and petrographical features (Kuikka *et al.* 2023).

The main purpose of this master's thesis is to improve the understanding of the evolution and formation of the LCT pegmatite dykes in the Potoskavaara area, Kitee-Tohmajärvi pegmatite province. To achieve these objectives, bedrock observations, petrographic thin sections, geochemical analyses, and structural interpretation of the area have been examined in this study with the following main aims:

1. To find compositional differences between the pegmatite dykes in the Potoskavaara area and classify pegmatites into classes.
2. To determine the degree of fertility of the pegmatite dykes in the Potoskavaara area.

3. To gain a better understanding of the source and evolution of the pegmatite dykes in the Potoskavaara area.
4. To assess the economic lithium potential in the Potoskavaara area.

2 Pegmatites

Pegmatites are coarse-grained intrusive igneous rocks, typically associated with granitic composition (eg. London 2005; London 2008; Simmons & Webber 2008; Müller *et al.* 2022). Pegmatites are characterized by coarse to extremely coarse grain size, where individual crystals can grow up to several meters in size. Compositionally granitic pegmatites are the most common type, although intermediate, basic, and alkaline pegmatites are also known. Granitic pegmatites are composed predominantly of granite-forming minerals such as quartz, feldspar, and accessory micas as biotite or muscovite. However, pegmatites may contain rare minerals and may be enriched in lithophile high-field strength elements such as B, Be, Ce, Cs, Li, Nb, Sn, Ti, Ta, Th, U, W, and Zr (London 2008). Pegmatites are typically found as sharply defined, homogeneous, or zoned bodies and can appear as dykes, dyke swarms, or intrusions within igneous or metamorphic rocks. According to London (2008), the host rocks such as volcanic rock, gneiss, and amphibolite tend to form persistent continuous dykes, whereas pegmatites that are emplaced into metasedimentary rocks are more irregular and discontinuous dykes. Dyke swarms are common to the pegmatites formed from granitic sources. Brittle and ductile structures of the bedrock, such as fractures, shear or fault zones, are good pathways for the residual fractionated granitic melt to intrude (Černý 1991b; Selway *et al.* 2005).

Pegmatites are most simply divided into two types: simple pegmatites and rare-element (RE) pegmatites. RE-pegmatites are divided by petrogenetic and mineral compositions into lithium, cesium, and tantalum (LCT)-family and niobium, yttrium, fluorine (NYF)-family (Černý 1991a; Černý & Ercit 2005; London 2008; Simmons & Webber 2008). Both families are product of extreme fractionation, but LCT pegmatites formed during fractional crystallization of orogenic S-type granites, and are enriched in Li, Cs, Ta, Be, B, F, Ga, Hf, Mn, Nb, Rb, P, and Sn. Relative to this, most NYF pegmatites are derived from anorogenic or within plate A-type granites (Černý & Ercit 2005). In addition, NYF pegmatites are enriched in Be, B, F, Nb > Ta, Th, Ti, rare earth elements (REE), Sc, Sn, Y, Zr, and U. The development of complex RE-pegmatites provides

enrichment of valuable rare metals within pegmatites (Černý 1991a; Černý & Ercit 2005; London 2008; Simmons & Webber 2008). The rare metals Li, Cs, Nb, Ta, Be, and Sn occur in minerals such as spodumene, petalite or lepidolite (Li), pollucite (Cs), columbite-tantalite (Nb, Ta), beryl (Be) and cassiterite (Sn), respectively and are predominantly enriched in the LCT-type pegmatites. These minerals are economically interesting for various ore industries (London 2005; London 2008; Simmons & Webber 2008).

2.1 Petrogenesis of pegmatites

Pegmatites are typically emplaced at temperatures between 500–700°C (eg. London 2005; London 2008). The most widely used theory for the formation of granitic pegmatites is that they originate from residual melts during the crystallization of a granitic pluton (Černý 1991b; London 2005; Simmons & Webber 2008). In the crystallization model by Jahns & Burnham (1969), during the development of LCT pegmatites magma becomes saturated with volatile substances H₂O, B, F, P, and CO₂ (Jahns & Burnham 1969, as cited in London 2005; Simmon & Webber 2008). The melt gradually evolves from common granite to fertile granite and the transformation is driven by the enrichment of incompatible elements (B, Be, Li, Cs, Nb, Mn, Rb, Sn, and Ta), RE components, and volatiles in the remaining melt (Černý 1991b; London 2005; Simmons & Webber 2008).

The presence of a vapor phase is important in the process, as the interaction of the melt and the vapor phase create pegmatitic textures, when the transition from granite to pegmatite begins at the H₂O saturation point (Jahns & Burnham 1969, as cited in London 2005; Simmon & Webber 2008). Pegmatites are formed when a fluid rich phase separates from the silicate rich melt, due to the temperature differences. Simmons & Webbers (2008) suggests fluxing components and volatiles play a crucial role in lowering crystallization temperatures, reducing nucleation rates, and decreasing melt polymerization and viscosity of the fluid rich magma. The presence of fluxes and volatiles in pegmatite melts may enable crystallization temperature as low as 350 °C (London 2005; London 2008; Simmons & Webber 2008). However, according to London's (2005) more recent theory of constitutional zone refining, the presence of a vapor phase is not necessary for the development of the complex pegmatite texture. London (2005) suggests rapid crystallization of an undercooled melt creates a boundary layer, which allows fluxes and incompatible elements to concentrate in the final products of crystallization. The boundary layer is highly enriched in excluded components. In the process fluxes and other

incompatible elements concentrate, which play a more decisive role in the enrichment of rare elements in LCT pegmatites than vapor saturation does (London 2005).

Further along fractional crystallization, pegmatites can also form as a result of partial melting and anatexis (Simmons & Webber 2008). A source rock is sedimentary, usually a metamorphic or migmatitic rock in an orogenic environment which partially melts at high temperatures and pressures. In metasediments, incompatible elements influencing the melting processes can promote the formation of a granitic melt, which may then crystallize into a pegmatite. In this process, rare elements such as Li, Cs, and Ta are eventually enriched in the formed S-type granitic melt (Simmons & Webber 2008).

2.1.1 Fertile granites

Fertile granite is heterogeneous and differs from barren granite in its geochemical, mineralogical and textural characteristics (Breaks & Tindle 1997; Selway *et al.* 2005). In addition to the typical minerals of pegmatites, a fertile pegmatite granite contains garnet, tourmaline, and apatite as accessory minerals, which are not present in a barren granite. Coarse grained K-feldspar in fertile granites is normally white rather than reddish in color which in turn is typical for the barren type, just as coarse-grained muscovite appears yellowish to greenish compared to the gray or brown muscovites of barren granites (Breaks & Tindle 1997; Selway *et al.* 2005). Further, graphic textures such as mineral intergrowths are common. The geochemical composition of granitic melt evolves as crystallization progresses, which leads to a granite melt crystallizing in different stages (Černý & Meintzer 1988, as cited in Selway *et al.* 2005). This leads to the formation of different pegmatite rock units with geochemical variations in the same batch of magma and fertile granite intrusion.

The first unit of Černý & Meintzer (1988) contains the primitive fine-grained biotite granite type. In the unit biotite is a common mineral, and the minerals typically are in a fine-grained form, although in some cases, biotite may crystallize as porphyroblasts. In this unit, biotite is often enriched in Fe and Mg and is indicative of sedimentary or volcanic host rock contamination. With increasing fractionation, the compositions of fertile granites evolve from the most primitive fine-grained or porphyroblastic biotite granite to two-micas leucogranite. This unit is light white-colored and fine-grained, which

commonly is composed of muscovite and biotite, as well as garnet and tourmaline minerals.

As fractionation progresses, the formation of coarse-grained pegmatitic leucogranite becomes possible, which differs from leucogranites due to its large mineral grains, often seen as large quartz and feldspar crystals (Černý & Meintzer 1988, as cited in Selway *et al.* 2005). The type can range in color from light to reddish and may contain tourmaline and garnet, apatite, zircon, and Zn-oxide minerals, as well as quartz and muscovite intergrowths. Pegmatitic leucogranites can have layers of sodic aplite, potassic pegmatite, or RE-rich pods.

Sodic aplite is light gray to white in color consisting mainly of quartz and Na-rich plagioclase and is often characterized by a sugary and easily crumbling texture, which makes the unit much more easily identifiable compared to the previous unit. The sodic aplite unit often contains layered stringers of garnet and tourmalines. In addition, it contains greenish muscovite, fluorapatite, and Ta-oxide minerals such as tantalite and columbite. The reduction in grain sizes of sodic aplite is explained by the removal of volatile substances from the melt (Jahns & Burnham 1969, as cited in London 2005). Aplites occur with rapid crystallization and increased viscosity that happens when volatile substances are removed from the melt. This has led to a change in the alkali compositions of the magma, resulting in fine-grained, Na-rich sodic aplite units, while the potassic pegmatite units are coarser-grained and enriched in K-feldspar.

Potassic pegmatite often contains abundant K-feldspar grains and may also be enriched in RE minerals. Potassic pegmatites differ from previous units in that they contain only K-feldspar and plagioclase is not present. In addition, tourmaline, garnet, beryl, molybdenite, and Nb-oxide mineral such as ferrocolumbite may occur (Černý & Meintzer 1988, as cited in Selway *et al.* 2005). The most developed unit of fertile granites is RE-enriched pegmatite types, which are important sources of RE minerals. RE-pegmatites differ from all other types with high amounts of Li-rich minerals such as petalite, spodumene, lepidolite, colorful tourmalines, Cs-rich beryl, and Ta-oxide minerals.

2.1.2 Regional zonation

Granitic pegmatites are formed from very fractionated granitic magma, ejected at the end of the development of granitic bodies (Černý 1991b). In the regional zonation, LCT-type

pegmatites typically crystallized from the parental pluton to the surrounding area, as shown in figure 1 (Černý 1991b; Simmons & Webber 2008). The volatile substances remain liquid at low temperatures 450–650°C and can therefore be carried further away from the source rock, as well as enriched in RE- and volatile components during the advancing crystallization (Černý 1991b; Simmons & Webber 2008). The farthest pegmatite dykes from a source granite are the most evolved pegmatite dykes, with increased mineral alteration and complexity of internal zonation (Černý 1991b; Selway *et al.* 2005). The most economically viable RE-pegmatites can fractionate at distances up to ten kilometers from the parent granite and spread over an area of 10 to 20 km² (Breaks & Tindle 1997). As stated in Selway *et al.* (2005), the mineral composition of pegmatites changes with increasing fractionation, and some minerals appear with decreasing distance to RE-pegmatites while others such as biotite disappear (Figure 1). Beryl is found in nearly all zones, because of its incompatibility with common minerals and silicic melt, in addition to its relatively early timing of crystallization. In contrast, columbite-tantalite and lithium minerals precipitate in later zones, and as crystallization progresses, pollucite eventually precipitates in the most evolved LCT pegmatite dykes (Černý 1991b). In addition to brittle and ductile structures, lithological boundaries or pre-existing batholithic contacts enable the regional zonation of the pegmatite dykes (Selway *et al.* 2005).

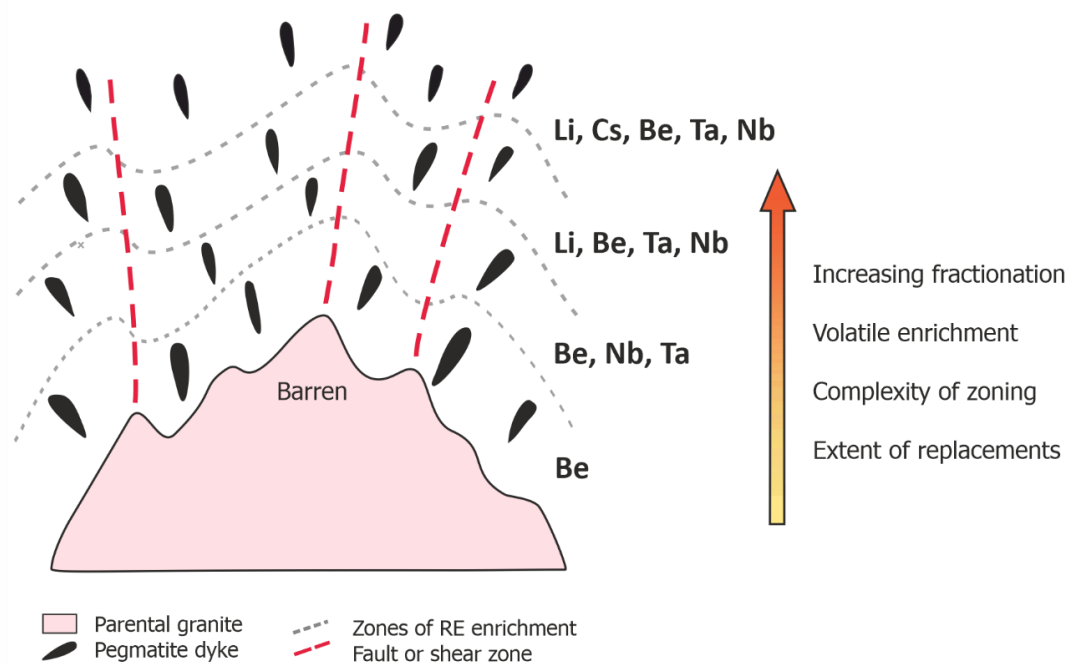


Figure 1. Schematic model of the regional zonation of the LCT pegmatite group, around a parental granite intrusion in map view. The schematic model is not presented to scale. (Modified from Černý 1991b)

2.2 Internal zonation

One clear feature of pegmatites is internal zoning, which shows the mineralogical and textural differences in units of the individual pegmatite bodies, as shown in figure 2 (Černý 1991a; London 2014). Based on this, pegmatites can be further divided into simple, zoned, and complex categories. As Černý (1991a) states, the structure of a pegmatite commonly consists of zoned and layered structures, with zoned pegmatites representing the most varied and common type. Simple pegmatites are homogeneous, while zonal and complex pegmatites are identified as heterogeneous, and often consist of different zones and metasomatic alteration (Černý 1991a; London 2014). The complex type is characteristic of the most common RE-pegmatite class, Li-enriched pegmatites which contain minerals such as spodumene, petalite, lepidolite and amblygonite (Černý 1991a; Černý & Ercit 2005), and Nb-Ta rich pegmatites are enriched in niobium and tantalum, which are found in columbite and tantalite oxide minerals (Černý & Ercit 1985). In addition, complex RE-pegmatites include Sn-rich pegmatites, where Sn is also enriched in oxide minerals, often in cassiterite or wodginite (Černý & Ercit 2005).

The degree of evolution increases from the primitive outer zone toward the evolved core zone of the pegmatite. According to Černý (1991a), textural changes are identified as granitic or aplitic units in the outer zones, graphic or heterogeneous in intermediate zones, and blocky and coarse-grained in the monomineralic core, as is presented in figure 2. Aplitic units lie within the footwall of layered pegmatites, while coarse-grained units near to the top alternate between K-feldspar- and quartz-rich. The border zone of the internal zonation represents the most primitive unit, measuring only a few centimeters and containing fine-grained mineral textures of plagioclase, K-feldspar, quartz and muscovite. Both the wall zone and the intermediate zone contain K-feldspar and quartz. The wall zone is coarser grained and can be several meters wide and displays intergrowth of K-feldspar and quartz. In the intermediate zone, the range in texture varies from fine to coarse-grained and blocky minerals. The intermediate zone often contains pockets, that are repositories for large and rare crystals. In LCT pegmatites, the most evolved part of the zonation is a monomineralic quartz core and a core margin, which commonly consists of tourmaline, beryl and spodumene (Černý 1991a; London 2014). As explained by London (2008), the internal zoning of pegmatites is influenced by bulk composition, liquidus undercooling before crystallization, isothermal fractional crystallization, boundary layer and constitutional zoning, as well as chemical diffusion in the melt.

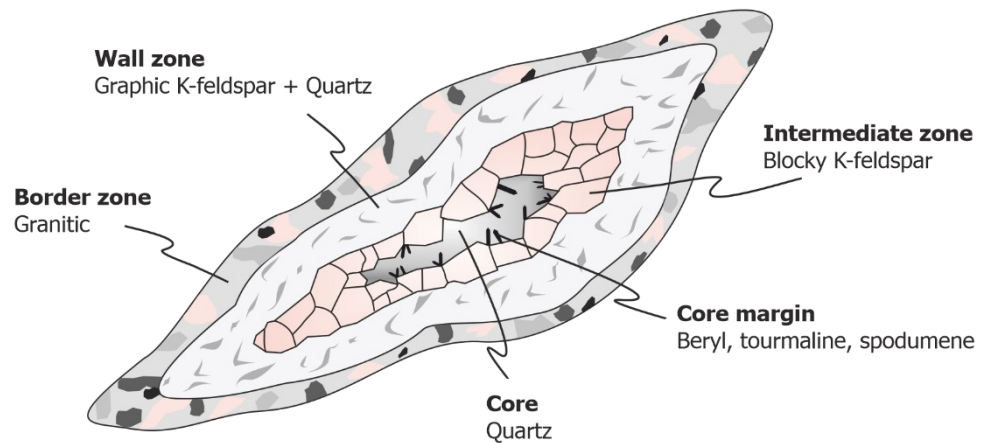


Figure 2. Schematic model of internal zonation of an LCT pegmatite dyke. The schematic model is not presented to scale. (Modified from Černý 1991a)

2.3 Pegmatite classification

2.3.1 Granitic pegmatites classification

Černý's (1991a) classification of granitic pegmatites is in common use today (Table 1). The classification is based on emplacement depth, metamorphic grade and minor element content of pegmatites, which shows relationships between classes, families, types and subtypes. The main classification is divided into abyssal, muscovite, RE, and miarolitic classes. The muscovite-RE class is the fifth published classification within the Černý's (1991a) classification by Černý & Ercit (2005).

In the Černý & Ercit (2005) classification, the abyssal pegmatites are developed in the low to high pressure granulite facies, under 4–9 kbar and 700–800°C conditions. Černý (1991a) referred them to be segregations of leucosome without relation to granites. Typically, mineralization is poor to moderate, and enriched in the trace elements U, Th, Nb, Ti, Y, REE, and Mo. Muscovite-class pegmatites are unrelated to granites, formed under kyanite-sillimanite amphibolite facies, at pressures of 5–8 kbar and temperatures of 580–650°C. Both pegmatite types can form during partial melting and anatexis as well. The muscovite, RE-, and miarolitic pegmatites have diverse element composition. According to Černý & Ercit (2005), RE-pegmatites of this class have formed at temperatures of 500–600°C and under 2–4 kbar. Miarolitic pegmatites are the primary sources of gem quality materials and exceptional mineral specimens found in pegmatitic

environments, which have been formed in especially low temperature and low pressure under 1–3 kbar conditions.

While the Černý (1991a) classification has been predominantly used for the classification of granitic pegmatites for many decades, Müller *et al.* (2022) discuss the challenges associated with it. Challenges in the classification are based on the crystallization pressure and depth, even though the mineralogy of pegmatites retains little information about the crystallization depth. Metamorphic events recorded in the host rocks might have occurred before the pegmatite was formed, and in addition the metamorphic grade of the host rocks may not accurately depict the crystallization conditions of the pegmatites (Müller *et al.* 2022). Especially NYF-family do not fit into the classification, because of the diversity of the pegmatites. Furthermore, Simmons (2005) noted another problem is that the classification disregards the possibly of pegmatites formed on direct anatexis.

Table 1. Granitic pegmatite classification (modified from Černý & Ercit 2005; Müller 2021). Classification into pegmatite class, subclass, type, and subtype are based on mineralogy, and classification into lithium-cesium-tantalum (LCT) and niobium, yttrium, fluorine (NYF) families are based on geochemistry. The classification into magma source is based on anorogenic (A), sedimentary (S), or igneous (I) plutonic source of pegmatites.

Pegmatite Class	Subclass	Type	Subtype	Family	Granitic magma
1. Abyssal		HREE		NYF	A to I-type
		LREE		NYF	A to I-type
		U		NYF	A to I-type
		B-BE		LCT	S to I-type
2. Muscovite					
3. Muscovite-RE	REE			NYF	A to I-type
	Li			LCT	
4. RE	REE	Allanite-monazite		NYF	A to I-type
		Euxenite		NYF	A to I-type
		Gadolinite		NYF	A to I-type
		Beryl	Beryl-columbite	LCT + NYF	A and I-type combination
			Beryl-phosphate	LCT	S to I-type
			Complex	Spodumene	LCT
			Petalite	LCT	S to I-type
			Lepidolite	LCT	S to I-type
			Elbaite	LCT	S to I-type
			Amblygonite	LCT	S to I-type
			Albite-spodumene	LCT	S to I-type
	5. Miarolitic	REE	Albite		LCT
Topaz-beryl				NYF	A to I-type
Gadolinite				NYF	A to I-type
Fergusonite				NYF	A to I-type
Beryl-Topaz				LCT	S to I-type
Li		Spodumene		LCT	S to I-type
		Petalite		LCT	S to I-type
		Lepidolite		LCT	S to I-type

2.3.2 *Pegmatites petrologic classification*

The petrologic classification of pegmatites is based on their plutonic derivation, which may be formed from different sources (Černý 1991a; Černý & Ercit 2005). The Černý & Ercit (2005) classification divided pegmatites into three different categories which are the LCT-family, NYF -family, and mixed NYF+LCT-family pegmatites (Table 1). The LCT- and NYF-type pegmatites are the so-called RE-pegmatites. The classification of RE-pegmatites shows that mainly LCT pegmatites are related to S-type granitic magma from orogenic events, conversely NYF-pegmatites are A-type granites from late- to post-tectonic and anorogenic events (Černý 1991a; Simmons & Webber 2017; Müller *et al.* 2022). Mixed NYF+LCT family consists of mixed geochemical and mineralogical characteristics in pegmatites. In the classification, the RE-pegmatites are divided further into RE, beryl, complex, albite-spodumene or albite type and subtypes, as shown in figure 1. Černý (1991b) categorized subtypes to be barren, RE-type, beryl-columbite sub-type, beryl-columbite-phosphate subtype, spodumene, petalite or amblygonite subtypes, lepidolite, albite-spodumene or albite type (Table 1).

The differentiation of genetic families of NYF and LCT-pegmatites is complex, which is why Wise *et al.* (2021) proposed a contemporary classification alongside Černý & Ercit (2005) classification (Müller *et al.* 2021). The classification of Wise *et al.* (2021) covers pegmatites more broadly, relating them to granite plutons, anatexis of metaigneous or metasedimentary protoliths. The classification divides pegmatites based on their origin from residual melts of granite magmatism (RMG) or direct products of anatexis (DPA) (Müller *et al.* 2021, 2022). According to Müller *et al.* (2021), the RMG pegmatites are linked to granite intrusions and magmatic processes, while the DPA pegmatites are formed directly from the melting rocks, without significant granite intrusion influence. The RMG classification is further divided into three types, where RMG-1 represents S-type pegmatites, RMG-2 corresponds to A-type pegmatites, and RMG-3 refers to I-type pegmatites. The DPA classification divides pegmatites into three different classes; DPA-1, DPA-2, and DPA-3. The DPA-1 class derived pegmatites with a granitic S-type signature and these pegmatites are characterized by geochemical signatures of Be, Nb, Ta, P, and Li. The DPA-2 are A-type granitic with geochemical markers such as REE, U, and Be. The DPA-3 pegmatites are rich in Al, and the pegmatites are marked by Al, Be and B elements. Both RGM and DPA pegmatite classifications can be effectively differentiated using Li, Ge and Al concentrations of the pegmatites (Müller *et al.* 2021).

2.4 LCT pegmatites mineralogy and geochemistry

The mineral and geochemical compositions of RE-pegmatites are variable. Quartz, feldspars, and micas are the most dominant minerals in pegmatites, even in the most complex pegmatites (Bradley *et al.* 2017). According to London (2008), the microcline type potassium feldspar, as well as albite or cleavelandite type plagioclase are common in LCT pegmatites. The plagioclase is usually elevated in Sr, Ba, Ga and P, while potassium feldspar is enriched in Ba, Pb, P, and Rb contents (London 2008). The most fractionated LCT pegmatites contain white blocky K-feldspar, with elevated Rb and Cs contents (Breaks *et al.* 2003; Selway *et al.* 2005; Bradley *et al.* 2017). Quartz and feldspar usually form graphic intergrowths, which often grow towards the pegmatite body from the outer zone (Selway *et al.* 2005). Increasing fractionation enables the growth of silicate-bearing Li-bearing minerals such as lepidolite $\text{KLi}_2\text{Al}(\text{Al},\text{Si})_3\text{O}_{10}(\text{F},\text{OH})_2$, spodumene ($\text{LiAlSi}_2\text{O}_6$), and petalite ($\text{LiAlSi}_4\text{O}_{10}$). Cs- and Ta-bearing minerals such as pollucite ($\text{CsAlSi}_2\text{O}_6 \cdot \text{H}_2\text{O}$) and columbite-tantalite are common in LCT pegmatites. Nb-rich columbite typically forms early in the development. Common Nb-Ta oxides includes ferrotantalite ($(\text{Fe} > \text{Mn})(\text{Ta} > \text{Nb})_2\text{O}_6$), ferrocolumbite (FeNb_2O_6), manganocolumbite (MnNb_2O_6), and manganotantalite (FeTa_2O_6) (Černý & Ercit 1985).

Certain accessory minerals are also more common in LCT pegmatites. These are beryl, tourmaline, and phosphate series (PO_4^{3-}) minerals, such as fluorapatite, montebrazite-amblygonite, and monazite (Breaks *et al.* 2003; Selway *et al.* 2005). Tourmaline ($\text{XY}_3\text{Z}_6(\text{BO}_3)_3(\text{Si}_6\text{O}_{18})(\text{OH})_3(\text{OH}, \text{F})$), is a very common accessory mineral in LCT pegmatites. The color of the tourmaline changes during increasing fractionation from black in outer zones to pink, green or blue Li-rich tourmaline in the most fractionated RE-pegmatites. The presence of white beryl within pegmatites usually indicates enrichment in Cs and is thus a good indicator of pegmatites belonging to the LCT type family (Selway *et al.* 2005). In addition, the highly fractionated LCT-pegmatites are enriched in Li, Cs, Mn, Rb, and F in micas (Selway *et al.* 2005; Bradley *et al.* 2017). As fractionation progresses, muscovite changes from silver to greenish Li-rich muscovite and eventually to lilac lepidolite, which is usually found in the fractionated zone of RE-pegmatites (Selway *et al.* 2005). Another important accessory mineral in complex pegmatites is garnet, which is usually found as a red Fe-rich almandine in fertile pegmatites or an orange Mn-rich spessartine in RE-pegmatites (Baldwin & von Knorring 1983; Černý 1989a).

2.5 Potential of RE-pegmatites in Finland

About 50 RE-pegmatite moderate and minor deposits have been found in Finland, of which a majority represent the LCT-type pegmatites (Alviola 2003, 2012). A limited extent of NYF and mixed LCT+NYF pegmatite families also appears in Finland. However, according to Rasilainen *et al* (2018), all the well-known mineral deposits are LCT-type. They have divided the pegmatite groups into different deposit areas all over Finland. In figure 3, these areas include both moderate and minor deposits, where the bedrock contains ore minerals that are economically interesting.

Most of the pegmatite groups are known from the schist belt of Southern Finland Granitoid zone, while only a few of the deposits are in Lapland (Alviola 2012). There are also several deposits in the so-called Ostrobothnia region, which includes the Kaustinen-Kauhava-Seinäjäjoki-Kuortane areas (Figure 3), and share the same 1.81–1.78 Ga ages as LCT pegmatites of the Southern Finland (Alviola 2012). Furthermore, 1.89 Ga aged NYF-type pegmatites can be found in the Central Finland Granitoid Complex. The youngest rapakivi granite hosted pegmatites in Finland are dated at 1.6 Ga and are found in the Wiborg area, which consist of the Luumäki-Kymi deposits (Figure 3; Alviola 2012). The Kaustinen Li-pegmatite province, located in western Finland and part of the Ostrobothnia region is the most well-known Li province in Finland (Rasilainen *et al.* 2018). The Kaustinen area consists of several spodumene pegmatite deposits. The pegmatites are RE-pegmatite type and belong to the albite-spodumene type of the Li subclass. The Kaustinen pegmatite deposits have been estimated to contain more than 15 Mt total mineral resources (Keliber 2023). Presently, Keliber Oy's aim is to start ramping up mine production in 2025 in the area, by responding to the growing global economy need for Li.

According to Rasilainen *et al.* (2018), compared to the global scale, the median number of Finnish pegmatite deposits is lower than average, and reserves constitute only 0.1% of the world's known reserves. However, according to Alviola (2003) and Rasilainen *et al.* (2018), the number of poorly exposed pegmatites is estimated to be high, and undiscovered resources in LCT pegmatites are estimated to contain more than 510 tonnes of Li in Finland (Rasilainen *et al.* 2018). Rasilainen *et al.* (2018) estimate that most of the undiscovered deposits are estimated to found in the Ostrobothnia region, and Somero-Tammela areas (Figure 3).

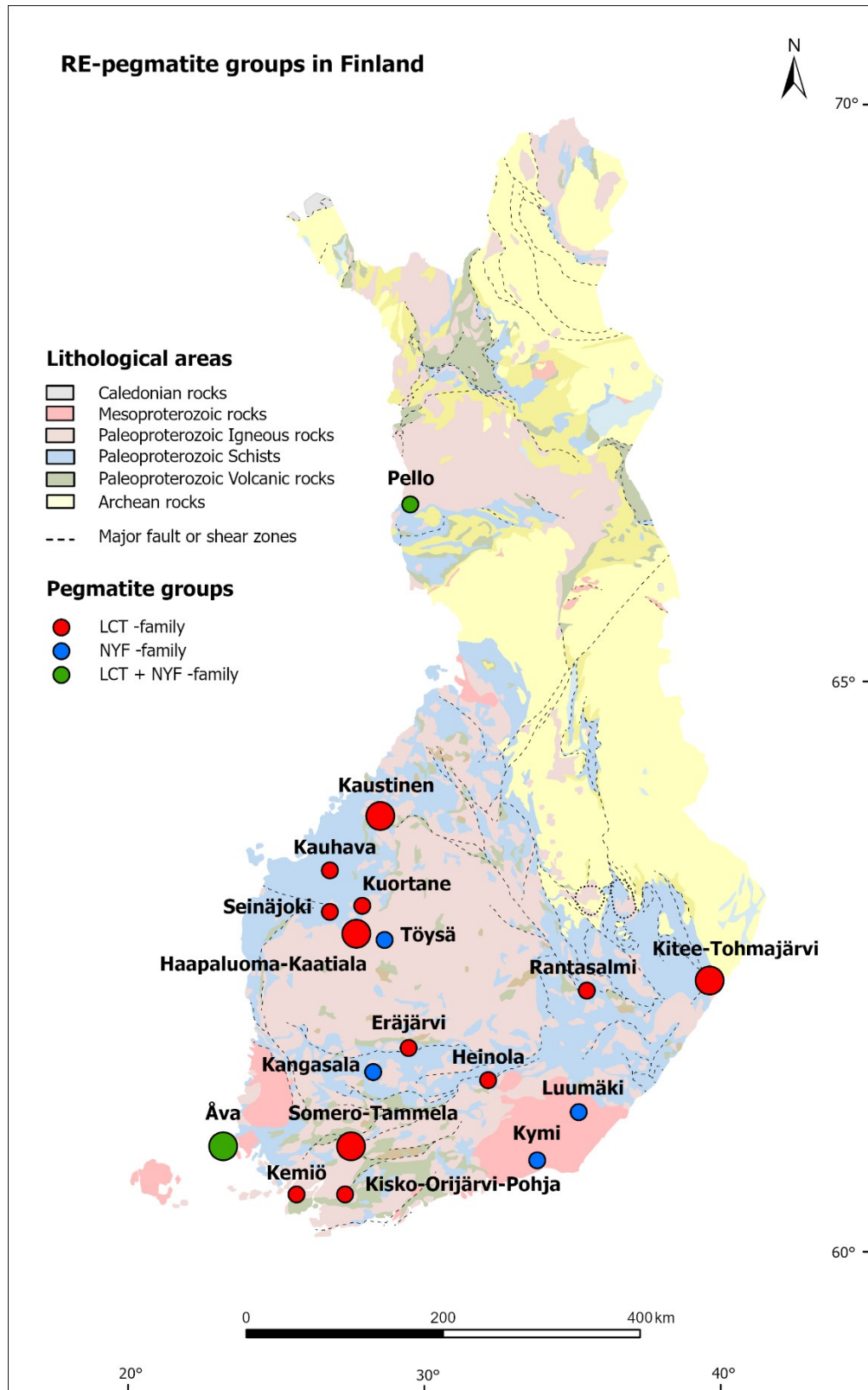


Figure 3. Geological map of RE-type pegmatites in Finland (modified from Alviola 2003; Rasilainen et al. 2018). The increased size of the pegmatite group reflects the size of the deposit. The Southern Finland Granitoid Complex contains the Kaustinen, Kauhava, Seinäjoki, Kuortane, Haapaluoma-Kaatiala, and Töysä pegmatite deposits. The Wiborg area contains the Luumäki-Kymi NYF pegmatite deposits. The modified Bedrock map of Finland is at a 5:000 000 scale from GTK (2024). Coordinates are in ETRS-TM35FIN coordinate system.

3 Regional geology

3.1 Karelia province

The Finnish Archean bedrock, part of the Precambrian Fennoscandian shield, is divided into several different provinces, with the Karelia province representing the western part (Figure 4; eg. Luukas *et al.* 2005; Hölttä *et al.* 2012a,b). The Karelia province formed during Svecofennian orogeny, by several metamorphic and deformation events during 1.9–1.8 Ga (Hölttä *et al.* 2012a,b). The dominant geological features of the Karelia province comprise the Archean basement and Paleoproterozoic supracrustal rocks of the Karelian schist belt. The western border area of the Karelia province features magmatic paragneiss and minor mafic metavolcanic rocks from the Savo belt (Figure 5), which are thrust over the Archean basement (Luukas *et al.* 2017). The subprovinces have their own different geological history as well as lithological, structural and age characteristics (Hölttä *et al.* 2012a,b).

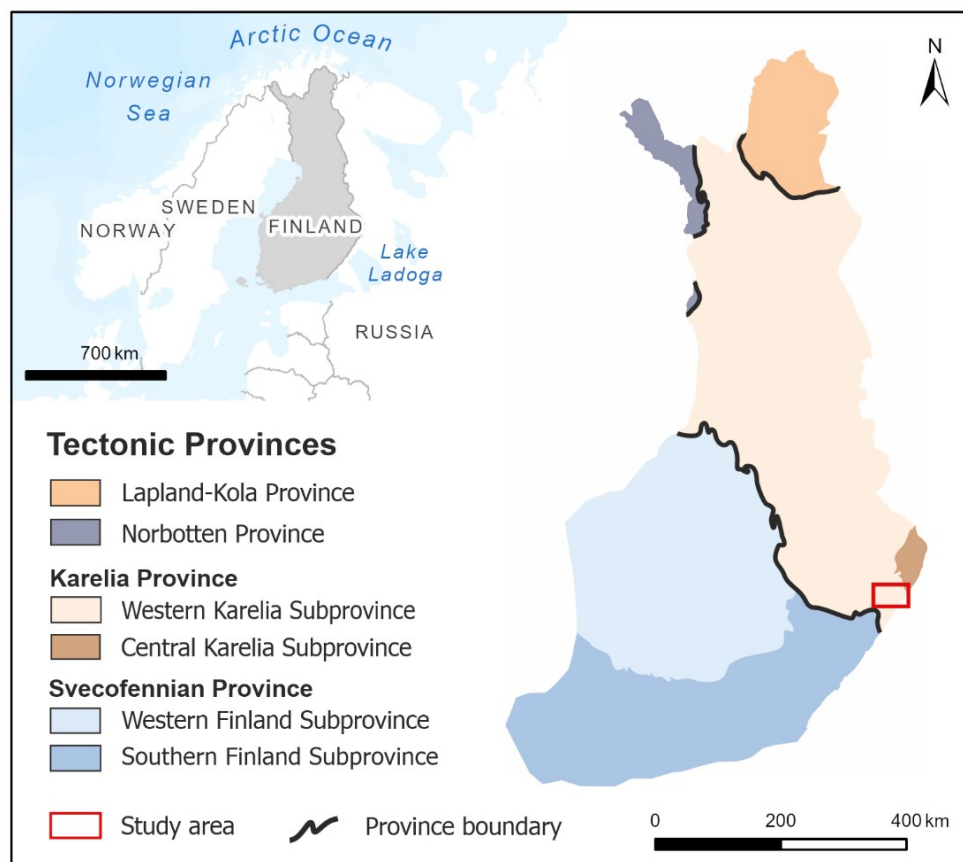


Figure 4. Simplified geological map of tectonic provinces in Finland (Luukas *et al.* 2005). The Bedrock map of Finland is at a 5: 000 000 scale from GTK (2024).

3.2 Karelian schist belt

Paleoproterozoic supracrustal rocks, aged 2.50–1.90 Ga, of the Karelian schist belt, were formed during the Svecofennian orogeny (eg. Laajoki 2005). The Karelian formations exist around and between the Archean basement blocks as the Kainuu belt, North Karelia belt, and Savo belt, located in eastern and central Finland (Figure 5; Laajoki 2005). The Karelian formations has been influenced by different deformation and metamorphic events, which transformed sedimentary and volcanic-origin rocks into metamorphic rocks, as well as developed different fault and shear zones in the areas. Based on the definition by Laajoki (2005), the Karelian formations are divided into six tectofacies which are Sumi, Sariola, Kainuu, Jatuli and Kaleva units. The formations of Kaleva are divided further into Lower Kaleva, Sub-Lower Kaleva and Upper Kaleva. The 2.06–1.97 Ga aged lower Kaleva represents a continental-epicontinental and a rift-marginal basin deposit while 1.92–1.87 Ga aged Upper Kaleva tectofacies represents an allochthonous marine basin. It is also the youngest tectofacies of the Karelian formations. Metamorphosed volcanic and sedimentary rocks developed in the eastern parts of Kainuu and North Karelian belts at greenschist facies, whereas in the western parts of the Kainuu and Savo at upper amphibolite facies (Laajoki 2005; Figure 5).

3.3 Puruvesi granite

The late-orogenic plutonic Puruvesi granite, located in Eastern Finland, formed during Svecofennian orogeny at 1.9 Ga (Figures 5 & 6; Nironen 2017). The Puruvesi granite is an ovoidal intrusion, containing 1.8 Ga initiated continental intrusive rocks and representing the youngest intrusive stage. The intrusive granites take a significant role in the understanding of the geological formations of the Precambrian cratons (eg. Nironen 2017). In general, the Puruvesi granite is mainly represented by a reddish homogeneous and undeformed late-orogenic granite (Kurhila *et al.* 2010). The mineral composition includes alkali feldspar, quartz, biotite and myrmekite plagioclase, as well as other accessory minerals like garnet, muscovite, apatite, monazite and zircon. Kurhila *et al.* (2010, 2011) specify that the Puruvesi granite is represented by two different types of granite marginal phases. In the marginal phases, granite displays an almost white coloration, featuring mica gneiss and irregularly garnet. These inclusions vary in size from a few centimeters up to one meter-scale fragments and exhibit several deformations features. The leucocratic granite composition is characterized by small concentrations of

alkali feldspar, myrmekite and zoned plagioclase, but is enriched in Na and garnet (Kurhila *et al.* 2011). Some parts of it represent heterogeneous pegmatite as well. The central phase of Puruvesi granite, in comparison, is a porphyritic microcline granite that features weak magmatic lineation in feldspar megacrysts. The proposed interpretation by Nykänen (1983), the southern part of the Puruvesi intrusion consists of synorogenic oligoclase granite, rather the east side represent late-orogenic granite. The late-orogenic pegmatite granite dykes and small intrusions cut synorogenic quartz diorite, granodiorite and oligoclase granite. Nykänen (1983) and Kurhila *et al.* (2010, 2011) have defined the age of Puruvesi granite at about 1.79 Ga. Referring to the examinations, Kurhila *et al.* (2010) states that the leucogranites of Puruvesi granite rather than originated from mantle-derived parent magmas are more likely indicative of a crustal melt and likely have a source in Svecofennian sedimentary rock (Kurhila *et al.* 2010, 2011).

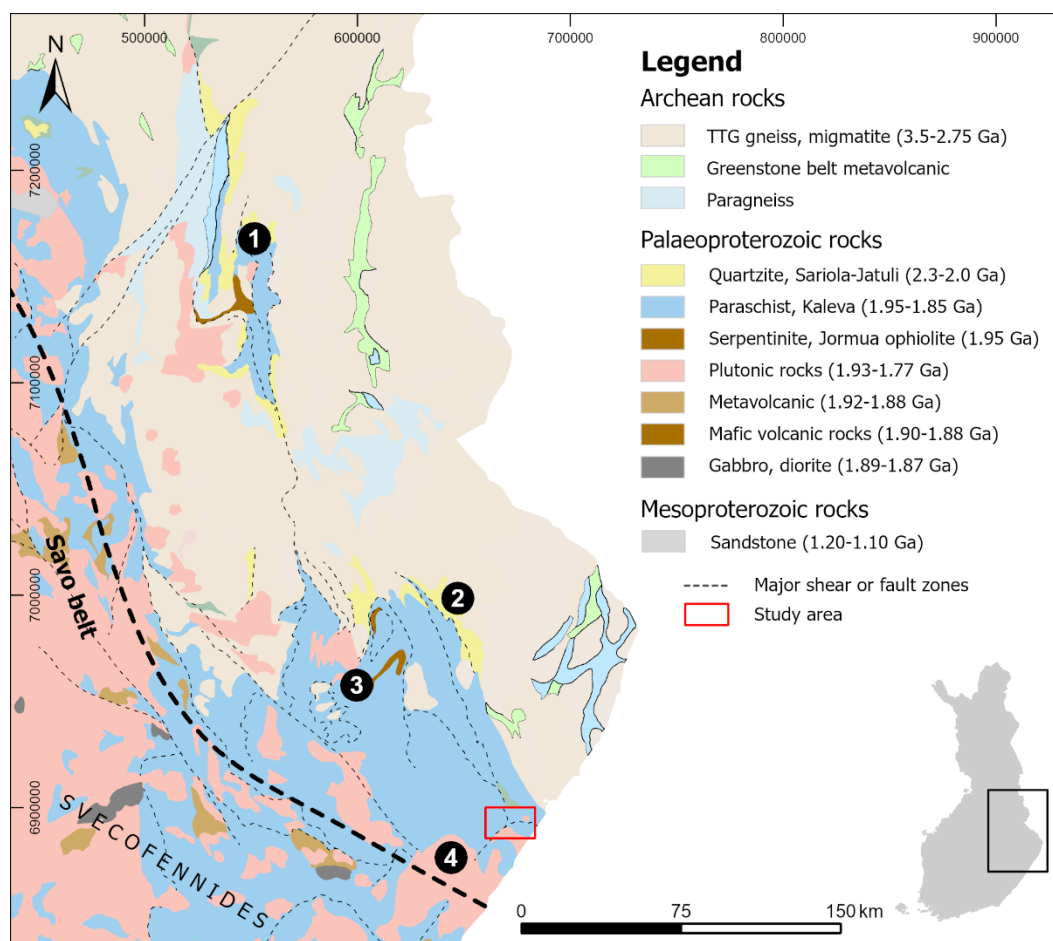


Figure 5. Simplified geological map of Central and Eastern Finland. Number 1-3 represents the Karelian Schist belt: 1) Kainuu belt, 2) North Karelian belt, and 3) Outokumpu nappe complex. The black dashed line is the boundary of the Karelian craton (modified from Laajoki 2005; Hölttä *et al.* 2012b). The geological map is at a 5: 000 000 scale from GTK (2024). Coordinates are in ETRS-TM35FIN coordinate system.

3.4 Kitee-Tohmajärvi pegmatite province

3.4.1 Evolution and structural evolution

The study area of this thesis is in the Kitee-Tohmajärvi pegmatite province, located in North Karelia in eastern Finland (Figure 6). The Kitee-Tohmajärvi area belongs into the Tohmajärvi, Viinijärvi, Höytiäinen, Kontionlahti and Tikkala suites part of the Karelian lithodemic units, as shown in figure 6 (Luukas *et al.* 2017). The Tohmajärvi area is divided into two different complexes: the western part into Karelian schist belt, and eastern part into Archean Karelia province. The Karelian schist belt deposited on the underlying gneiss complex, both of which continued to deform and fold during the Svecofennian orogeny. The eastern part of Kitee-Tohmajärvi is the syncline basin of Höytiäinen (Figure 6; Nykänen 1968), which is separated by an anticlinal ridge on the west, extending from Tohmajärvi toward NNW (Nykänen 1971). The regional lineament trend of the Karelian schist belt and the basement gneiss complex are oriented NNW-SSE in Tohmajärvi. In the interpretation by Hölttä & Heilimo (2017), the peak metamorphic conditions are between low and mid-amphibolite facies in the Kitee-Tohmajärvi areas.

The plutonic rocks of Kitee and Tohmajärvi range from ultramafic hornblendite to felsic granites and pegmatites (Figure 6; Nykänen 1971; Alviola 1974a,b). In addition, the regional bedrock consists of gabbro, diorite, schists, amphibolite, diabase, and volcanite, as well quartz- and granodiorite. The small intrusions of the pegmatite granites in the area belong to the so-called Kitee granite (Figure 6), which covers an area of 200 km², and are part of the late-kinematic Svecofennian plutonic rocks (Nykänen 1971; Nykänen 1985). The Kitee pegmatite granite is most prominent in the Potoskavaara area on the border between Kitee and Tohmajärvi. The Kitee pegmatite granite and Kitee granite are very coarse grained, light or light gray in color, and the main mineral characteristics of feldspar, oligoclase, quartz, muscovite, tourmaline, garnet, apatite, and biotite (Nykänen 1971). According to Nykänen (1985) interpretation, the Kitee pegmatite granites are the youngest late-orogenic granites in the area and have an age of 1.83–1.81 Ga.

The geological structures in the Kitee-Tohmajärvi are complex. The bedding and schistosity structures in the bedrock are generally parallel, however the conglomerates, quartzites, amphibolites and the staurolite-mica schist typically show transversal schistosity in the anticlinal ridge of the Tohmajärvi suite near of the Tohmajärvi area

(Figure 6; Nykänen 1968). In the proposed interpretation by Nykänen (1968, 1971), in the synclinal parts of the Kontionlahti suite, the dips of the schistosity and stratification are primarily steep or vertical. The Karelian schist belt can be found within a broad axial depression in the Tohmajärvi suite, and the fold axis inclines gradually or more steeply towards Lake Ladoga. Furthermore, the axial planes of the folds slope steeply westward. Nykänen (1971) interpreted that the cataclastic structure of the basement gneiss complex formed during the movements of the Karelian schist belt. The Puruvesi and Kitee granite seemingly caused cross-cutting deformation in the general direction of the Karelian schist belt (Nykänen 1968).

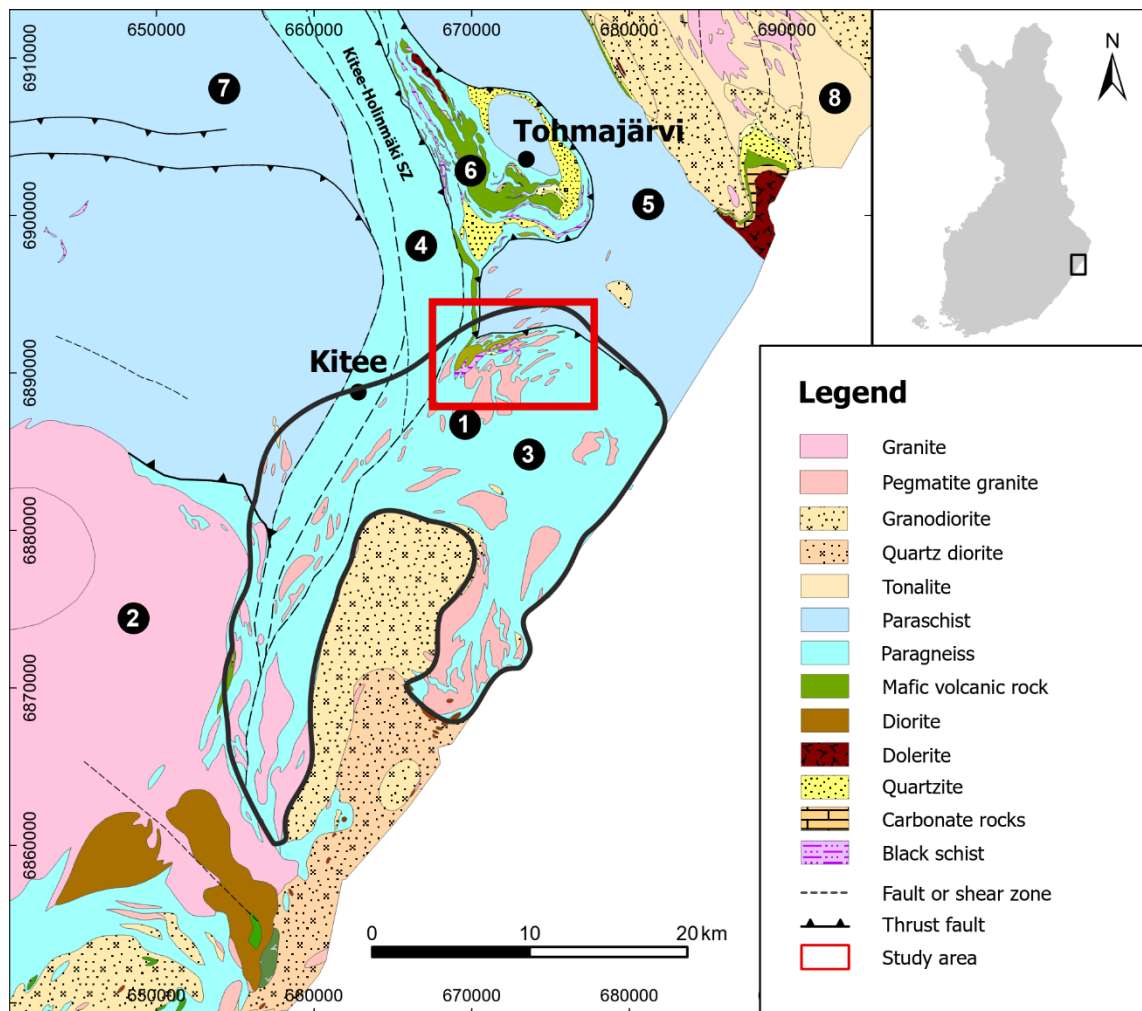


Figure 6. Simplified regional geological map of the Kitee-Tohmajärvi pegmatite province (solid black line) and the Potoskavaara area (red square). 1. Kitee granite, 2. Puruvesi granite, 3. Tikkala suite, 4. Höytiäinen suite, 5. Kontionlahti suite, 6. Tohmajärvi suite, 7. Viinijärvi suite, 8. Ilomantsi complex. (modified from Laajoki 2005; Hölttä et al. 2012b; Kuikka et al. 2023). The geological scale-free Bedrock map of Finland from GTK (GTK 2024). Coordinates are in ETRS-TM35FIN coordinate system.

3.4.2 Earlier pegmatite studies

Numerous pegmatite intrusions and dykes are found in the Kitee and Tohmajärvi area (Figure 6; Alviola 1974 a,b; Nykänen 1971, 1983). The first signs of complex pegmatites were discovered by Kalkkitechdas Oy in 1969 during andalusite research, when they found the first beryl-bearing pegmatite dykes from the southern part of Tohmajärvi (Alviola 1974b). The first Li-pegmatite was discovered during boulder exploration by GTK in the summer 1971. More detailed bedrock explorations followed from 1972 until 1973, in addition to later exploration carried out as part of the battery minerals project from 2019 until 2022.

The latest research suggests the Kitee-Tohmajärvi pegmatites represent mostly leucogranite type, with typical minerals as quartz, feldspar, plagioclase, muscovite, and as accessory minerals black tourmaline, garnet and apatite. According Alviola (1974a, b), a total of 70 complex pegmatites are found around in the Kitee-Tohmajärvi boundary during 1972–1973, where pegmatites of the Potoskavaara area represent the most complex ones (Alviola 1974b, Kuikka *et al.* 2023). In the Potoskavaara area (Figure 7) the pegmatites are mainly leucogranite, but potassic pegmatites, sodic aplite, and RE-pegmatite types are also found (Kuikka *et al.* 2023). According to Alviola (1974b) and Kuikka *et al.* (2023) studies, the Surmasuo and Kumpu pegmatites in northern Potoskavaara contain Li-rich silicates and spodumene and represent a distinct type of pegmatite in the whole Kitee-Tohmajärvi area. The Surmasuo pegmatite dykes consist of two parts, Surmasuo S and Surmasuo E, which are located 200 m from each other. In Both dykes are coarse-grained containing the most important complex minerals, including spodumene, lilac-gray lepidolite, amblygonite, and cassiterite. Plagioclase is found as cleavelandite dykes. However, Surmasuo S has a higher content of these minerals, as well as additional Mn-tantalite mineral (Alviola 1974b). The pegmatites found in the Potoskavaara area, Surmasuo S, Surmasuo E, Oriselkä SW or Selkäpäivänrinne, Kumpu and Kuusela N pegmatites are the most enriched in grayish, yellow-greenish or reddish colored beryllium. The deep drilling carried out in the surroundings of the Surmasuo S pegmatite indicated that mineralization of Li is unlikely to be present deeper than about 10 m (Alviola 1974b; Kuikka *et al.* 2023). The radiometric age determinations of uraninite by GTK give the Surmasuo E to be formed at age 1.81 Ga (Alviola 1974b).

4 Materials & methods

4.1 Bedrock observations

For this study, 13 bedrock observations were collected from pegmatite dykes within the Potoskavaara area in Kitee-Tohmjärvi province during the summer field season in August 2022. The observations include information of the outcrop, for example GPS-location, rock type, pegmatite classification, grain size, mineralogy, textures, structural information, color, field photographs and any other relevant comments on the pegmatites. The observations were mainly documented using Kapalo mobile software provided by GTK. Samples were collected from the bedrock with a geological hammer and in total, 15 mini-drill cores were collected from the study outcrops for later petrography and geochemical analysis. Using the mini-drill technique, a diamond drill tool was employed to extract samples from the outcrop beneath the erosion surface of the bedrock. The drill-core sample ranged in size from about 5–15 cm in length and 5 cm in diameter. Furthermore, external bedrock GTK databases from the Kitee-Tohmjärvi area outside the study area were also used in this research.

4.2 Petrography

For the optical petrography studies a total of 11 thin sections were prepared from the mini-drill core samples by GTK. The thin sections were studied with an optical microscope in the Geohouse, University of Turku. The examination of the petrographic thin sections involves the documentation of the mineralogy, textures, grain size, alterations, photos and any other relevant comments of the pegmatite samples. The aim of the petrography study was to get a better understanding of the mineralogy and identify the differences between pegmatite samples.

4.3 Geochemical analyses

Whole-rock geochemical analyses were made from the 15 mini-drill cores samples by Australian Laboratory Services (ALS) Finland Oy laboratory in Outokumpu, Finland. The major rock-forming elements (SiO_2 , Al_2O_3 , BaO , CaO , Cr_2O_3 , Fe_2O_3 , K_2O , MgO , MnO , Na_2O , P_2O_5 , SrO , and TiO_2) were analysed using the whole-rock analytical method with Inductively Coupled Plasma Atomic Emission Spectrometry (*ICP-AES*) (ALS 2024). The trace elements Ag, As, Ba, Be, Bi, Ca, Cd, Ce, Co, Cs, Cu, Dy, Er, Eu,

Fe, Ga, Gd, Ge, Hf, Ho, In, K, La, Li, Lu, Mg, Mn, Mo, Nb, Nd, Ni, Pb, Pr, Rb, Re, Sb, Se, Sm, Sn, Sr, Ta, Tb, Te, Th, Ti, Tm, U, V, W, Y, Yb, and Zn were analysed by using ME-MS89L method. The technique employed was the sodium peroxide fusion method with an elemental analysis technique Inductively Coupled Plasma Mass Spectrometry (*ICP-MS*), which is recommended especially for Li-enriched pegmatites, which usually consist of acid-resistant minerals. The method is optimal for samples with high Li or B concentrations, or with sulphide minerals (>4%). For the trace element Zr, the ME-MS85 method was used, which involves a Li borate fusion in ICP-MS measurement followed by acid dissolution. (ALS 2024)

The Geochemical Data Toolkit (GCDkit) program by Janoušek *et al.* (2006) was used for the interpretation of the whole-rock geochemical data. The geochemistry of the pegmatites in the study area are presented collectively in the diagrams, highlighting the distinct trends and variations in elemental composition. Samples with a geochemical element concentration below or above its detection limit are represented in diagrams as half of the detection limit value. In the tables and appendixes, elements are simply labeled with a "less than" or "greater than" sign to indicate their presence at levels outside the detectable range.

4.4 Lineament interpretation

A 2D-lineament interpretation using ArcGIS Pro software was conducted by manually drawing polylines to interpret the structural geological features of the Kitee-Tohmajärvi area. This includes on a large scale interpreting the positioning of ductile foliation trends, brittle major faults, and shear zones in the area, which help in interpreting the location and extent of the pegmatites in relation to the surrounding geological structures. The interpretation of the foliation trends is based on an independent analysis of the area's structural features, with modification of shear and structural data supported by GTK's existing open shear and fault database. The 2D-lineament interpretation was primarily based on negative and positive low-altitude aeromagnetic geophysical data obtained from GTK's open database, which revealed the area's structures as continuous linear features. Additionally, the interpretation utilized lithological information about the variability and properties of the rocks, which influence the behavior of deformation. The open hyperspectral light detection and ranging (LiDAR) data provided by National Land Survey of Finland (2024) was utilized in interpretation. LiDAR is a three-dimensional

laser-scanning point data, which effectively represents the ground features on the surface, and helps to accurately identify geological structures.

5 Results

5.1 Bedrock observations

The pegmatite dykes in the study area (Figure 7) were classified into four different categories according to pegmatites characteristics and mineral compositions. These categories are pegmatitic leucogranite, potassic pegmatite, sodic aplite, and RE-pegmatite, which are presented from the most evolved type to the most primitive type. The RE-enriched pegmatites are found in the northern part of the study area, while the other pegmatites vary across the area. However, pegmatitic leucogranites are primarily found in the central part of the study area, whereas potassic pegmatites and sodic aplites are found in the surrounding areas. These different rock pegmatite types suggest a geologically diverse area with potential significance for the occurrence of mineral deposits.

The bedrock observations from the study area reveal the presence of various types of fertile granite, predominantly leucogranite type. The least developed pegmatite types such as fine-grained or porphyroblastic biotite granite, and entirely fine-grained leucogranite, are not represented in the study area. The pegmatites in the study area mainly contain typical pegmatite minerals such as quartz, feldspar, plagioclase, muscovite, varying amount of secondary biotite and as accessory mineral black tourmaline, garnet, and apatite. The pegmatites dykes' grain size varies between small to extremely coarse-grained. Additionally, their coloration varies from light gray to reddish gray, depending on the composition of the feldspar present. Many of the pegmatite dykes are in sharp contact with surrounding host rock which is mainly sedimentary.

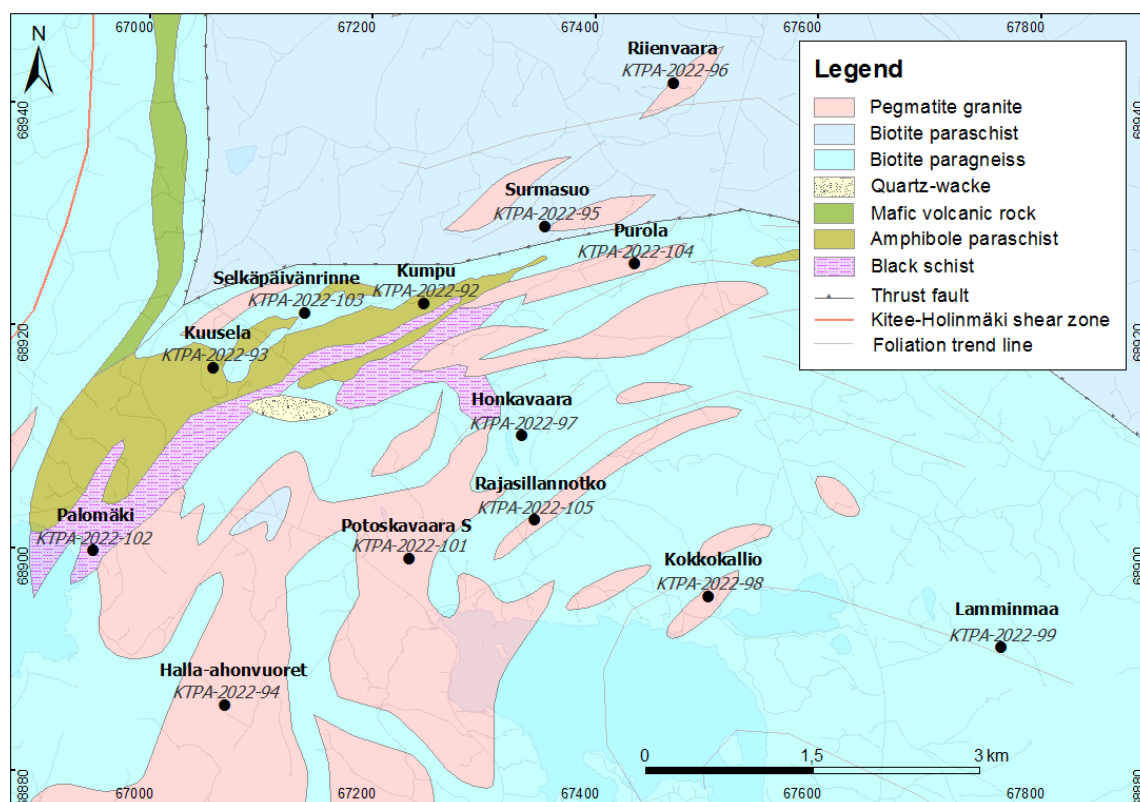


Figure 7. Geological map and the study targets in the Potoskavaara area, Kitee-Tohmajärvi pegmatite province. The scale-free Bedrock map of Finland is from GTK (2024) and the background Topographic Database is from National Land Survey of Finland (2024). Coordinates are in ETRS-TM35FIN coordinate system.

5.1.1 RE-enriched pegmatites

The most RE-enriched pegmatites are found in Kumpu *KTPA-2022-92* and Surmasuo *KTPA-2022-95*, in the northern part and boundary of the Kitee-Tohmajärvi regions (Figures 7). The pegmatites represent the most evolved pegmatites in the study area, containing many RE-bearing minerals (Figure 8).

The Surmasuo area features a mineralogically very complex pegmatite dyke and this study is focusing on the southern part of the dyke (Figures 8A-B). According to field observations, the pegmatite is grayish in color and composed of typical pegmatite minerals, as well as a variety of complex minerals, such as yellowish muscovite, spodumene, colored green, blue, and red tourmaline, cleavelandite, and lilac lepidolite (Figure 8B). The general grain size of the minerals ranges from coarse to very coarse, with almost 1 m sized crystals of quartz and feldspar. Colored tourmalines are often surrounded by finer-grained accessory muscovite grains, as well coarse-grained quartz

grains. Lepidolite is slightly more grayish in color than in Kumpu and commonly appears in fine-grained masses. Plagioclase cleavelandite also appears locally in a fan-shaped form and is visible to the naked eye in the outcrop. Further, the pegmatite dyke contains minor phosphate minerals such as amblygonite, heterosite and purpurite. The pegmatite dyke is divided into three distinct zones based on mineral concentrations: cleavelandite-rich, spodumene-rich, and feldspar-rich parts of the dyke. This observation suggests that the dyke represents a zoned pegmatite type. Additionally, the pegmatite is in strong contact with a large and coarse-grained quartz vein. Three different mini-drill samples were taken from different zones of the outcrop, with one from a spodumene-rich (*KTPA-2022.95.1*) (Figure 8A), one from a feldspar-rich (*KTPA-2022-95.2*), and one from a cleavelandite-rich (*KTPA-2022.95.3*) part of the pegmatite dyke.

The pegmatite from Kumpu is also a complex pegmatite (Figures 8C-D) and contains various amounts of RE-bearing minerals. The pegmatite is light gray in color, and the grain size is mainly coarse-grained. It contains largely quartz, plagioclase, K-feldspar, muscovite, and rare minerals. Kumpu, also known as rubellitepegmatite, is characterized by several differently colored Li-rich tourmaline, which are blue, green, and red in coloration (Figure 8C). The dyke contains significantly more reddish tourmaline compared to the dyke at Surmasuo. Further, the pegmatite contains Li-bearing spodumene, abundant lilac lepidolite, and muscovite with ranges in color from silver to yellow and greenish (Figure 8C). Coarse-grained spodumene and in its typical striated texture is clearly visible in the outcrop (Figure 8D). Micas in the pegmatite are commonly found as fine-grained and massive aggregates.

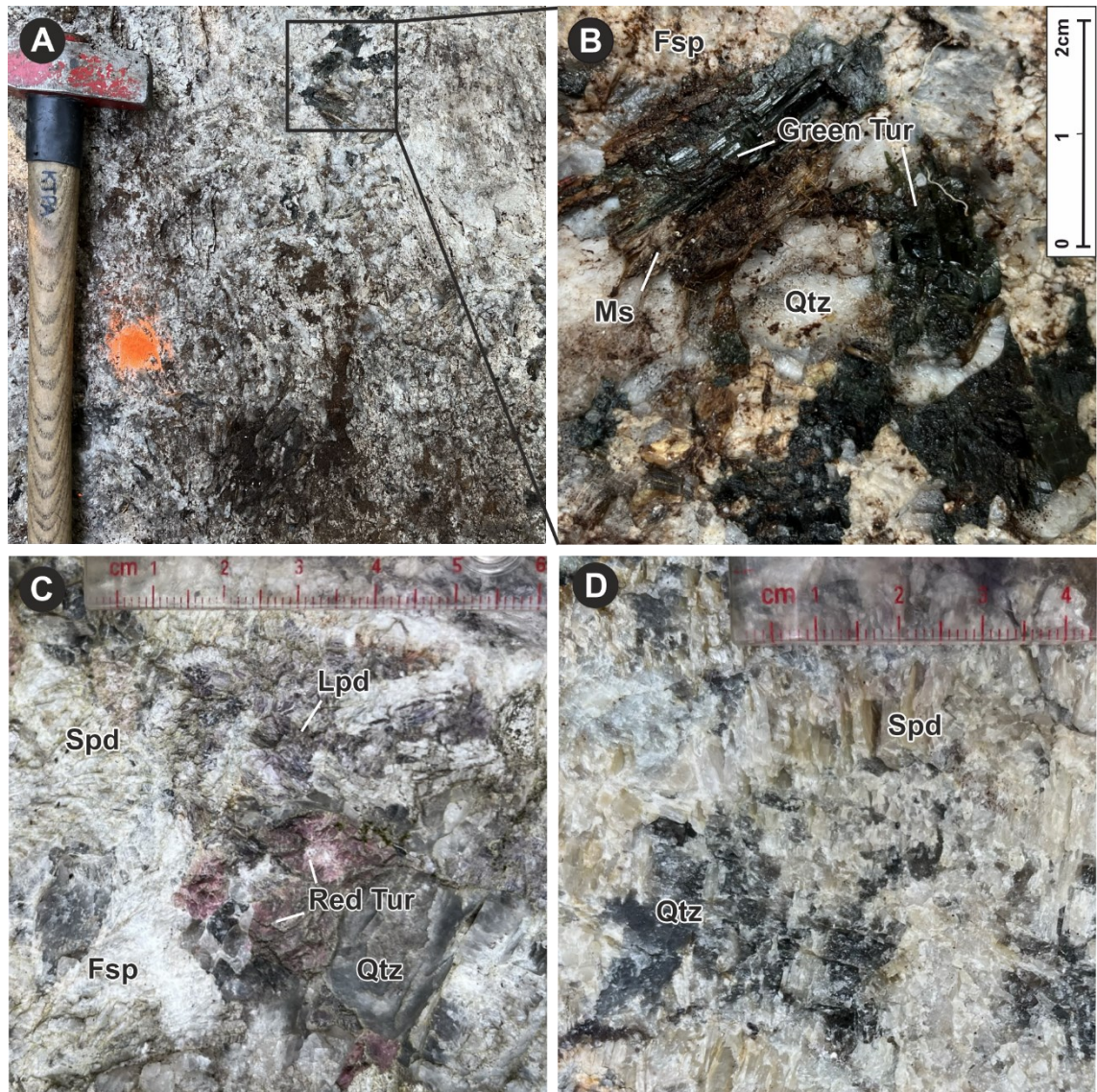


Figure 8. Outcrop pictures of the RE-enriched pegmatites in Potoskavaara area, Kitee-Tohmajärvi pegmatite province. A) Overview of the coarse-grained spodumene-rich RE-pegmatite and green tourmaline (black square) in Surmasuo (KTPA-2022-95). The marked orange spot is the mini-drill sample point number KTPA-2022-95.1. The hammer is 63 cm in length. B) Li-rich green tourmalines in muscovite, feldspar, and quartz matrix in Surmasuo. C) Li-rich lilac lepidolite, red tourmaline, and spodumene (light beige) grains, which are surrounded by feldspar and quartz grains in the pegmatite from Kumpu (KTPA-2022-91). D) A closer picture of the striated texture of spodumene.

5.1.2 Potassic pegmatites

The pegmatites from Riienvaara (*KTPA-2022-96*), Lamminmaa (*KTPA-2022-99*), Palomäki (*KTPA-2022-102*), and Selkäpäivänrinne (*KTPA-2022-103*) represent the potassic pegmatite type (Figures 9 & 10). Typical potassic pegmatites are light gray, with a grain size ranging from fine to very coarse grained (Figure 10A). The mineral composition of the pegmatites includes quartz, blocky K-feldspar, muscovite, tourmaline, beryl and garnet. Intergrowths of quartz and K-feldspar are common and clearly visible to the eye in the outcrop.

The pegmatite from Selkäpäivänrinne is an interesting target. Signs of deformation are clearly visible in the pegmatite dyke, with the eastern and western sides representing different types of pegmatites (Figure 9). The eastern side is a more typical reddish pegmatitic leucogranite type, while the western side is a significantly more evolved type. The eastern side of the pegmatite contains quartz, two feldspars (K-feldspar and albite-rich plagioclase), muscovite, and black tourmaline (Figure 9A). The contact between the surrounding host rock of schist and the pegmatite dyke is sharp, trending E–W. The more evolved western side of the pegmatite is an advanced pseudomorphic potassic pegmatite containing quartz, blocky K-feldspar, black tourmaline, large reddish garnet grains (Figure 9B), and abundant coarse-grained yellowish muscovite, as well masses of light brownish cookeite. Cookeite is a hydrothermal alteration product of spodumene that is observed when Li-bearing minerals are replaced in silicate (London 2008). Cookeite appears as an individual alteration product, surrounded by coarse-grained quartz and feldspar grains, which is especially visible to the eye in the hand sample shown in figure 9C. Unaltered spodumene is not visible to the naked eye in the outcrop, or has not been identified among the alteration. Furthermore, intergrowths of quartz and K-feldspar are commonly visible in western side of the outcrop. However, the dyke does not show the same type of rare mineral enrichments, such as colored tourmalines or other Li-mineralization's, as the RE-enriched dyke at Surmasuo and Kumpu. A mini-drill sample of the pegmatite dyke was taken from the evolved western side of the dyke.

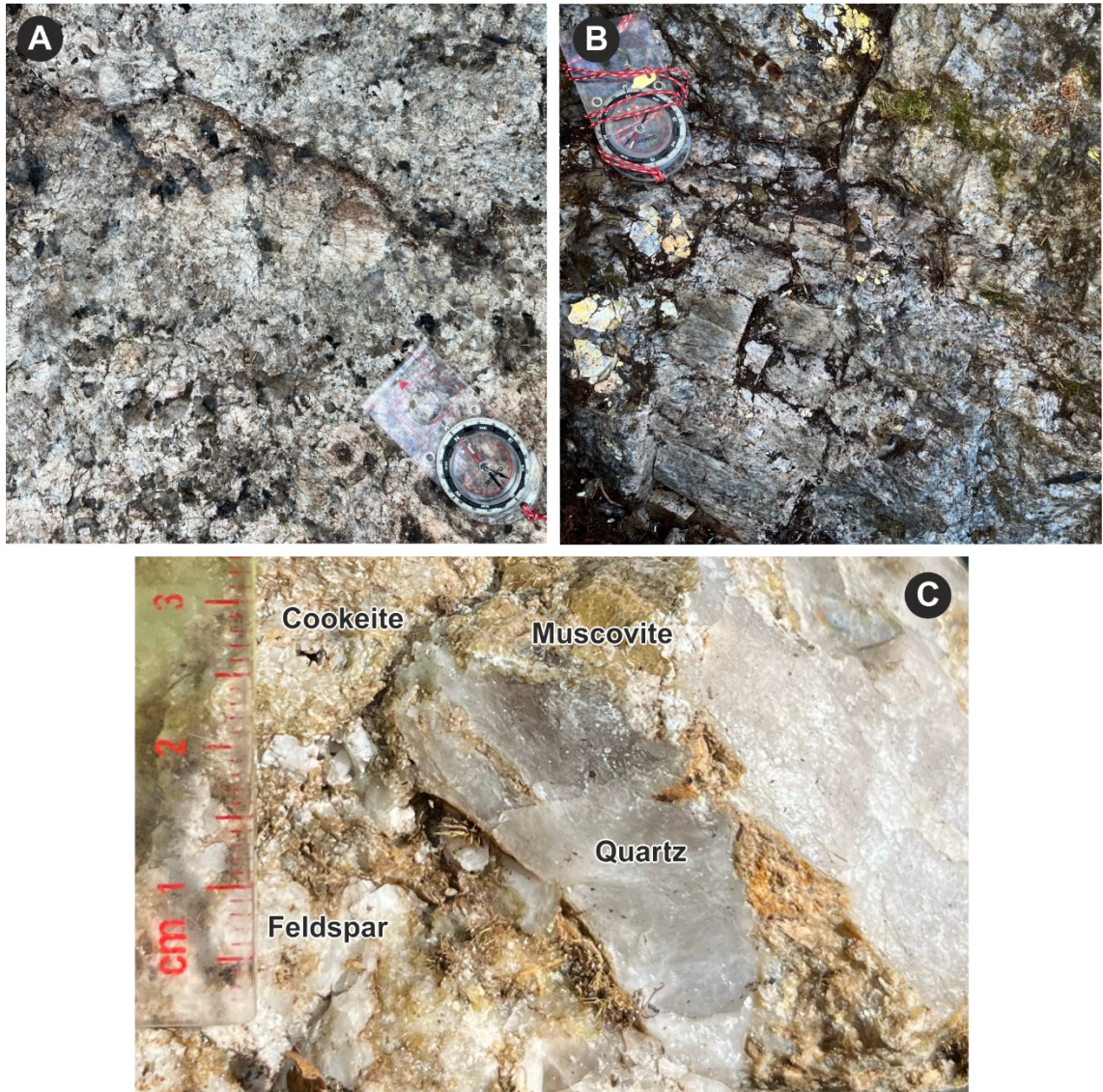


Figure 9. Outcrop pictures of the pegmatite dyke from Selkämpivänrinne (KTPA-2022-103), Kitee-Tohmajärvi pegmatite province. The compass is 12 cm in length and pointing toward N. A) A potassic pegmatite type of the eastern part of the pegmatite dyke in Selkämpivänrinne. B) An evolved pegmatite type of the western part of the pegmatite dyke in Selkämpivänrinne. C) A hand sample of the cookeite-rich pegmatite. Cookeite represent from fine to small grained yellowish grains, which is an alteration product of spodumene. Cookeite appears with coarser-grained yellow muscovite, quartz, and feldspar crystals.

There are several dyke swarms in the Riienvaara area, from which observations have been taken from one pegmatite dyke for this study (Figure 10A,B). The Riienvaara pegmatite contains quartz, feldspar, yellowish muscovite and black tourmaline as the main minerals with beryl and garnet as minor minerals. The small-grained spessartine garnet is orange in color. Abundant yellow-orange beryl is present as coarse-grained crystals, where individual crystals are usually over 2 cm in size. In addition, quartz and K-feldspar appears as extremely coarse-grained, even >10 cm in size (Figure 10A). The outcrop exhibits a sharp contact between the pegmatite and the surrounding schist, to the west side of the pegmatite dyke. The contact has a dip of 85° and dip direction of 045°. Furthermore, clear internal zonation is visible in the pegmatite dyke (Figure 10B). In addition, tourmalines are aligned according to the zoning, and general mineral grain size increases toward the interior from the border zone.

The Lamminmaa pegmatite dyke differs in mineralogy from the previous dykes. The pegmatite dyke from Lamminmaa (Figure 7) is light gray in color and ranges in grain size from medium to very coarse-grained. The pegmatite dyke is composed mainly of quartz, K-feldspar, and coarse-grained muscovite. Muscovite appears silver-colored rather than yellow, as in the previous dykes. Additionally, the pegmatite contains accessory minerals such as large reddish garnet grains, a small amount of light creamy-colored beryl and exceptionally coarse-grained rose and smoky quartz, which are represented locally as patches. Individual beryl crystals are present as coarse-grained. The mineralogical observations suggest that the pegmatite represents a zoned pegmatite.

The Palomäki pegmatite shows some similar textural features with the dyke of Lamminmaa dyke, but there are differences especially in mineralogy. The pegmatite represents a typical potassic pegmatite, which is light grayish to reddish in color, with the general grain size varies from small to very coarse-grained. The dyke contains pegmatite minerals such as coarse-grained K-feldspar, quartz, yellowish muscovite, and black tourmaline grains. Tourmalines are present as very coarse-grained individual crystals, up to >5 cm in size. Furthermore, the pegmatite contains locally plumose quartz and muscovite intergrowths, reddish garnet, and small-grained blue apatite grains. In addition, the grain size of garnet varies from fine to coarser, and at places it appears as small-grained masses between K-feldspar and quartz grains.

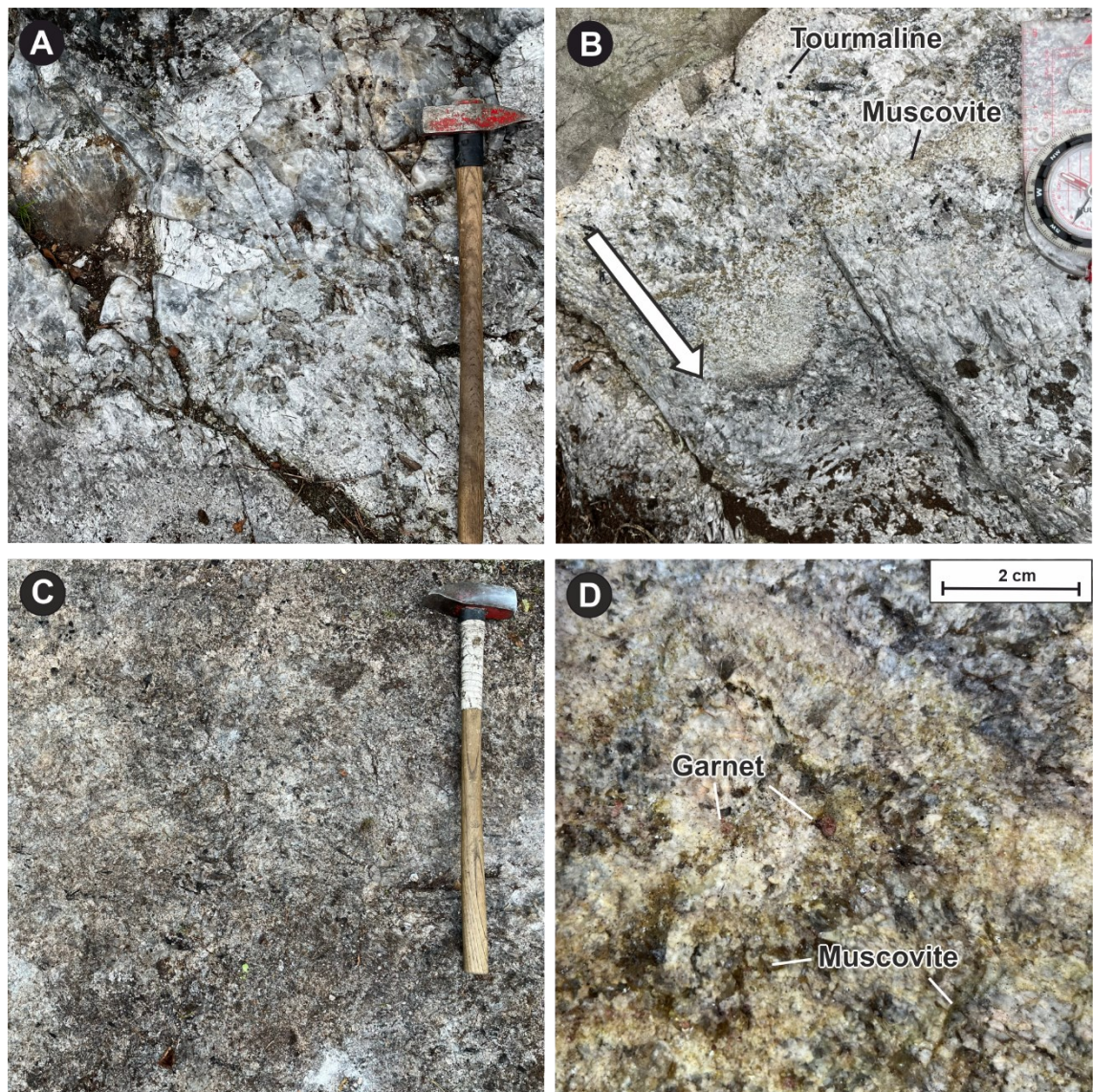


Figure 10. Outcrop pictures of potassic pegmatite type (A-B) and sodic aplite pegmatite type (C-D) in the Potoskavaara area, Kitee-Tohmajärvi pegmatite province. A) Overview of the extremely coarse-grained potassic pegmatite type in Riienvaara (KTPA-2022-96). The hammer is 63 cm in length and pointing toward North. B) Layering internal zonation of the pegmatite dyke in Riienvaara, featuring small-grained yellowish muscovite and black tourmaline in distinct layers. The general mineral grain size increases toward the center of the pegmatite dyke from the border zone (white arrow). The compass is 12 cm in length and pointing toward North. C) Overview of the fine-grained sodic aplite pegmatite in Rajasillanotko (KTPA-2022-105). The hammer is 63 cm in length and pointing toward North. D) A sugar-like crumpling texture with layered featuring red garnets, black tourmalines, and greenish muscovite masses in the pegmatite from Purola (KTPA-2022-104).

5.1.3 Sodic aplite pegmatites

The sodic aplite-type pegmatites were observed in two areas of the study region, in the Purola (*KTPA-2022-104*) and Rajasillannotko (*KTPA-2022-105*) areas (Figures 10C-D). The grain size is fine to small, and in some places, it is sugar-like in texture, crumbling easily. The pegmatite dykes contain albite, quartz, muscovite, tourmaline, garnet, apatite, and in some places Ta-oxide minerals. The coloration of the pegmatites is light gray or almost white, which is typical for albite-rich pegmatites.

The pegmatite dyke represents a typical sodic aplite pegmatite type in Rajasillannotko (Figure 10C). The pegmatite contains feldspar, quartz, small amounts of black tourmaline, and very fine-grained reddish almandine garnet. Quartz, K-feldspar and tourmaline grains size varies from small to coarser grained, but in general the grain size is smaller than in the potassic pegmatite type dykes. In addition, feldspars show clearly visible perthitic texture, which is visible to the naked eye in the pegmatite. The mineral composition is typical of the sodic aplite pegmatite type but lacks some common features like graphic intergrowth of K-feldspar and quartz or muscovite. The outcrop measures 10 × 10 × 6 meters and features a sharp, NNE–SSW-oriented contact between the host rock of schist and the pegmatite dyke.

The pegmatite dyke at Purola shares similar texture characteristics with the dyke at Rajasillannotko. The pegmatite dyke from Purola (Figure 10D) is light gray in color and the grain size ranges from fine to medium-grained. In general, the grain size is smaller than in the Rajasillannotko dyke, but both exhibit a sugar-like texture. Another difference compared to the Rajasilta dyke is the clearly internal zoning within the Purola area. Further, there is a visible quartz core and layering of the mineral masses. In figure 10D, the wall zone contains a very fine-grained layered and greenish muscovite mass, as well light small-grained red garnets and black tourmalines. Garnet appears in grain clusters in parts of the pegmatite. The intergrowth of feldspar and quartz visible to the naked eye is common and appears throughout the outcrop. The pegmatite dyke is in sharp contact with the surrounding schist, which is the host rock in the area. The contact of pegmatite and schist is trending NNE–SSW.

5.1.4 Pegmatitic leucogranites

The pegmatite dykes of Kuusela (KTPA-2022-93), Halla-ahonvuoret (KTPA-2022-94), Honkavaara (KTPA-2022-97), Kokkokallio (KTPA-2022-98), and Potoskavaara S (KTPA-2022-101) are classified as pegmatitic leucogranite type (Figure 11). The pegmatites are light gray, reddish, or grayish in color, and the mineral composition includes quartz, feldspar, plagioclase, muscovite, and in varying amounts black tourmaline, garnet, and beryl as accessory minerals. A common observation is the visible intergrowth of quartz and feldspar, that are visible to the eye in the outcrop.

The bedrock observations of the pegmatite dyke in Kuusela suggest that the pegmatite represent a typical pegmatitic leucogranite (Figure 7). The coloration is light gray, and grain size varies from small to coarse grained. Quartz, plagioclase, K-feldspar, muscovite and black tourmaline are the main visible minerals. The pegmatite dyke contains a notably large 30–40 cm beryl crystal, which is partially altered to feldspar. However, the grain size varies across zones, indicating that the pegmatite dyke could represent a zoned pegmatite.

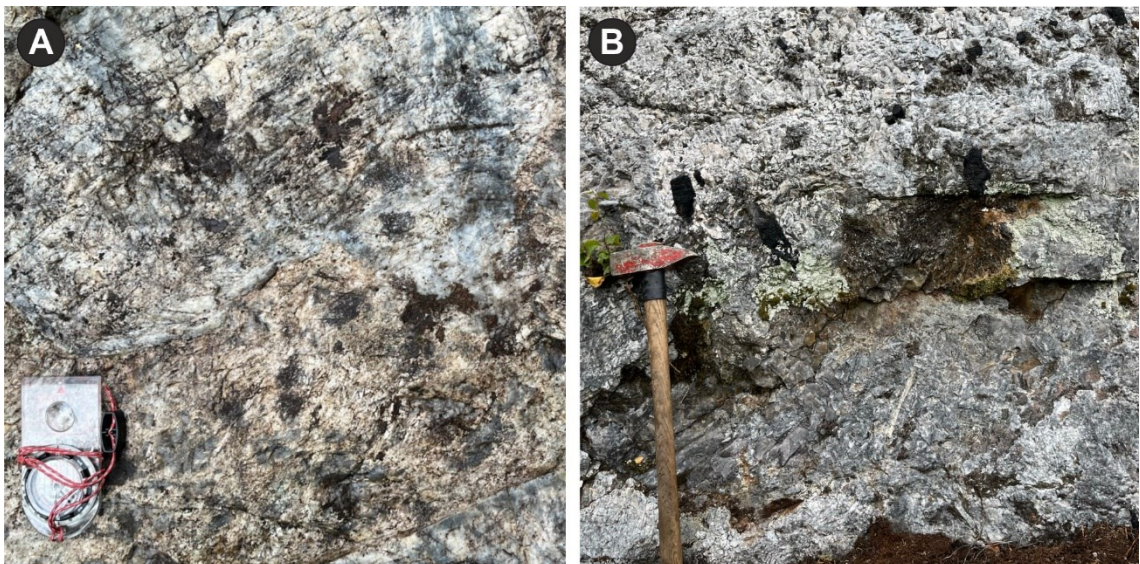


Figure 11. Typical coarse-grained pegmatitic leucogranites in the study area, Kitee-Tohmajärvi pegmatite province. A) Overview of the pegmatite leucogranite in Halla-ahonvuoret (KTPA-2022-94). The compass is 12 cm in length and pointing toward North. B) Overview of the extremely coarse-grained pegmatite leucogranite, and black tourmaline crystals from Potoskavaara S (KTPA-2022-101). The hammer is 63 cm in length.

The Halla-ahonvuoret pegmatite dyke also appears to represent a similar type of pegmatite in terms of mineralogy as the Kuusela dyke. The pegmatite from Halla-ahonvuoret ranges from light gray to reddish in color and consists of medium to very coarse-grained matrix of quartz, plagioclase, and muscovite (Figure 11A). Furthermore, it also contains black tourmaline, but in contrast to the Kuusela dyke, a clearly visible reddish almandine garnet is present as a secondary mineral. Intergrowth of potassium feldspar and quartz, showing a graphic texture, is also observed. The exposed outcrop measures 400 m x 50 m, but the whole pegmatite dyke is estimated to be at least 700 m in size. Small sections of mica schist are exposed, but the pegmatite remains the dominant rock type.

The pegmatite dyke of Potoskavaara S (Figure 11B) is multi-phase compared to the Halla-ahonvuoret and Kuusela dykes with several special compositional and textural features. Mineralogically, it shares similar features with Kuusela and Halla-ahonvuoret pegmatites, containing feldspar, quartz, muscovite, and minor amounts of black tourmaline as well as creamy-colored beryl. It differs significantly from the previous dykes in grain size, as the dykes has an extremely large grain size, and locally some minerals, like tourmaline and beryl, are extremely coarse-grained >10 cm (Figures 11B & 12D). Furthermore, the pegmatite also features megacryst pods of rose and smoky quartz. Beryl and tourmaline are also exhibited in larger quantities compared to the earlier dykes. Based on its mineral composition and bedrock observations, the pegmatite represents the more evolved pegmatitic leucogranite type than Kokkokallio or Kuusela. The pegmatite dyke exhibiting a sharp contact with the surrounding schist. In addition, the observed contact is left of the pegmatite dyke, and the dip of the contact is 70° and dip direction 110°.

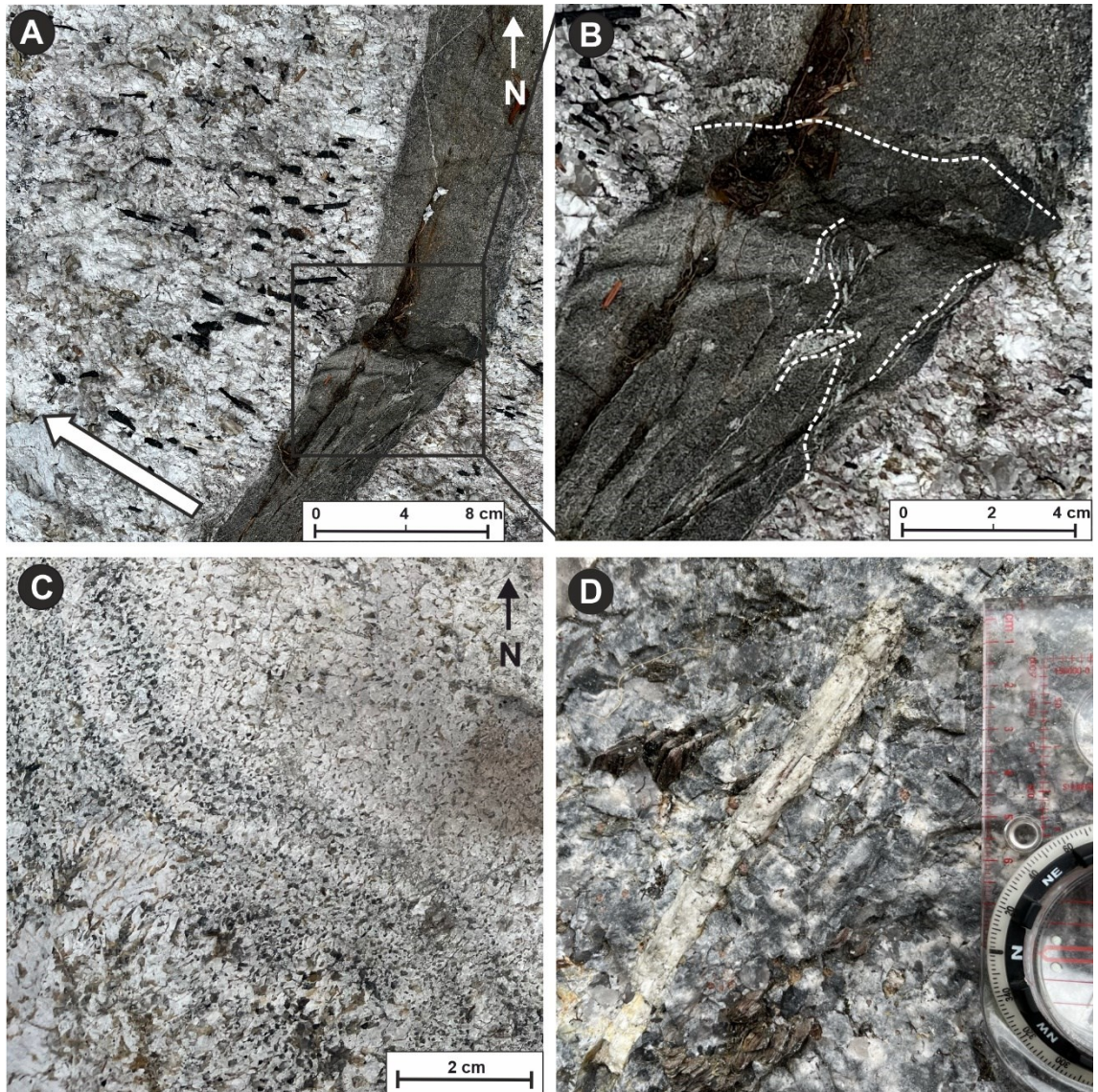


Figure 12. Outcrop pictures of the typical pegmatitic leucogranites in the Potoskavaara area, Kitee-Tohmajärvi pegmatite province. A) Internal zonation of the pegmatite dyke in Honkavaara (KTPA-2022-97). Black tourmalines are aligned perpendicular to the contact of the schist and pegmatite, and the general mineral grain size increases from the border zone (white arrow). B) A closer view of the contact of the pegmatite and schist with internal graphic texture. The layering and foliation of the schist and pegmatite melt (dashed line) are clearly visible. The schist does not extend into the border zone. C) Layering graphic intergrowth of quartz and feldspar in the pegmatite from Honkavaara (KTPA-2022-97). D) A creamy-colored and very coarse-grained beryl crystal in the pegmatite from Potoskavaara S (KTPA-2022.101).

The Kokkokallio dyke (Figure 7) appears to represent a similar type of dyke in the texture as the Kuusela and Halla-ahonvuoret. The dyke is reddish gray in color and grain size ranges from coarse to very coarse-grained. Mineralogically, the dyke is not very well-developed, containing mainly quartz, feldspar, and plagioclase. A peculiar feature, however, is the very coarse-grained megacrysts of K-feldspar and quartz, with grains reaching up to 15 cm in size. In addition, the pegmatite dyke also contains silver muscovite and black tourmaline. However, muscovite is less abundant compared to the pegmatite dykes from Halla-ahonvuoret and Honkavaara. The pegmatite dyke of Kokkokallio measures 300 m x 50 m, and the orientation of strike of the pegmatite dyke is NNW-SSE.

The Hokavaara pegmatite dyke differs from the previous dykes due to its clear internal zoning. As shown in figure 12A-B, the pegmatite is in sharp contact with the schist, which is the general surrounding rock type in the area. The strike of contact is oriented NNE-SSW. Internal zonation is observed within the pegmatite dyke, and foliation of the schist extends into the pegmatite but does not penetrate the border zone. The granitic border zone is fine-grained, and the grain size increases toward quartz, plagioclase, and tourmaline-rich wall zone. As presented in figure 12A, black tourmalines are oriented perpendicular to the pegmatite dyke, and the general foliation trend. The layering intergrowths of quartz and feldspar (Figure 12C), as well internal zonation are clearly visible in the outcrop (Figures 12A-B). In coloration, the pegmatite dyke is light gray to reddish, containing typical pegmatitic leucogranite minerals and large white plagioclase and pinkish K-feldspar crystals (Figures 12A-C). Further, the coloration of muscovite is yellowish, and the pegmatite contains Fe-rich alluaudite. The outcrop contains various phases, including granitic and pegmatitic sections.

5.2 Petrography

5.2.1 Mineralogical and textural features

The pegmatite thin sections from the Potoskavaara area show the typical primary pegmatite minerals such as quartz (20–30%), plagioclase (20–40%), K-feldspar (10–15%), muscovite (5–10%), tourmaline (5–10%), and in some samples garnet, beryl, secondary biotite, apatite, and zircon as accessory minerals (1–5%) (Figures 13 & 14). Plagioclase is observed as albite type, and K-feldspar as microcline type. Further,

plagioclase grains display characteristic polysynthetic albite twinning (Figure 13B), and in certain thin sections, flame-shaped deformation twinning is observed under cross-polarized light. Compared to that, microcline exhibits typical cross-hatched twinning, and quartz shows undulatory extinction (Figure 16). Rarer Li-silicates, such as spodumene and lepidolite are not visible in the thin sections, or they could not be identified with certainty. Overall, the grain size of the minerals varies from fine <1 mm to extremely coarse grain <5 cm in size. However, most of the samples exhibit a phaneritic, and occasional porphyritic texture. The most common minerals are quartz, K-feldspar, plagioclase, and occasionally muscovite, and tourmaline in some thin sections. The crystal form of the mineral grains varies from euhedral to anhedral, and they represent mostly a so-called hypidiomorphic texture, meaning they consist mainly of subhedral outlines. In particular muscovite, tourmaline and garnets appear as partially euhedral grains with regular crystal surfaces.

The most muscovite-rich pegmatite samples are the more evolved dykes from Selkäpäivänrinne, Riienvaara, the potassic pegmatite dykes, sodic aplite dyke of Rajasillannotko as well the pegmatitic leucogranite dyke from Halla-ahonvuoret. The grain size is predominantly coarse, with the exception of variations ranging from fine to coarse in size from Rajasillannotko. Instead, the pegmatites which contain both muscovite and tourmaline minerals are the pegmatitic leucogranite dykes from Kuusela, Honkavaara, Potoskavaara S, and the sodic aplite dyke from Purola. Generally, the grain size is coarse in these samples. The extremely coarse-grained pegmatitic leucogranite sample from Kokkokallio does not directly contain either tourmaline or muscovite. However, it does contain some mica sericitization and fine-grained recrystallization of quartz (Figure 16A). Both feldspar minerals, K-feldspar and plagioclase, are present generally in all thin sections, except for the potassic pegmatite samples from Lamminmaa (Figure 15), and Palomäki (Figure 16B), and pegmatitic leucogranite dyke from Kokkokallio, where only K-feldspar was observed, with no evidence of plagioclase present.

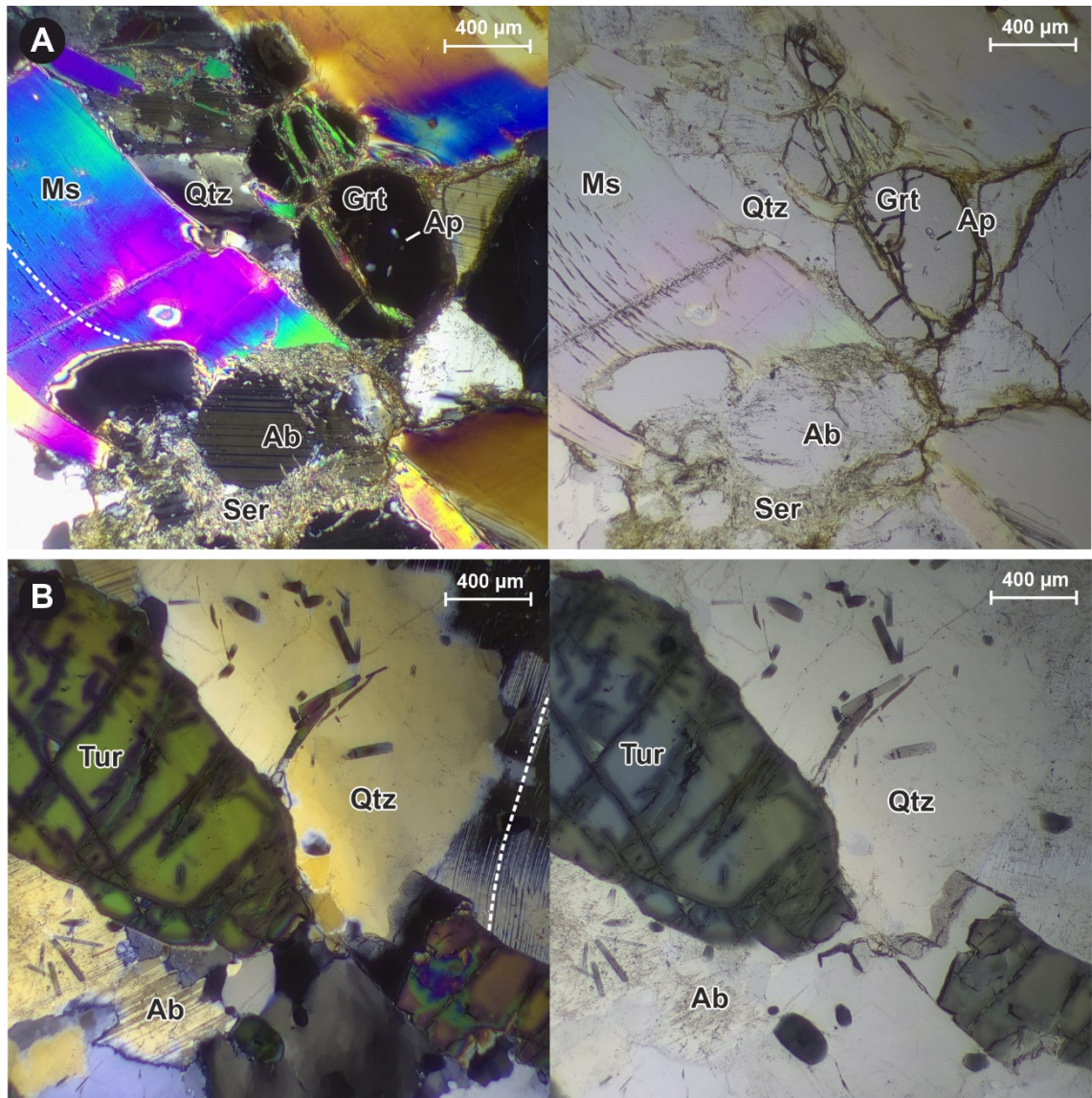


Figure 13. Cross polarized light (left), and plane polarized (right) images of the thin sections from the pegmatite dykes in Potoskavaara area, Kitee-Tohmajärvi pegmatite province. A) Muscovite (Ms), quartz (Qtz), garnet (Grt), albite plagioclase (Ab), and apatite inclusions in garnet (Ap) are present in Halla-ahonvuoret (KTPA-2022-94). Deformation bending (white dashed line) of muscovite, and mineral sericitization (Ser) are clearly visible. B) Coarse-grained euhedral tourmaline (Tur), quartz (Qtz), and albite plagioclase (Ab) are observed in Purola (KTPA-2022-104). Kink bands and deformation twinning in plagioclase are visible (white dashed line).

Accessory minerals are present in varying amounts in the pegmatite thin sections. Garnet (Figure 13A) is found in the thin sections from the varying degrees within each pegmatite type, except for the potassic pegmatites. These dykes are Halla-ahonvuoret, Purola, Riienvaara, and Honkavaara pegmatite dykes. Apatite has been observed in the thin sections from the pegmatitic leucogranite dyke of Halla-ahonvuoret, and in more evolved Selkäpäivänrinne, and Riienvaara pegmatite dykes. In the pegmatite samples from Halla-

ahonvuoret and Riienvaara, apatite often appears alongside garnet grains. In the thin section from the Halla-ahonvuoret pegmatite, zircon may present, frequently identified as inclusions in muscovite grains (Figure 14B). In addition, the unique feature of the pegmatite thin section from more evolved Riienvaara dyke is an extremely coarse-grained beryl crystal (Figure 14A).

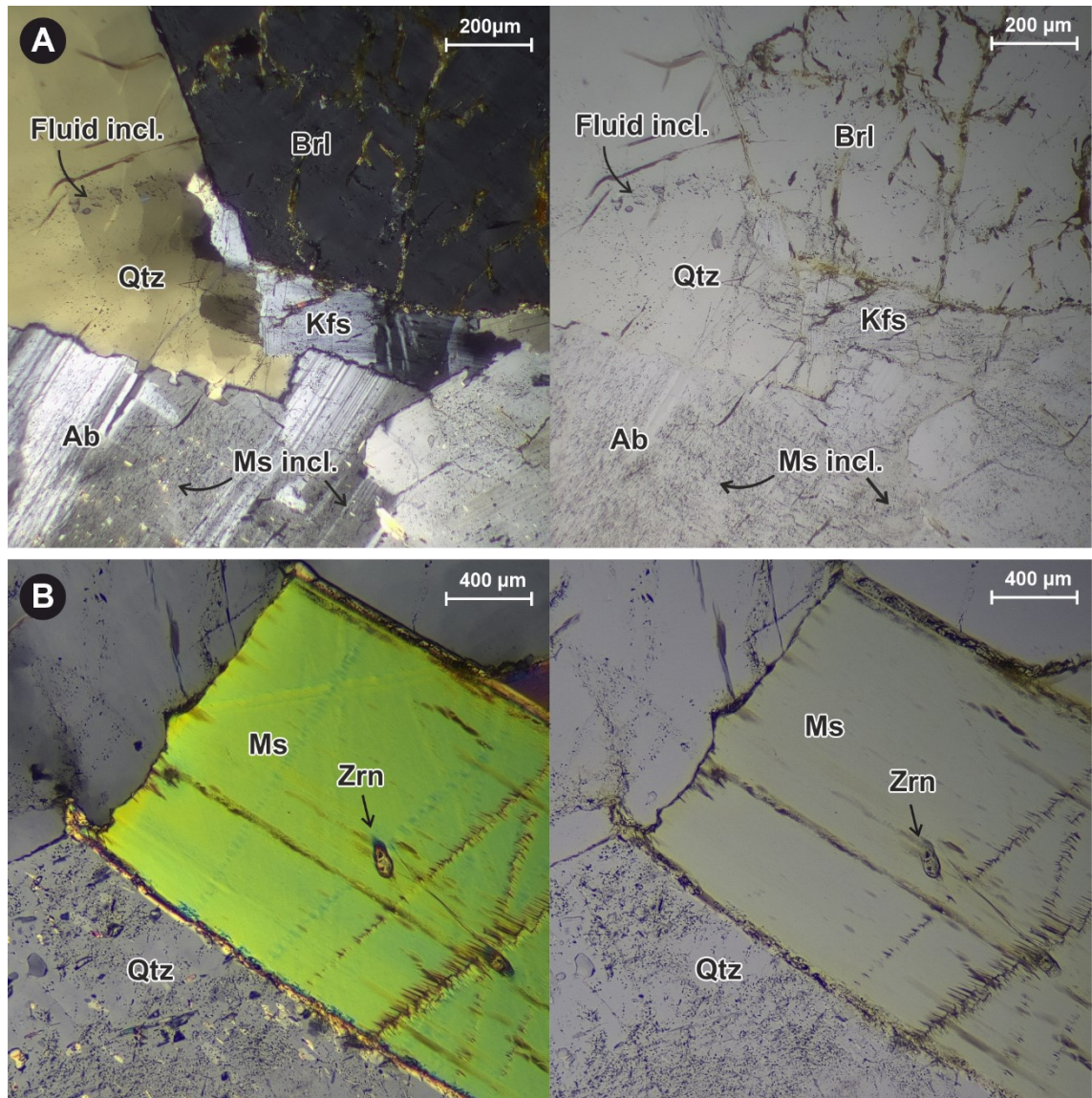


Figure 14. Cross polarized light (left) and plane polarized (right) images of the thin sections from the pegmatite dykes in Potoskavaara area, Kitee-Tohmajärvi pegmatite province. A) Fluid inclusions in quartz and muscovite inclusions in albite plagioclase (Ab), beryl (Brl), and K-feldspar (Kfs) in Riienvaara (KTPA-2022-96). B) Inclusions in mineral grains. Zircon (Zrn) inclusion in a coarse-grained muscovite grain (Ms), and multiple smaller muscovite inclusions in a coarse-grained quartz (Qtz) grain in Halla-ahonvuoret (KTPA-2022-94).

5.2.2 Deformation and metamorphic features

The pegmatite samples in the Potoskavaara area exhibit signs of mineral alteration, recrystallization, and both brittle and ductile deformation in the thin sections. Brittle deformation appears as brittle fractures of the minerals, while ductile deformation can be seen as elongation and recrystallization of the minerals. Generally, mineral grains are characterized by typical mineral cleavage or brittle fracturing. In figure 13, the thin sections of the pegmatites exhibit plastic deformation of mineral grains such as bending and kinking in muscovites and feldspars, and deformation lamellae in quartz. In the thin section from the Lamminmaa potassic pegmatite dyke, the large en echelon shearing with dextral kinematic cuts through the entire thin section (Figure 15A). In addition, a small sinistral shear zone is observed in thin section from the pegmatitic leucogranite Potoskavaara S dyke. As shown in figure 15B, small-grained muscovite grains have deformed along shearing, and very coarse-grained muscovite and feldspar grains are oriented perpendicular to the shearing.

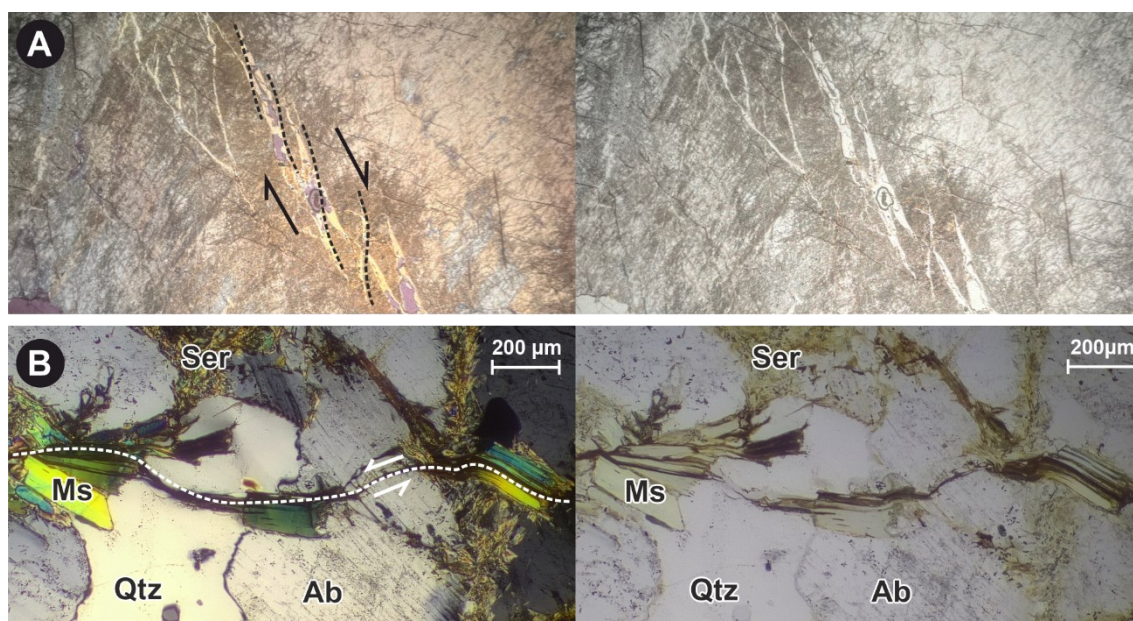


Figure 15. Cross polarized light (left) and plane polarized (right) images of the thin sections from the deformed pegmatites in Potoskavaara area, Kitee-Tohmajärvi pegmatite province. A) The dextral en echelon structure in Lamminmaa (KTPA-2022-99). The model is not presented in scale. B) Ductile shearing with sinistral kinematic and deformed muscovite grains along it (white dashed line), sericitization (Ser) the boundaries of the mineral grains, quartz (Qtz), and albite plagioclase (Kfs) in Potoskavaara S (KTPA-2022-101).

Metamorphic events caused deformed poikiloblastic texture in the minerals from the Potoskavaara area. Particularly the pegmatite samples from Selkäpäivänrinne, Riienvaara, and Rajasillannotko, which are otherwise altered, have a significant number of mineral inclusions. Fine-grained muscovite grains appear as inclusions within larger grains, particularly plagioclase, quartz, and garnet, exhibited commonly in the pegmatite dyke thin sections (Figure 14A). In addition, quartz crystals often contain fluid inclusions (Figure 14A). Fluid inclusions are small pockets of liquid, gas, or solid phases that formed under hydrothermal conditions and provide information about the genesis of pegmatites (London 2008).

In the K-feldspar-rich thin sections, microperthite lamellar texture is common. It is a production of the mixing of K-rich alkali feldspar and Na-rich sodic plagioclase (London 2008). Large perthite textures were observed in the thin sections from the Kokkokallio (Figure 16A), Potoskavaara S, and Palomäki pegmatites. However, as shown in figure 16A, the thin section from the Kokkokallio pegmatite dyke is not the most representative, and the thin section mainly contains perthitic texture and recrystallized quartz. Recrystallization is influenced by regional metamorphism and deformation events. Generally, thin sections contain mosaic-like recrystallization of quartz and mineral sericitization in feldspar (Figure 16). In addition to the Kokkokallio pegmatite, recrystallization of quartz was observed in many other pegmatites which is observed in the thin sections from the Honkavaara, Halla-ahonvuoret, Palomäki, Rajasillannotko, and Purola pegmatites. In sericitization, minerals such as feldspar usually transform into a fine-grained mass of mica during hydrothermal alteration (London 2008). These are mainly found around fractures and boundaries of the different mineral grains (Figures 13A, 15C & 16B). The alteration has often progressed most intensely in the central parts of the original grain. Sericitization is especially common in the many pegmatite samples and extensively in various pegmatite types, with the most notable presence observed in the Halla-ahonvuoret, Palomäki, Rajasillannotko, Honkavaara, Selkäpäivänrinne, and Purola thin sections. Moreover, the potassic pegmatite thin section from Palomäki shows extremely coarse-grained graphic texture.

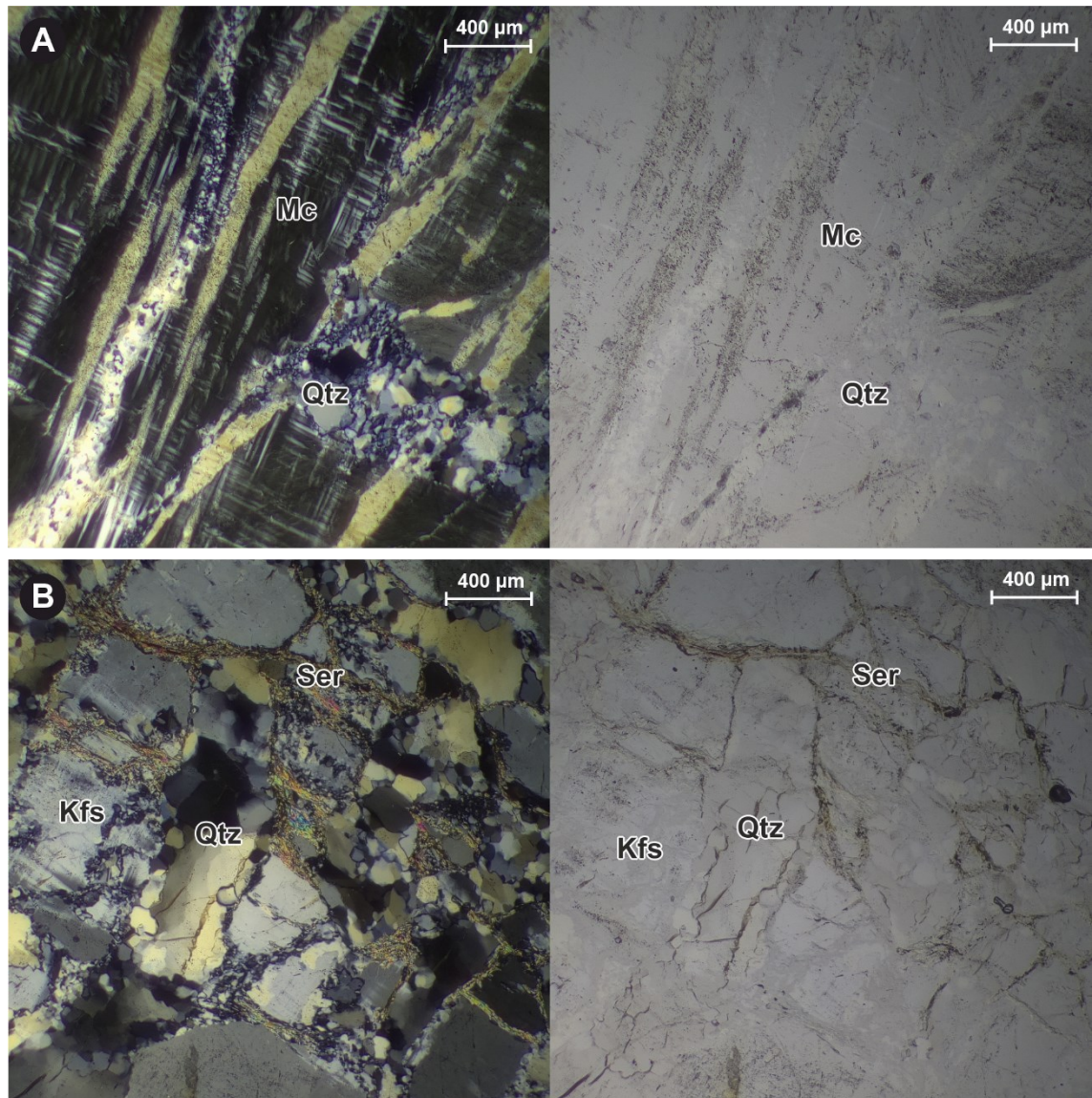


Figure 16. Cross polarized light (left) and plane polarized (right) images of the thin sections from the pegmatite dykes in Potoskavaara area, Kitee-Tohmajärvi pegmatite province. A) Perthite texture of feldspar, cross-hatched twinning in microcline (Ms) feldspar, and small-grained recrystallization of quartz (Qtz) in Kokkokallio (KTPA-2022-98). B) Sericite alteration (Ser) in the boundaries of the mineral grains, granoblastic recrystallization of undulating quartz (Qtz), and K-feldspar (Kfs) in Palomäki (KTPA-2022-102).

5.3 Geochemical analyses

5.3.1 Major elements

All the Kitee-Tohmajärvi pegmatites from the study area exhibit varying amounts of SiO_2 contents between 64.0–79.3 wt% (Figure 17A). In the Middlemost (1994) alkali $\text{Na}_2\text{O}+\text{K}_2\text{O}$ vs silica SiO_2 (TAS) -diagram, pegmatite samples plotted expectedly mainly in a granite field. However, two RE-enriched pegmatites and one pegmatitic leucogranite sample plotted in the quartz monzonite field. A common characteristic among them is a lower SiO_2 content compared to the other pegmatites. As shown in TAS-diagram in figure 17B, an exceptionally high $\text{Na}_2\text{O}+\text{K}_2\text{O}$ content is found from the Kokkokallio dyke, whereas in the sample from Surmasuo (*KTPA-2022-95.1*) has very low Na_2O and K_2O concentrations, as a result, it plotted in the granodiorite field.

The $\text{CaO}-\text{Na}_2\text{O}-\text{K}_2\text{O}$ ternary diagram is used to determine which alkali or alkali earth elements are dominant in the pegmatite samples (Selway *et al.* 2005). The diagram in figure 17B shows a clear decrease in CaO content in all the pegmatite dykes along with the expected variability in Na_2O and K_2O concentrations. The RE-enriched pegmatites are close to the Na_2O peak indicating a Na-rich fluid composition (Selway *et al.* 2005). The diagram reveals that the pegmatitic leucogranites show the greatest variability in Na_2O and K_2O contents and indicates variability in the fractionation degrees. In comparison, the potassic pegmatite and sodic aplite pegmatite dykes exhibit less variability in concentrations and plot approximately in the central part of the diagram.

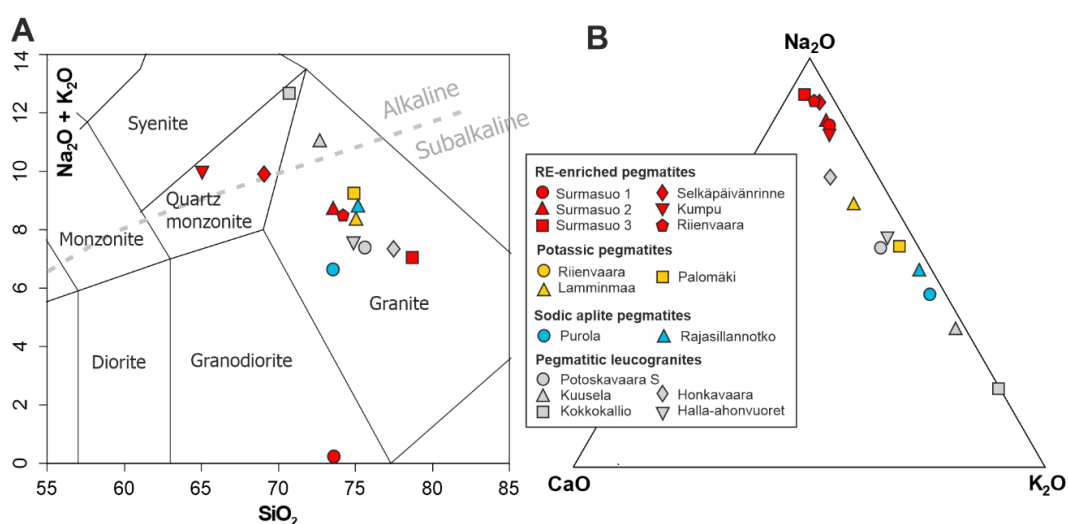


Figure 17. A) Binary Total alkali versus SiO_2 diagram (Middlemost 1994) and B) Ternary $\text{CaO}-\text{Na}_2\text{O}-\text{K}_2\text{O}$ diagram for pegmatites from Potoskavaara area, Kitee-Tohmajärvi pegmatite province.

The most applied diagrams for classifying granitic rocks are the comparison of aluminosity and alkalinity compositions, the contrast between ferroan versus magnesian contents, and alkali-lime index of granitic rocks (Frost *et al.* 2001). A more recent classification of granites, based on the $\text{FeO}_{\text{tot}} / (\text{FeO}_{\text{tot}} + \text{MgO})$ versus SiO_2 diagram (Figure 18A) classifies pegmatites into magnesian ($\text{Fe}^* < 0.8$) and ferroan ($\text{Fe}^* > 0.8$) types, based on the balance of Fe and Mg (or Fe^*) content (Frost *et al.* 2001). Most of the pegmatite samples plot with the ferroan class, however the Mg-rich pegmatites from Potoskavaara S and Kumpu plotted in the magnesian type.

The granite tectonic discrimination of alkalinity A/NK (molar ratio of $\text{Al}_2\text{O}_3 / (\text{Na}_2\text{O} + \text{K}_2\text{O})$) and aluminosity A/CNK (molar ratio of $\text{Al}_2\text{O}_3 / (\text{CaO} + \text{Na}_2\text{O} + \text{K}_2\text{O})$) plot of Shand (1943) discriminate pegmatites in their peraluminous, metaluminous, and peralkaline characteristics. In the diagram in figure 18C, all the pegmatite samples from the study area are clearly plotted into strongly peraluminous S-type granites ($\text{A/CNK} > 1.2$) (Chappel & White 2001). One of the Surmasuo samples (*KTPA-2022-95.1*) plotted in the extreme high A/NK vs. A/CNK value over 60 wt%, therefore having an extremely high Al content compared to Na and K.

The tectonic discrimination $\text{Na}_2\text{O} + \text{K}_2\text{O} - \text{CaO}$ versus SiO_2 diagram by Frost *et al.* (2001) shows feldspar contents in the pegmatites relating to the magma source. The different varieties of the results are recognized in figure 18B, nevertheless the pegmatites represent mainly the alkali-calcic (index > 61 wt%) or calcic-alkalic rocks (index between 51 and 56 wt%) (Frost *et al.* 2001). The pegmatites from the RE-enriched pegmatites of Kumpu and Selkämäivänrinne, and the leucogranite pegmatites of Kuusela and Honkavaara plotted in the alkalic field. The pegmatite samples from Surmasuo (*KTPA-2022-95.1*, *KTPA-2022-95.3*) are in the calcic field and it is notable that the Surmasuo pegmatite (*KTPA-2022-95.1*) has a value closest to zero of $\text{Na}_2\text{O} + \text{K}_2\text{O} - \text{CaO}$ content. The pegmatite sample from Honkavaara plotted at the boundary of the calc-alkali and calcic series.

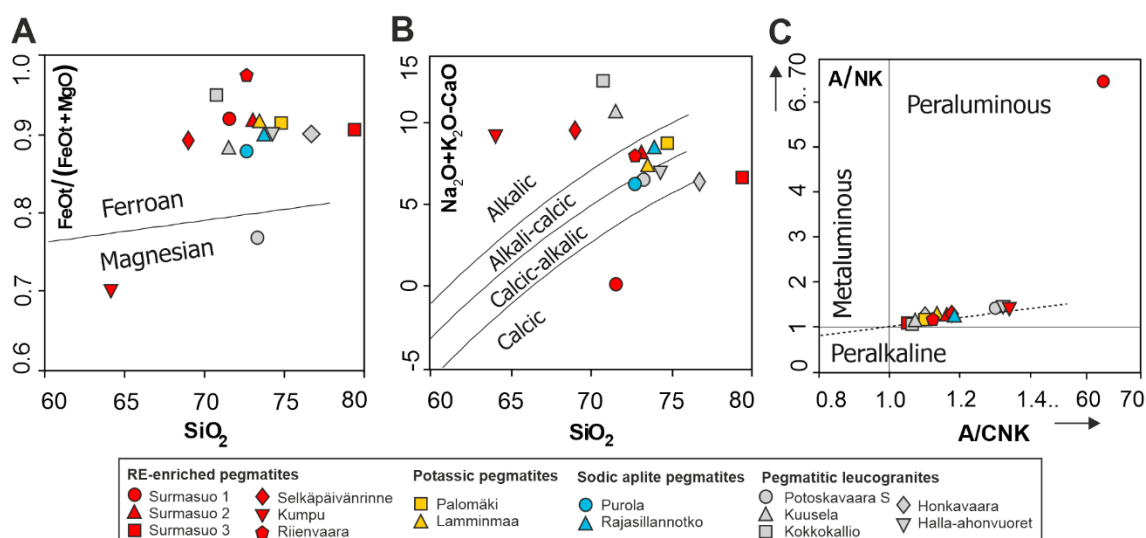


Figure 18. The granite tectonic discrimination diagrams for pegmatites from Potoskavaara, Kitee-Tohmajärvi pegmatite province. A) A/NK (molar $Al_2O_3/(Na_2O+K_2O)$) versus A/CNK (molar $Al_2O_3/(CaO+Na_2O+K_2O)$) diagram (Shand 1943). B) Na_2O+K_2O-CaO diagram (Frost et al. 2001). C) $FeO_{tot}/(FeO_{tot}+MgO)$ versus SiO_2 diagram (Frost et al. 2001).

In the classification of the pegmatite dykes the variation in elements of the concentrations of Al_2O_3 , CaO , K_2O , Na_2O , and P_2O_3 plays a key role (eg. Černý 1991a,b). The geochemical binary diagram of the major elements versus SiO_2 content shows a clear difference in the concentrations (Figure 19). The pegmatites mainly have high Al_2O_3 content which shows a negative correlation with increasing SiO_2 content (Figure 19A). In general, the Al_2O_3 contents in the pegmatites vary greatly, and the highest contents of Al_2O_3 (>19 wt%) are found in the RE-enriched pegmatites. However, in the samples from Surmasuo, the contents vary significantly (13.0–24.6 wt%). The average Al_2O_3 content of all the samples is 15.5 wt% in the area (Table 2). Compared to the high Al_2O_3 contents, the CaO contents are low in all the samples and mainly vary between 0.25–0.40 wt% (Figure 19B). The RE-enriched and sodic aplite pegmatites generally show relatively similar CaO contents, whereas the pegmatitic leucogranites and potassic pegmatites exhibit more variability. Remarkably low CaO contents are found in the RE-enriched pegmatite of Surmasuo (KTPA-2022-95.1) (0.01 wt%) and the leucogranite pegmatite of Kokkokallio (0.04 wt%).

There is considerable variability in the K_2O contents of the pegmatite types, but in general ranges between 1.5 to 4.2 wt% (Figure 19E; Table 2). The lowest contents are found in the RE-enriched pegmatites where the K_2O contents are very low (<1 wt%). Further, an especially low K_2O content (0.03 wt%) is found in the highly RE-enriched Surmasuo

sample (*KTPA-2022-95.1*). The sodic aplite and potassic pegmatites show roughly similar values, but the pegmatitic leucogranites exhibit more variability in contents. The highest contents (>7 wt%) are found in the leucogranite pegmatites from Kokkokallio and Kuusela. The Surmasuo sample (*KTPA-2022-95.1*) distinguishes itself from the other pegmatites, for its remarkably low CaO, K₂O, Na₂O, MgO, and P₂O₅ contents. The Na₂O contents show an inverse trend, and in contrast to K₂O contents, the pegmatites from the RE-pegmatite types have high Na₂O contents (>6 wt%) (Figure 19D). In the other pegmatite samples, the Na₂O content mainly varies 2.87–5.76 wt% with increasing SiO₂ content, and the pegmatite samples plot very close to their respective types. The diagram shows a low Na₂O content (0.21 wt%) in the Surmasuo sample (*KTP2022-95.1*).

The MgO values are almost invariably low and vary between 0.01–0.08 wt% (Figure 19C). However, the highest MgO >10 wt% contents are found in the pegmatitic leucogranite dykes from Potoskavaara S and Halla-ahonvuoret and the notably high MgO value (0.32 wt%) is in the RE-enriched pegmatite sample from Kumpu. In addition, all the samples have invariably very low TiO₂ concentrations (Figure 19F), which is typical for highly fractionated pegmatites (Selway *et al.* 2005). Additionally, the Surmasuo sample (*KTPA-2022-95.1*) have TiO₂ <0.01 wt% below the specified detection limit value (Appendix 2).

In the pegmatitic leucogranites from Honkavaara (0.05 wt%), and Potoskavaara S (0.09 wt%) have low P₂O₅ contents, while in the other samples it is high and varies between 0.1–0.24 wt% (Figure 19G). The highest contents (>0.35 wt%) are found in the RE-enriched pegmatites. In general, the concentrations of Fe₂O₃ and MnO are very low in the pegmatites. The Fe₂O₃ content varies from 0.24 to 0.84 wt%. However, the Fe₂O₃ concentration of Halla-ahonvuoret is high at 1.36 wt% (Figure 19H). The MnO content in the samples is generally around 0.01 wt%, which is the MnO specified limit value (Figure 19I). MnO concentrations greater than 0.01 wt% are found in RE-pegmatites, with the highest MnO concentration of 0.35 wt% is observed in Halla-ahonvuoret. Additionally, the pegmatite samples from Kokkokallio and Lamminmaa have MnO contents below the limit value of 0.01 wt%.

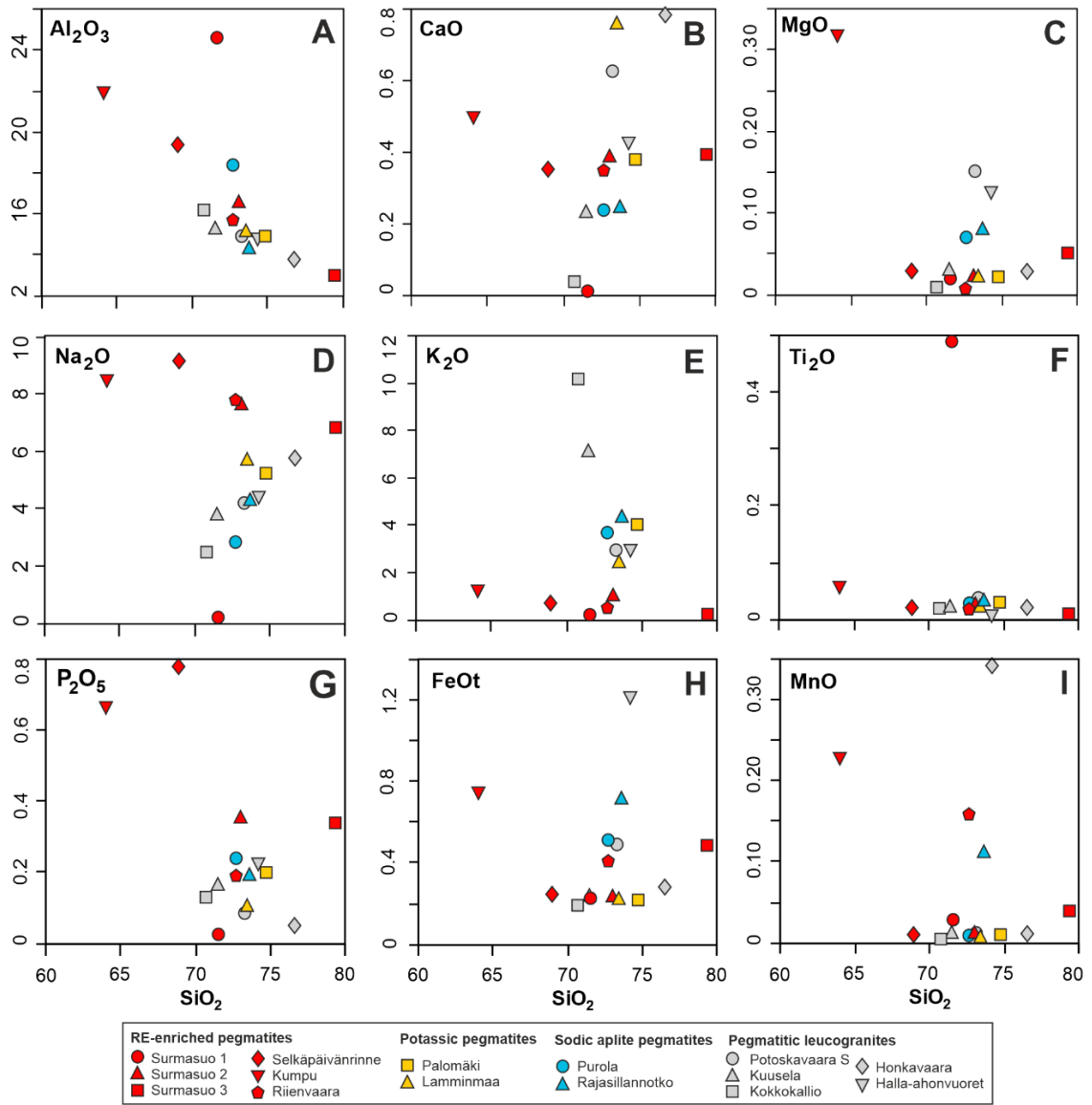


Figure 19. Geochemical binary diagram of major elements versus SiO₂ content (wt%) of pegmatites from Potoskavaara, Kitee-Tohmajärvi pegmatite province. A) Al₂O₃ versus SiO₂. B) CaO versus SiO₂. C) MgO versus SiO₂. D) Na₂O versus SiO₂. E) K₂O versus SiO₂. F) Ti₂O versus SiO₂. G) P₂O₅ versus SiO₂. H) FeOt versus SiO₂. I) MnO versus SiO₂.

5.3.2 Trace elements

Whole rock analyses of the selected trace elements Ba, Be, Cs, Ga, Li, Nb, Rb, Sn, and Ta reflect the degree of fertility of the pegmatites (Table 2) (Selway *et al.* 2005). As seen in table 2, the pegmatites are variably enriched in these elements, and there is also variability within the same pegmatite classes.

A significant variation in the concentrations of Li, Cs, and Ta can be observed in the samples, where highest values are in the RE-enriched pegmatites (Table 2). The Li >200 ppm are found in RE-pegmatites, and a particularly high Li content, above the detection limit value Li >25 000 ppm is found from Surmasuo (*KTPA-2022-95.1*). In other pegmatites Li content range mainly between 19–64 ppm, and the lowest contents are in the pegmatitic leucogranite dykes. The Cs concentrations show elevated values in all the pegmatite samples (>3.7 ppm), with the highest contents are found in the RE-enriched pegmatites. The potassic pegmatites of Lamminmaa and Palomäki show variability in the concentrations, while other types have relatively consistent Cs contents. The lower contents (<5 ppm) exhibited in the pegmatitic leucogranites of Honkavaara, Potoskavaara S, and RE-pegmatite of Riienvaara. In addition, Ta contents are mainly <1 ppm in all the pegmatite samples, but elevated Ta >6.64 ppm are found in the RE-pegmatites and Purola.

All pegmatites show elevated Rb contents with varying concentrations, and the RE-enriched pegmatites do not show significantly higher Rb content compared to other samples (Table 2). The Rb content varies mainly between 104–411 ppm in the samples. Low Rb contents are found in the RE-enriched pegmatite samples from Surmasuo (14.6 ppm and 20.0 ppm). Further, samples with Rb >100 ppm are found from Riienvaara (64.2 ppm) and Honkavaara (68.2 ppm). The Sn concentrations are also elevated (mainly <5.5 ppm) and variable, with the highest concentrations mainly found in the RE-enriched pegmatites (Table 2). The significantly high Sn contents are found in the samples from Selkäpäivänrinne (1 320 ppm) and Surmasuo (459 ppm), while the pegmatitic leucogranite types are mostly poorer in Sn. In comparison, the pegmatite samples do not show significant enrichment in Nb, and the contents varies mainly between 1.0 and 4.3 wt% in the pegmatites. Otherwise, the highest Nb >9 ppm content is present in the RE-pegmatites of Kumpu and Selkäpäivänrinne, as well in the pegmatitic leucogranite dyke from Halla-ahonvuoret and sodic aplite dyke from Purola. The Nb concentration is below the reference value of 0.8 ppm in the pegmatitic leucogranite sample from Kokkokallio.

Ba contents generally range between 11–42 ppm in the pegmatite samples (Table 2). The highest values >60 ppm are found in the pegmatitic leucogranites, whereas the lowest (<10 ppm) in the RE-pegmatites of Surmasuo and Riienvaara, and the pegmatitic leucogranite of Honkavaara sample. Furthermore, the Be concentrations vary

significantly regardless of the pegmatite type, but mainly the samples show elevated enrichment (>3 ppm). The Be concentrations varies mainly between 10 ppm and 23.7 ppm in the samples, of which the lowest contents (<3ppm) are found in the pegmatitic leucogranites from Kokkokallio and Kuusela, and in the RE-enriched sample from Surmasuo. Compared to this, a relatively high Be content >100 ppm is found at the RE-pegmatites and elevated values are also found at the sodic aplite pegmatite from Purola (60.9 ppm).

Table 2. Selected trace elements (ppm) whole-rock geochemical analyses of the pegmatite dykes from the Potoskavaara area, Kitee-Tohmajärvi pegmatite province. The average ratio of the samples is denoted by the "avg".

	1	2	3	4	5	6	7	8
Ba	37	23	42	7	4	8	5	7
Be	380	3.3	10	2.4	23.7	9	133	7.8
Cs	155.5	6.1	11	25	24.3	6.7	5.1	4
Ga	40.7	8.5	23.9	27.2	21	13.6	17	9.6
Li	440	52	45	>*	270	64	19	38
Nb	160	1	15.6	4.3	9.5	2.9	12.8	1.4
Rb	411	302	210	14.6	168	20	64.2	68.2
Sn	46	5	18	459	18	3	10	3
Ta	21.2	0.28	3.22	8.1	6.6	1.0	10.7	0.2
U	166.5	7	7.9	0.5	6.5	2	1.4	10.6

1. Kumpu (KTPA-2022.92.1) 2. Kuusela (KTPA-2022.93.1) 3. Halla-ahonvuoret (KTPA-2022-94.1)
4. Surmasuo (KTPA-2022.95.1) 5. Surmasuo (KTPA-2022.95.2) 6. Surmasuo (KTPA-2022-95.3)
7. Riienvaara (KTPA-2022.96.1) 8. Honkavaara (KTPA-2022.97.1)

	9	10	11	12	13	14	15	avg.
Ba	120	15	33	11	16	69	15	15
Be	1.1	8.5	4.6	5.8	12.5	60.9	5.2	8.5
Cs	11.2	8.6	4.1	21.4	50.2	7.3	9	9
Ga	7.8	12.6	13.6	15.1	19.5	25.4	10	15.1
Li	46	16	58	6	660	58	19	52
Nb	<0.8	4.1	4.2	3.1	59.7	22.8	3.2	4.2
Rb	365	104	103	222	166.5	303	197.5	168
Sn	4	8	6	15	1320	33	8	10
Ta	0.2	1.2	0.5	0.7	141	12.4	0.4	1.26
U	3.5	3.7	2	5.8	3.5	2.5	18.9	3.7

9. Kokkokallio (KTPA-2022.98.1) 10. Lamminmaa (KTPA-2022.99.1) 11. Potoskavaara (KTPA2022-101.1)
12. Palomäki (KTPA-2022.102.1) 13. Selkäpäivänrinne (KTPA-2022-103.1) 14. Purola (KTPA-2022-104.1)
15. Rajasillannotko (KTPA-2022-105.1)

The Primitive Mantle normalized spider plot in figure 20 shows a clear continuous trendline in peg (Sun & McDonough 1989). The pegmatites show positive enrichment in Cs, K, Pb, Rb, and U. Conversely, the diagram shows negative anomalies and depletion of Ba, Nb, Sr, Zr, and Ti. The most complex RE-pegmatites show a steeper normalized pattern compared to the other pegmatite types. The pegmatites from Potoskavaara S, Purola, Rajasillanotko, Kumpu, Halla-ahonvuoret, and Surmasuo (*KTPA-2022-95.3*) are the only samples that are above the detection limit of Ti. At Kumpu, an exceptionally high U concentration (166.5 ppm) is detected (Table 2). Furthermore, the chondrite-normalized REE-diagram shows uncertainties in the results as many of the elements are below the detection limit value, and therefore it's not been presented in these results.

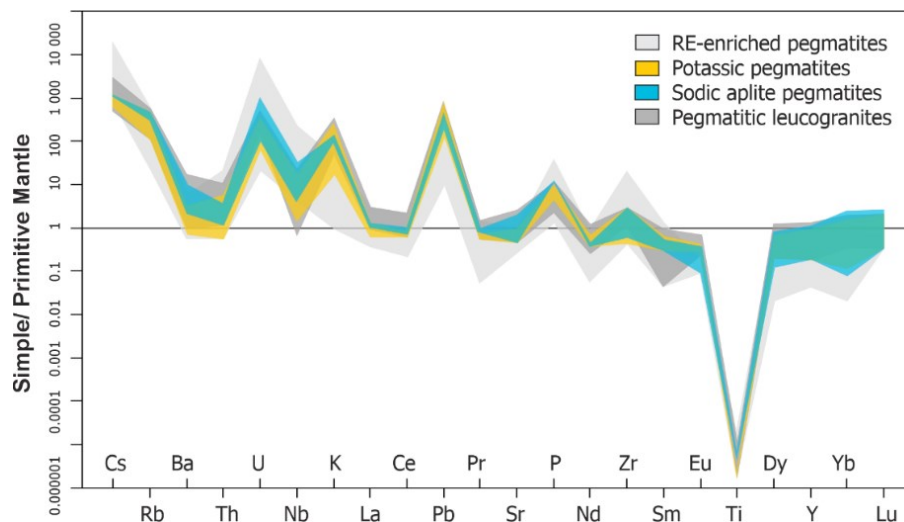


Figure 20. Primitive Mantle-normalized multi-element spider diagram (Sun & McDonough 1989). The pegmatite samples with Ti values below the detection limit of 0.005 wt%, have their Ti values represented as half of the detection limit value.

5.3.3 Fractionation indicators

The pegmatitic melts represent the final products of magmatic differentiation, where previously incompatible lithophile elements begin to exhibit differing behaviors (Černý *et al.* 1985). The differentiation of pegmatites is typically compared using a diagram with the absolute concentration of the REE of interest on the X-axis and an indicator of the degree of differentiation associated with the same element on the Y-axis. The Mg/Li, K/Cs, K/Rb, K/Ba, Nb/Ta, Sr/Rb, Fe/Mn, and Al/Ga ratios are good indicators for the degree of fractionation of pegmatites (Figure 21; Table 3; Černý *et al.* 1985).

Table 3. Geochemical fractionation indicators of the pegmatite dykes from the Potoskavaara area, Kitee-Tohmajärvi pegmatite province. The average ratio of the samples is denoted by the “avg”.

	1	2	3	4	5	6	7	8
A/CNK	2.11	1.38	1.87	4.36	1.83	1.73	1.81	1.71
Mg/Li	3.63	1.92	13.33	0.004	0.18	3.12	2.63	2.63
K/Cs	68.16	8 9409.83	2 172.72	10	337.44	358.20	882.35	3 225
K/Rb	25.79	190.06	113.80	17.12	48.80	120	70.09	189.14
K/Ba	286.48	2 495.65	569.04	35.71	1 025	600	900	1 842.85
Nb/Ta	7.54	3.56	4.84	0.52	1.43	2.84	1.19	5
Sr/Rb	0.048	0.066	0.095	0.68	0.11	0.5	0.15	0.29
Ba/Rb	0.09	0.07	0.07	0.2	0.47	0.2	0.47	0.2
Fe/Mn	3.21	36.66	3.41	7	24	14.33	2.71	33.75
Al/Ga	2847.53	9 525.6	3 299.19	4 786.14	4 183.2	5 058.52	4 902.88	7 607.25
Zr/Hf	11.05	2.9	3	0.5	1.5	3.2	2.3	1.2

1. Kumpu (KTPA-2022.92.1) 2. Kuusela (KTPA-2022.93.1) 3. Halla-ahonvuoret (KTPA-2022-94.1)
 4. Surmasuo (KTPA-2022.95.1) 5. Surmasuo (KTPA-2022.95.2) 6. Surmasuo (KTPA-2022-95.3)
 7. Riienvaara (KTPA-2022.96.1) 8. Honkavaara (KTPA-2022.97.1)

	9	10	11	12	13	14	15	avg.
A/CNK	1.27	1.70	1.90	1.55	1.89	2.70	1.62	1.81
Mg/Li	1.08	6.25	13.79	16.66	0.30	5.17	21.05	3.12
K/Cs	7 607.14	2 406.97	6 219.51	1 565.42	113.54	4 000	3 944.44	2 172.72
K/Rb	233.42	199.03	247.57	150.90	34.23	96.36	179.74	120
K/Ba	710	1 380	772.72	3 045.45	356.25	423.18	2 366.66	772.72
Nb/Ta	1.48	3.25	7.11	3.92	0.42	1.83	6.53	3.25
Sr/Rb	0.10	0.19	0.48	0.04	0.06	0.13	0.05	0.11
Ba/Rb	0.32	0.14	0.32	0.04	0.9	0.22	0.07	0.10
Fe/Mn	63.33	57.5	64.28	30	22	40.90	6.42	24
Al/Ga	10 991.08	6 363	5 817.30	5 239.43	5 278.43	3 843.99	7 567.56	5 239.43
Zr/Hf	1.3	0.5	22	1.1	0.9	0.7	2.9	1.5

9. Kokkokallio (KTPA-2022.98.1) 10. Lamminmaa (KTPA-2022.99.1) 11. Potoskavaara (KTPA2022-101.1)
 12. Palomäki (KTPA-2022.102.1) 13. Selkäpäivänrinne (KTPA-2022-103.1) 14. Purola (KTPA-2022-104.1)
 15. Rajasillannotko (KTPA-2022-105.1)

The Mg/Li ratio is one of the best fractionation indicators for LCT pegmatites (Selway *et al.* 2005). As data show in the Mg/Li binary diagram (Figure 21A), the Mg/Li ratio of the study samples clearly varies, mainly between 1.9–5.2. The RE-enriched pegmatites show the highest Li enrichment with generally low Mg/Li ratio. In other pegmatite types, there is significant variability. However, the Mg/Li ratio >10 is found from the leucogranite pegmatites of Halla-ahonvuoret (13.3) and Potoskavaara S (13.7), and potassic pegmatite from Palomäki (16.6), while the highest Mg/Li ratio is from the sodic aplite Rajasillannotko pegmatite (21). The RE-pegmatite samples of Surmasuo (KTPA-2022-95.1, KTPA-2022-95.2) and Selkäpäivänrinne have a very low Mg/Li <1.0 ratio.

According to Selway *et al.* (2005), a very low ratio of K/Rb indicates potential of increased LCT-concentrations. The highly fractionated and RE-enriched pegmatites have the lowest K/Rb ratios (<75), while other pegmatite types show more variation in the concentrations (Figure 21B; Table 3). In the study samples, K/Rb ratio varies mainly from 70 to 199. The highest ratios of K/Rb >200 are found in the pegmatitic leucogranites from Potoskavaara S (247.5) and Kokkokallio (233.4).

The K/Cs ratio of the pegmatite samples varies widely in the study area but generally follows a decreasing trend from the pegmatitic leucogranite pegmatites to potassic and sodic aplite pegmatites, and finally to RE-enriched pegmatites (Figure 21C). The highest concentrations of K/Cs are found in the pegmatitic leucogranites from Kuusela (9 409.8), Kokkokallio (7 607.1), and Potoskavaara S (6 219.5), which also had high K/Rb ratios. Reduced values are found in the RE-pegmatites of Riienvaara (882.3), and Surmasuo (358.2 and 337.4). The low values of Cs <120 ppm are found in the RE-pegmatites and a remarkably low ratio (10) in Surmasuo (*KTPA-2022-95.1*). These pegmatites also have the lowest K/Rb ratios of all the samples (Table 3)

The K/Ba ratio again shows variability between the different pegmatite dykes (Figure 21D; Table 3). Mainly, the K/Ba ratios vary between 286.4–3045.4 in the samples. The highest contents are in the potassic pegmatite from Palomäki, instead the notable low K/Ba content (35.7) is in the RE-pegmatite sample from Surmasuo (*KTPA-2022-95.1*). Furthermore, the lower K/Ba $<1\ 000$ ratios are found in the RE-pegmatites of Selkäpäivänrinnea, Kumpu, and other Surmasuo samples, as well in the pegmatitic leucogranite dykes of Halla-ahonvuoret and Kokkokallio.

The Nb/Ta trend shows a clear pattern, indicating that the most fractionated RE-enriched samples have the lowest values (Figure 20F). The sodic aplite pegmatites show some variation in values, as do leucogranites, but the trend generally follows leucogranites, potassic pegmatites, sodic aplites, and finally RE-enriched pegmatites. As the results are shown in figure 20F, the geochemical analyses show variations in the Nb/Ta ratios mostly between 1.8 and 4.8. However, all the samples plotted into a fertile granite category Nb/Ta <8 (Selway *et al.* 2005).

The Fe/Mn and Al/Ga ratios also show a clear trend, with the most fractionated RE-enriched pegmatites having the lowest values (Figures 20G-H). The sodic aplite types

show some variability and particularly in the pegmatitic leucogranites. In the Fe/Mn diagram (Figure 20G), one notable observation is the especially low ratio in the pegmatitic leucogranite dyke from Halla-ahonvuoret (3.41). Notably high Fe/Mn ratios in the study area are found in the pegmatitic leucogranites from Potoskavaara S (61.28) and Kokkokallio (63.3), while the lowest ratios are found in the RE-enriched Riienvaara (2.71) and Kumpu (3.21) (Figure 20G; Table 3). The other samples have varying values of Fe/Mn ratio between 7.0 and 57.5 wt%. In figure 21H, the Al/Ga ratios in the pegmatite samples vary greatly, which is typical for granitic rocks (Černý *et al.* 1985). The Al/Ga ratios are low <4 000 in the pegmatites from RE-enriched Kumpu, the pegmatitic leucogranite of Halla-ahonvuoret, and the sodic aplite of Rajasillannotko, while the highest contents Al/Ga ratios (> 9 000) are found in the pegmatitic leucogranites from Kokkokallio, and Kuusela. Other pegmatites have Al/Ga ratios between 4 183.2–7 567.56 (Table 3).

The Sr/Rb and Ba/Rb ratios vary widely between the study samples and within the different pegmatite classes (Table 3; Figure 21E). The ratios indicate very similar results in the pegmatitic leucogranites, sodic aplites and potassic pegmatites, with the samples partially correlate with each other. However, in the RE-enriched pegmatites, the ratios vary more. Still, in general, both ratios vary significantly between different pegmatite types and do not show any distinct fractionation trend. The Sr/Rb ratios varies between 0.04 and 0.68, with the highest Sr/Rb ratio (0.68) found in Surmasuo (*KTPA-2022.95.1*) and Potoskavaara (0.48). The Ba/Rb ratio ranges between 0.04 and 0.47 in the samples, with the highest Ba/Rb ratios (0.47) are found in Surmasuo (*KTPA-2022-95.1*) and Riienvaara.

In granitic pegmatites, zircons become enriched in Hf relative to Zr, particularly during the later stages of pegmatite crystallization (Černý *et al.* 1985). The pegmatites mainly have Zr/Hf ratio between 1.1–3.2 (Table 3). Zr/Hf <1 is found in Purola, Rajasillannotko, Surmasuo, and Lamminmaa. A remarkably high Zr/Hf ratio is found in Kumpu (11.05). At Potoskavaara S, the Hf content is below the limit of the detection value (<10 ppm).

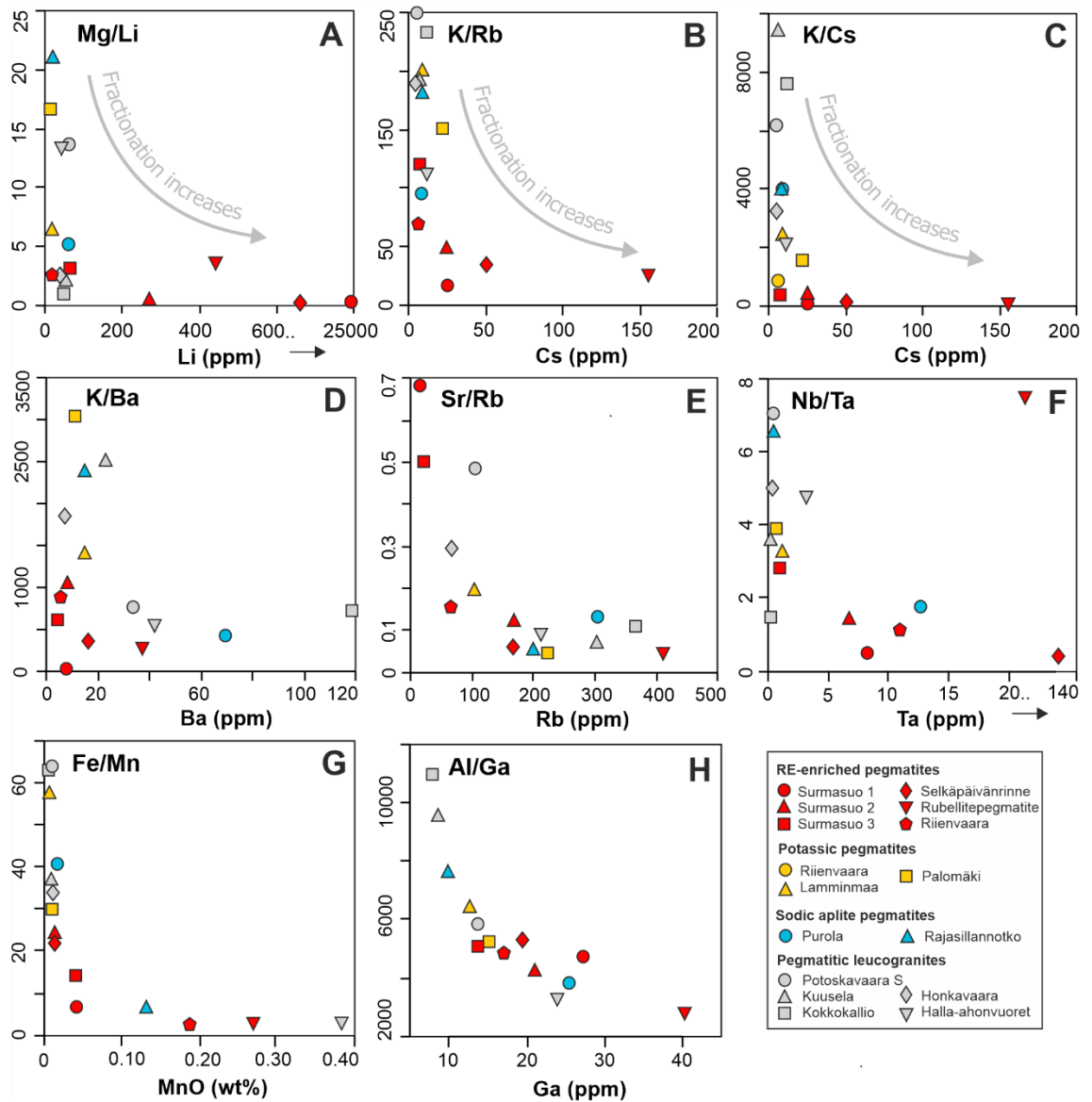


Figure 21. Selected geochemical fractionation indicators in pegmatites from Potoskavaara area, Kitee-Tohmajärvi pegmatite province. A) Mg/Li versus Li. B) K/Rb versus Cs. C) K/Cs versus Cs. D) K/Ba versus Ba. E) Sr/Rb versus Rb. F) Nb/Ta versus Ta. G) Fe/Mn versus MnO. H) Al/Ga versus Ga.

5.4 Structural interpretation

The aeromagnetic data of Kitee-Tohmajärvi areas display structural trend features tens of kilometers long (Figure 22A). The structural interpretation illustrated in figure 22 involves ductile deformation trends, which are shear, foliation and folding trends, as well as brittle deformations, such as several shear and fault zones. Deformation events mainly formed opposite to NNW-SSE orientation trends and in contrast to the general trend of the Karelian schist belt. The Puruvesi and Kitee granites are bordered by the NNE-SSW striking so-called Kitee-Holinmäki shear zone, extending across Kitee and Tohmajärvi turning towards the NNW-SSE trend of Karelian schist belt (Figure 22). The boundary between Kitee and Tohmajärvi outlines the bendy thrust fault zone, where the southern block has been thrust over the northern Archean basement (Luukas *et al.* 2017). The rocks in the area have undergone plastic deformation, and the general trend of foliation is reversed along the trends of the regional deformation zones. In the study area, the general trend of foliation structures are oriented NNE-SSW and ENE-WSW. The area lies within a complex thrust zone, bounded by lithological variations of mica schist, black schist, amphibolite, quartzite, and pegmatite rock types. To the north of the study area, the foliation trend reverses to ENE-WSW strike.

As presented in figure 22, the large-scale disharmonic folding, where the surfaces of the fold are variable and discontinuous, highlights the Kitee granite and the study area. On a large scale, the fold plunge is mainly parallel to the deformation towards NNW-SSE. However, the fold structures also exhibit several discontinuous axial planes oriented in different directions and folds themselves are rotated.

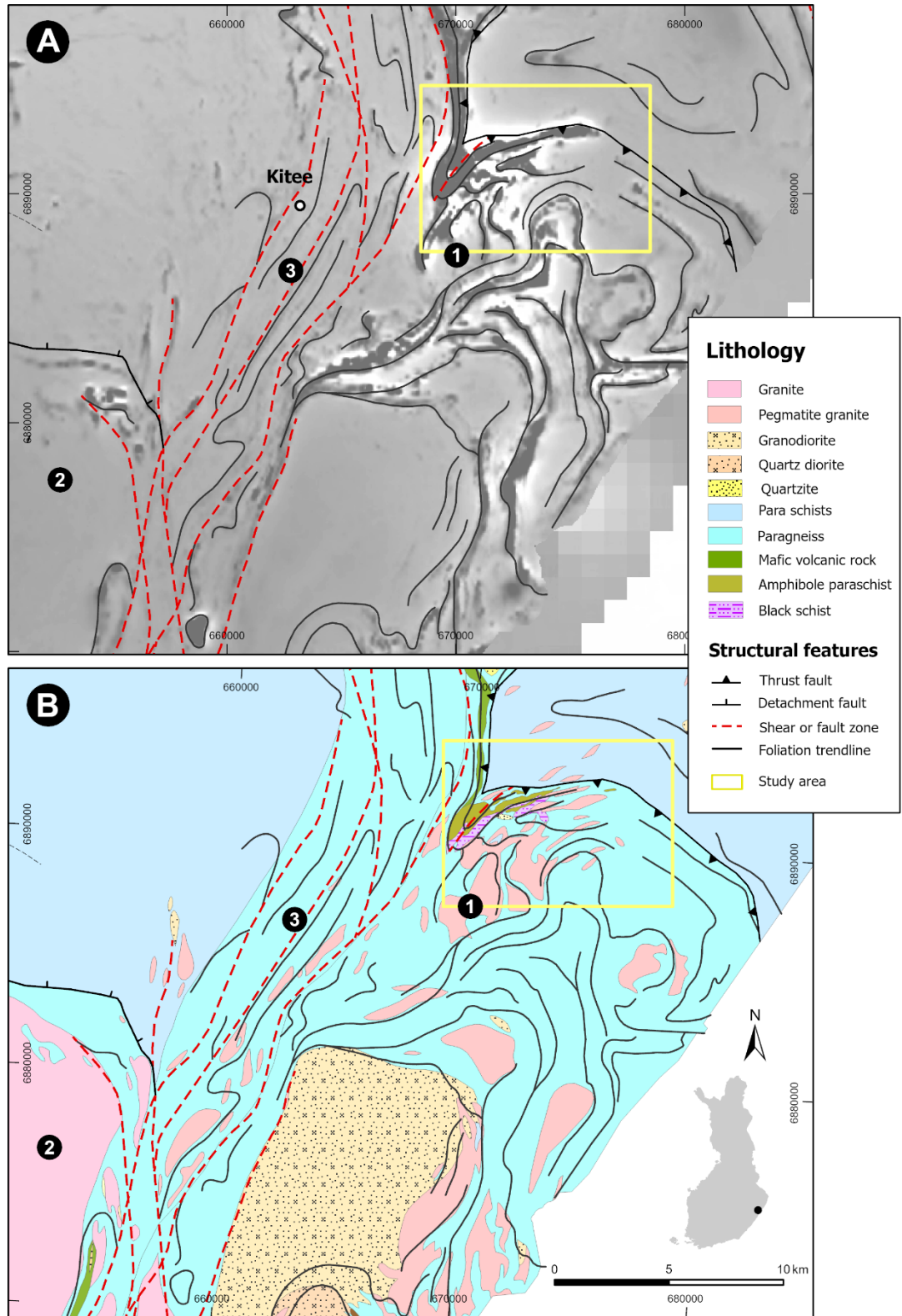


Figure 22. Structural 2D-line interpretation of the Kitee-Tohmajärvi pegmatite province A) with aeromagnetic map and B) bedrock map of Finland (GTK 2024). Fault, shear zone data and geophysical aeromagnetic data from GTK (2024). Shear and fault zones (red dashed line) and foliation trendlines are modified from GTK. Antiform is modified after Nykänen (1968). Meaning of numbers is 1. Kitee granite, 2. Puruvesi granite and 3. Kitee-Holinmäki shear zone. Coordinates are in ETRS-TM35FIN coordinate system.

6 Discussion

6.1 Classifications

The pegmatite dykes in the Potoskavaara area, Kitee-Tohmajärvi pegmatite province are provided to represent strongly peraluminous S-type granites (Figure 18C) and belong in the LCT-pegmatite family (Černý 1991a,b; Černý & Ercit 2005; Simmons 2005; London 2008). In the petrogenetic classification proposed by Wise *et al.* (2021), the pegmatite dykes in the Potoskavaara area can also be divided into the RMG-1 group in addition to the LCT-family (Müller *et al.* 2021). These observations are supported by geochemical results, which confirmed that the strongly peraluminous pegmatite dykes have a A/CNK ratio > 1.1 (Table 3), and they are enriched in RE-elements such as Li, Cs, Rb, Be, Sn, Ta, and Nb, along with the volatile substance P_2O_5 (Figure 19G). These are dominant features of LCT-type and RMG-group pegmatites (Černý 1991a,b; Černý & Ercit 2005; Müller *et al.* 2021). On the other hand, the challenge with Wise *et al.* (2021) classification is to determine whether the pegmatite dykes in Potoskavaara are derived from a residual granitic magmatism or are direct products of anatexis. If they are a direct product of anatexis, they alternatively represent then the DPA-1 group pegmatites (Müller *et al.* 2021, 2022).

As stated in previous studies by Alviola (1974a,b) and Kuikka *et al.* (2023), the granitic pegmatite dykes show variations in the mineralogical and geochemical characteristics in the Potoskavaara area. According to Černý & Ercit (2005) classification (Table 1), the regional zonation of the pegmatite dykes from the Potoskavaara area can roughly divided into two main types. The dyke type of pegmatites varies from complex to beryl type, with highly fractionated REL-Li complex-type pegmatites being Surmasuo, Kumpu and Selkäpäivänrinne (enriched in Li, Cs, Be, Rb, P) (Table 2). The Surmasuo and Kumpu pegmatites can be divided further into spodumene-lepidolite subtypes, based on their mineralogical features. Other dykes belong in the REL-Li beryl-type (enriched in Be, Cs, Rb, Nb, Ta) (Table 2). A more detailed mineralogical evaluation is necessary to confirm the subtypes of the dykes.

6.2 Fertility and fractionation

6.2.1 Determination of the fertile pegmatites

Like findings of Kuikka *et al.* (2023), the pegmatite dykes from the study area exhibit common characteristics that distinguish them from barren pegmatite to fertile in the Potoskavaara area, Kitee-Tohmajärvi pegmatite province. The geochemical results of this study (Tables 2 & 3) reveal the fertile peraluminous granite characteristics, mainly the high Al ratio, low Ca, Fe, and Mg compositions, as well as well variable K_2O/Na_2O composition (Figures 19C & D; Černý 1991b; Selway *et al.* 2005). Moreover, the conclusion is supported by the elemental ratios of $Mg/Li < 10$ and $Nb/Ta < 8$ (Figures 21A, F; Table 3), which are predominant features for highly fractionated and fertile pegmatites (Selway *et al.* 2005). In the fertile pegmatites, the RE concentration is over the upper continental crust compositions of Be (3 ppm), Cs (3.7 ppm), Ga (17 ppm), Li (20 ppm), Nb (25 ppm), Rb (112 ppm), Sn (5.5 ppm) and Ta (2.2 ppm) (Taylor & McLennan 1985), and these features are also found in the geochemical results of the pegmatite dykes from Potoskavaara, as presented in figure 23.

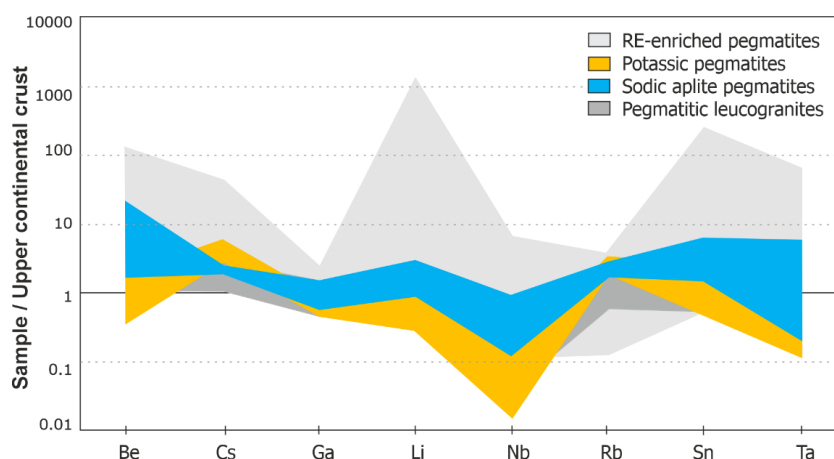


Figure 23. An illustrative diagram of selected Be, Cs, Ga, Li, Nb, Rb, Sn, and Ta elements of the pegmatite dykes from the Potoskavaara area versus average upper-continental crust values (ppm) (Taylor & McLennan 1985).

6.2.2 Geochemical fertility and fractionation variations

The key finding is that the results of this study align with earlier research by Alviola (1974a,b) and Kuikka *et al.* (2023), confirming fertility variations in the pegmatite dykes

of the Potoskavaara area, Kitee-Tohmajärvi pegmatite province (Figure 24). The geochemical results prove the main trend of the elemental enrichment to be $\text{Be} > \text{Cs} > \text{Rb} > \text{Nb} \geq \text{Ta} > \text{Li} > \text{Sn}$ in the pegmatite dykes (Figure 24), which is reflected roughly in this developmental trend from more evolved to primitive pegmatite type; RE-enriched pegmatites (Surmasuo >Kumpu >Selkäpäivänrinne >Riienvaara), potassic pegmatites (Palomäki >Lamminmaa), sodic aplite pegmatites (Purola >Rajasillannotko), and pegmatitic leucogranites (Halla-ahonvuoret >Honkavaara >Kuusela >Kokkokallio >Potoskavaara S).

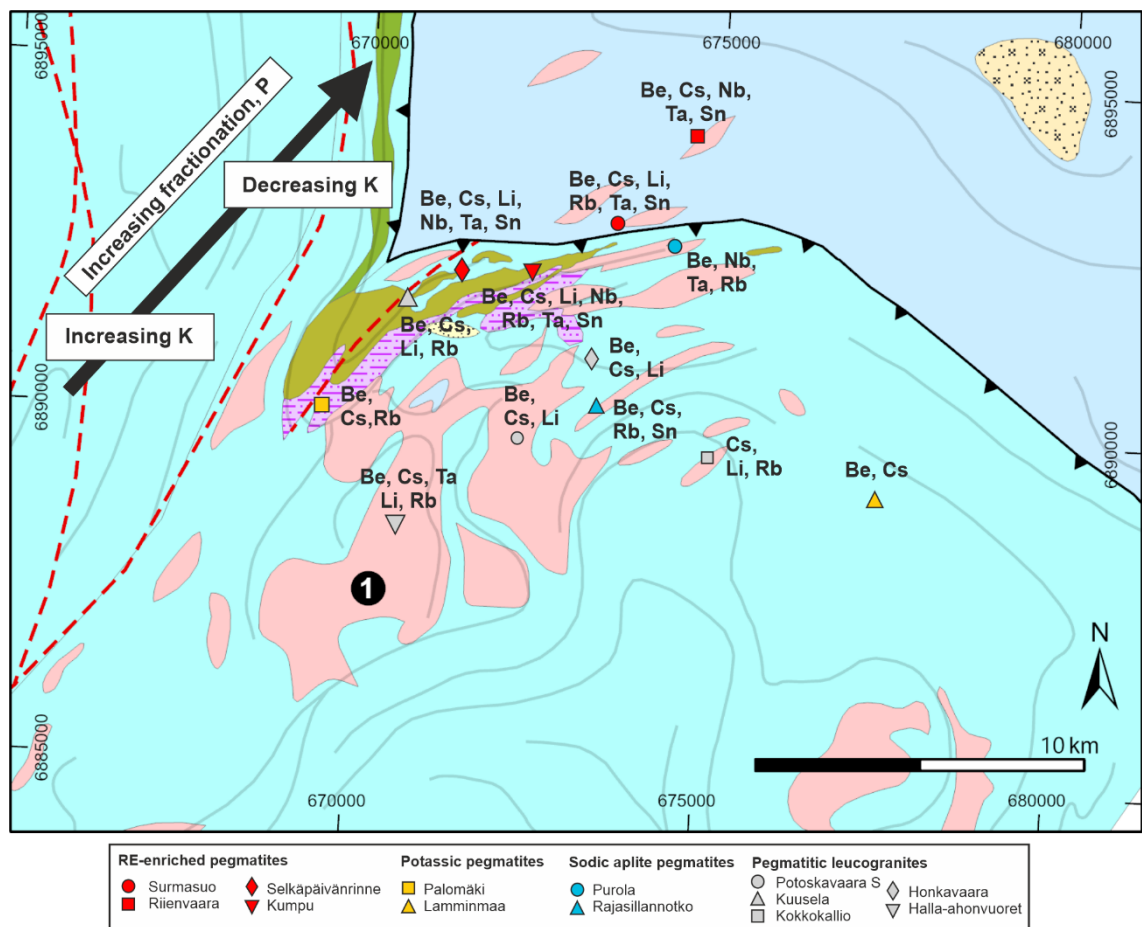


Figure 24. The regional zonation, structural features and rare elements $\text{Be} > \text{Cs} > \text{Rb} > \text{Nb} \geq \text{Ta} > \text{Li} > \text{Sn}$ enrichment trend of the pegmatite dykes in the Potoskavaara area, Kitee-Tohmajärvi pegmatite province. The black arrow illustrates an increasing trend of fractionation as the concentration of volatile P rises in comparison to K. Kitee granite is marked by the number 1 and other entries in the legend of the map are explained in figure 22. The scale-free Bedrock map of Finland is from GTK (2024). Coordinates are in ETRS-TM35FIN coordinate system.

The most complex RE-enriched pegmatite dykes from Surmasuo, Kumpu, and Selkäpäivänrinne (Figure 24) are well-documented in previous studies by Alviola (1974a,b) and Kuikka *et al.* (2023). They are the most fertile pegmatites in the area, having a high Li, Cs, Rb, Ta, Sn, and volatile P₂O₅ concentrations and are depleted in Sr (Table 3; Figure 19G). The especially variable low fractionation trends of Mg/Li, K/Rb, K/Cs, Nb/Ta, Fe/Mn or Al/Ga values (Figure 21; Table 3), with enrichment in REs support this evidence regarding the most highly fractionated pegmatite dykes in the northern Potoskavaara area (Černý *et al.* 1985; Černý 1991a,b; Breaks *et al.* 2003; Černý & Ercit 2005; Selway *et al.* 2005; London 2008). Contrary to earlier studies, the analytical results indicate that the pegmatite dyke from Riienvaara represents a significantly more fractionated pegmatite dyke than previously thought by its geochemical (Tables 2 & 3), mineralogical and internal zonation features (Figure 10A, B2). However, the Li and Cs concentrations and RE-enrichment are among the lowest compared to other RE-pegmatite dykes (Figure 24; Table 2) and these results support the interpretation that this pegmatite dyke has not undergone substantial enrichment in RE components and therefore represents fractionated but the least fertile pegmatite among the other RE-enriched pegmatite dykes.

Among all the samples from the study area, the Surmasuo sample's (*KTPA-2022-95.1*) exceptionally high Li (> 25 000 ppm) and Al₂O₃ (24.6 wt%) concentrations, and low fractionation ratios (Table 3) show extremely fractionated RE-pegmatite (Selway *et al.* 2005). A very low Mg/Li <1.0 ratio indicates spodumene type pegmatite (Selway *et al.* 2005), and together element concentrations indicate a very quartz-, Al- and Li-rich mineralization. As the geochemical analyses show (Tables 2 & 3; Figure 21), the three samples from the Surmasuo show a high variability in elemental concentrations and clearly indicate several different zones within the same pegmatite dyke (London 2008). The enrichment trend is the most evolved spodumene-rich core, to albite-rich unit, and less evolved feldspar-rich unit indicating the pegmatite dyke likely follows the internal zonation model like presented in figure 2.

The Mg/Li fractionation trend in this study area aligns partly with results of Kuikka *et al.* (2023). One clear exception is the RE-pegmatite dyke from Kumpu, where the geochemical results in table 3 show an Mg/Li ratio of 3.63, which differs from the value of less than 1.0 of spodumene pegmatite reported in the previous study. The pegmatite of the Kumpu is heterogeneous which can lead to varying geochemical analysis

results and the dyke can be the individual Li-rich podiform body in the surrounding host rock. One explanation could be also that the different sample techniques. The mini drill of this study is generally more reliable than hand sampling because the drill core sample is a continuous section of the rock, providing a more accurate and representative view of the mineralization and geological features over a certain depth under erosion level. The exceptionally high Mg concentration (Table 2) of the Kumpu pegmatite likely indicates that the pegmatite dyke is contaminated with Mg-rich hydrothermal fluids from the surrounding host rock of metavolcanic and amphibolite schist (Selway *et al.* 2005). Secondly, it is possible to be a result of the assimilation of the surrounding rock by granitic melt. As shown in table 2, enrichment of Nb-Ta and incompatible elements as Bi, Ti, Sb, Sn, U, Zn, Zr, and Hf, along with many enriched REE elements in the pegmatite dyke of Kumpu, distinguish the dyke from the other RE-pegmatite dykes in the Potoskavaara area. The Nb/Ta fractionation value is particularly high (>7), as well as the Hf/Zr ratios (Table 3). Nb/Ta and Hf/Zr behave similarly in the melt, and zircon crystals become enriched in Hf relative to Zr during the later stages of pegmatite crystallization (Černý *et al.* 1985). Selway *et al.* (2005) and Anderson *et al.* (2013) has stated that the abundance of Nb-Ta-Zr minerals increases as fractionation progresses, leading to a rise in Nb-Ta mineralization in columbite-tantalite and fractionation indicator ratios, particularly from the margins of the pegmatite body toward its core. Mineralization likely occurred under late-stage hydrothermal conditions, which is also supported by the low Nb/Ta ratios with K/Rb <150 ratios of the other RE-pegmatite dykes, which according to Shaw (1968) indicate hydrothermal events.

The potassic pegmatite dykes from Lamminmaa and Palomäki are fractionated, but they have relatively low enrichment of RE concentrations compared to the RE-enriched pegmatites. The pegmatite dyke from Lamminmaa shows significantly lower K/Ba and Mg/Li ratios than the pegmatite from Palomäki, while Ba/Rb, Nb/Ta, Al/Ga, and K/Rb ratios are relatively similar (Table 3). Especially the pegmatite dyke of Palomäki shows low Sr/Rb ratio, and variation in geochemical results suggest that Palomäki is more evolved. Similar low Ba/Rb and Sr/Rb findings have been observed in the sodic aplite pegmatite of Rajasillannotko (Table 3). The Sr/Rb and Ba/Rb ratios decrease when the concentration of K-feldspar increases during fractionation in plagioclase-rich melts, and while Rb is a more incompatible element and tends to remain in the melt rather than incorporate into minerals (London 2008).

Based on the results, the sodic aplite pegmatite dykes from Purola and Rajasillanotko are developed, but they do not reach the high fertility category compared to the RE-pegmatites in the study area. Nevertheless, the pegmatite dyke from Purola represents a significantly more fertile dyke among higher enrichment in Nb, Rb, Ta, Be, and Ga contents (Table 2). The low K/Rb ratio of the dyke (Table 3) indicates that the dyke is a product of late-magmatic and post-magmatic crystallization (Černý *et al.* 1985). Further, the dyke has lower K/Ba, Al/Ga, Mg/Li, and Nb/Ta fractionation indicator ratios (Table 3). These results make it more fractionated than the pegmatite from Rajasillanotko (Černý & Ercit 2005; Selway *et al.* 2005; London 2008).

The geochemical results of pegmatitic leucogranites show the most composition variations in the study area. They are mostly poorly enriched in REs and have high fractionation indicators (Tables 2 & 3). The pegmatitic leucogranite dykes from Kuusela and Honkavaara show similar results of K/Cs, K/Rb, Al/Ga, and Fe/Mn ratios and elemental concentrations (Table 2,3; Figure 21), which indicate minimal fractionation. Among leucogranite-type pegmatites, the low Fe/Mn and Al/Ga ratios, high P₂O₅, and elevated Cs, Ti, Li, and Rb concentrations of Halla-ahonvuoret (Tables 2 & 3) display higher signs of fractionation than initially expected (Černý *et al.* 1985). Still, the field observations of mineralogy and textures suggest that the Halla-ahonvuoret pegmatite dyke may not be as highly developed. The K/Rb versus Cs plot is one of the best diagrams used to determine the degree of fractionation in leucogranite pegmatites, because Cs and Rb replace K in K-feldspar and muscovite, as fractionation increases (Breaks *et al.* 2003, Selway *et al.* 2005). The K/Cs and K/Rb ratios of Halla-ahonvuoret is the lowest compared other pegmatitic leucogranites and especially high ratios (K/Cs >6 000 with K/Rb >190) are found in Kuusela, Kokkokallio and Potoskavaara S, therefore together with significantly poor evidence in RE-components the results indicate the most minimal fractionation (Table 3). However, the high K₂O concentrations (>7 wt%) of the Kuusela and Kokkokallio dykes along with the elevated P₂O₅ volatile (>0.10 wt%) concentration, can indicate increased fractionated pegmatite dykes than Potoskavaara S dyke.

The observed variation in elemental concentrations, particularly the increase in K and P₂O₅ concentration during early stages of fractionation, is consistent with the regional zonation and the progressive fractionation process (Figures 17B & 24). This behavior can be attributed to the mobilization of volatile components, such as water and P₂O₅, which facilitates the enrichment of K in the melt (Breaks *et al.* 2003; London 2008). As

fractionation continues and the melt composition shifts toward more Na-rich, the K content decreases, which is also observed in the Potoskavaara albite-rich pegmatites (Figure 24). Although the pegmatitic leucogranite dykes are fractionated, the magma may not have had enough volatiles to promote significant RE-enrichment (Černý 1991b; London 2005; Selway *et al.* 2005; London 2008; Simmons & Webber 2008). The absence of the flux components F and B in the analysis results complicates the interpretation, as their presence would provide more precise information about the fractionation of the pegmatite dykes.

6.2.3 Field observation and petrography studies

Field observations of mineralogical and textural variations, such as internal zonation, where evolution increases toward the pegmatite core zone (Figures 10A, D & 12A-C) strongly support the geochemical results regarding fractionation variations in the Potoskavaara area. Generally, mineralogical changes are primarily driven by the crystallization of RE into minerals as fractionation progresses (Selway *et al.* 2005; London 2008). Clear evidence is the coloration and textural changes in the minerals, such as in muscovite, tourmaline, and garnet, from pegmatitic leucogranites to the most fertile RE-enriched pegmatites. The field results show that colored tourmalines are found only in the most evolved RE-enriched pegmatites (Figure 8), muscovite shifts from silver to a coarse-grained Li-indicating yellowish-green in color (Figure 9), and the color of garnet changes from Fe-rich orange to Mn-rich spessartine (Baldwin & von Knorring 1983; Černý 1989a), a transition that is particularly prominent in the Riienvaara dyke. Muscovite, however, does not necessarily appear coarse-grained in fertile pegmatites (Breaks *et al.* 2003), which is visible in the fine-grained and occasionally massive texture of muscovite formed by the hydrothermal events of the Selkämpäivänrinne (Figure 9C) and Riienvaara (Figure 10B) dykes. The effect of the volatile components may be observed in the smaller grain size of the sodic aplite pegmatites (Figures 10C-D), even though the samples are more fractionated than pegmatitic leucogranite types (Jahns & Burnham 1969, as cited in London 2005). Further, the evidence of the alteration events is noticeable in thin sections as varying amounts of fluid inclusions and sericitization in the pegmatite dykes (Figures 13A, 14A & 16) proves the formation of the dykes from magmatic to hydrothermal conditions (London 2008).

On a related note, field observations are crucial for identifying discrepancies in the geochemical data. The field observations from the Selkäpäivänrinne shows that the dyke does not fully represent a RE-rich dyke but possibly it is a Li-enriched section of a larger potassic pegmatite (Figure 11). This observation is also in line with the Alviola (1974a,b) and Kuikka (*et al.* 2023) studies. One possible explanation for the compositional differences is that the Selkäpäivänrinne represents a zoned pegmatite (Cerný 1991a,b; London 2008). This can be explained by the fact that different crystallization phases may have occurred in different parts of the dyke, leading to variations in mineral compositions.

The geochemical results of the Honkavaara dyke are unable to show significant signs of fertility, whereas the field observations and petrological studies indicated clear internal zonation (Figure 10A-C), and evidence of alteration, based on which, Honkavaara is more developed than others pegmatitic leucogranite dykes of Kuusela and Kokkokallio. Furthermore, the geochemical results of the pegmatite dyke from Halla-ahonvuoret are also inconsistent with the field observations, which show a poorly developed pegmatite (Figure 11A). However, the petrographic studies that show signs of deformation and metamorphism (Figure 13A), support the notion that the dyke is more evolved compared to the other pegmatitic leucogranite dykes. These results highlight the importance of the different methods in determining the degree of development.

6.2.4 Uncertainties in sampling

Although the studies indicate signs of fertility and fractionation, more reliable results would have been achieved if multiple comparative samples had been taken from the pegmatite dykes. A single sample from each occurrence is unable to represent the bulk composition of the deposits well based on the whole-rock geochemical compositions. In coarse-grained and heterogeneous pegmatites, differences in mineral grain sizes can lead to uneven sampling, causing certain minerals to be over- or under-represented in the sample and element enrichment, in a non-representative way. The possibility of a so-called nugget effect can lead the concentrations in the pegmatites in a misleading way (Steiner 2019). In this situation, pegmatites contain randomly high concentrations of RE and valuable minerals in small portions like in Kumpu, Selkäpäivänrinne and Surmasuo (KTPA-2022-95.1) samples, which can lead to results that falsely suggest enrichment of minerals, even though it should represent only a small local pod in the dyke. Additionally, in the collection of mini-drill samples, particularly regarding the final sample sizes, and

by collecting sufficiently large samples, the uncertainties could have been reduced. In bedrock mapping and sampling, efforts should be made to identify multiple pegmatite dykes or pegmatite dyke swarms as well notable the internal zonation, textural differences, and sufficiently large sample size to avoid the nugget effect (Steiner 2019).

6.3 Regional origins and structural controls

6.3.1 Source of the pegmatite dykes

According to Hölttä & Heilimo (2017), the metamorphic grade in the Potoskavaara area is low amphibolite facies, which enables the partial melting and slow crystallization of minerals from the melt and formation of RE-pegmatites (Selway *et al.* 2005). The geochemical results and geological history of the area reveal that the LCT pegmatites are fractionated from orogenic granites derived from a metasedimentary source rock of S-granite (Černý 1991b; Chappel & White 2001; Selway *et al.* 2005; Laajoki 2005; London, 2008; Bradley *et al.* 2017). The pegmatite dykes in the Potoskavaara area are formed either directly from evolved granitic source, or from granitic melts by partial melting or anatexis of surrounding host rocks, which is usually pelitic metasediment (Chappel & White 2001; London, 2008; Bradley *et al.* 2017). To confirm this, the surrounding host rock should be further investigated to assess the enrichment of RE elements (Li, Cs, Ta) contents to the metasomatic aureole.

The mineralogical and geochemical results of this study highlight zonation of the dykes (Figure 24), which is typical for heterogeneous LCT-pegmatites (Figure 1; Černý 1991b; Simmons & Webber 2008). The development direction is roughly increasing from south to north and is mainly followed by the typical trend from the pegmatitic leucogranite pegmatites, to the sodic aplite pegmatites and potassic pegmatites, to the most RE-enriched pegmatites (Selway *et al.* 2005). As shown in the figures 22 & 24, the pegmatite dykes occur as dykes, dyke swarms, and intrusions within the study area, with the most fertile and fractionated pegmatite dykes occurring the north of the Potoskavaara study area, up to 25 km from the assumed source granite of Puruvesi granite. Upon comparing the Selway *et al.* (2005) and Breaks & Tindle (1997) studies, it becomes clear that the RE-enriched pegmatites typically crystallize up to 10 km away from the source granite, suggesting that the Puruvesi granite is not the source granite for the pegmatite dykes in the Potoskavaara area. Based on this, the Kitee granite would seem to be a likely source

of the pegmatite dykes. Alviola (1974b) have identified the pegmatite dykes in the Surmasuo as 1.81 Ga aged, but even so, in order to be certain of the source, more precise age determinations are needed to identify the age of the pegmatite dykes in the Potoskavaara area (Černý & Ercit 2005).

6.3.2 Regional structure and impact on formation

The movements of the melt are generally controlled by structures, and principal stress orientations of these structures (Deveaud *et al.* 2013; Silva *et al.* 2023), which together have influenced why the pegmatite dykes in the Potoskavaara area are favorably positioned relative to lithological variations, folding and fold axial planes (Figure 22). These structures also include the fault and shear zones, such as thrust faults which likely transport fluids during anatectic water-fluid processes in the study area (Silva *et al.* 2023). The pegmatite dykes in the study area, and the Puruvesi granite on the west are bounded by the NNE-SSW trending the Kitee-Holinmäki shear zone (Figures 7 & 22), which in addition could be a possible magma pathway for the formation of the pegmatite dykes (Černý 1991b; Selway *et al.* 2005). However, the RE-enriched rocks in the Potoskavaara area show a similar positioning along the compressional thrust-over zone and the contact between the lithological units of amphibolite, metavolcanite, and metasedimentary rocks (Figure 22B), similar to the Li-richest pegmatites in the Kaustinen-Ullava area (Nygård *et al.* 2023). This would support the idea that the thrust zone and lithological variations have provided a structural magma pathway in the area (Deveaud *et al.* 2013).

The structural interpretation and features of the area show that the Kitee-Tohmajärvi area is part of a larger complex structural-geological system on a large scale (Figure 22A), and the area has been affected by several deformations of different ages which complicate the interpretation of the pegmatite formation and the identification of the original source. The Kitee granite and pegmatite dykes appear to be aligned along the folding (Figure 22B), which would indicate the deformation caused by the large fold is younger than or of the same age as the pegmatite dykes. Some of the deformation events are younger than the pegmatite dykes, which is proven by observed the deformation signs in thin section studies (Figure 15). The large-scale structural interpretations remain uncertain, especially when they are mainly based on geophysical data. Geophysical data are primarily useful for structural interpretations but does not reveal RE-pegmatites in anomalies due to their poor density differences compared to surrounding rocks (Bradley *et al.* 2017). For a more

detailed structural analysis, an extensive structural field study of the area should be conducted to examine better the deformation features in pegmatites as well as the relationships between pegmatite dykes and the surrounding rocks.

6.4 Comparison to LCT-pegmatites in Finland

The Potoskavaara pegmatite dykes have similar features compared to the S-type LCT-pegmatites of the Kaustinen, Kuortane, Alajärvi, Haapaluoma, Kaatiala, and Seinäjoki areas (Table 4; eg. Nygård *et al.* 2024) in the Ostrobothnia region as shown in figure 3. Both regions belong to a variable, predominantly low amphibolite facies metamorphic grade regions (Hölttä & Heilimo 2017) and surrounding rock types are mainly metasedimentary and metavolcanic (Table 4). The pegmatites of the Kaustinen-Ullava area of the Ostrobothnia (Figure 3) represent mainly homogeneous albite-spodumene pegmatites (Alviola 2003; Martikainen 2012) and the average concentration of Li₂O is higher at 0.18–1.18 wt% (Ahtola *et al.* 2015) compared to the average 0.71 wt% of Li₂O concentration in the Surmasuo (Alviola 1974b). In the the Kaustinen area, the Dragbacken dykes show internal zonation and variations in lithium concentrations. These characteristics are also observed in the pegmatite dykes of Potoskavaara (Nygård *et al.* 2023). On the other hand, the Seinäjoki and Kaatiala-Haapaluoma area shows more similarities in fertility variations and elemental enrichment of Be, Nb, Sn, Li, and Cs (Table 4) features closest to the Potoskavaara pegmatites (Nygård *et al.* 2024).

When comparing volatile elements concentrations, the P₂O₅ concentrations in the Kaustinen-Ullava deposit range from 0.01 to 0.35 wt% according to Martikainen (2012) and from 0.09 to 0.44 wt% according to Ahtola (2015), exhibiting similar characteristics to the general P₂O₅ concentrations of the Potoskavaara area (0.03–0.35 wt%) (Table 4). For comparison, the Kaustinen-Kruunupyy and Dragbacken spodumene-pegmatite deposits contain 0.71 wt% of P₂O₅ (Nygård *et al.* 2023), which is very close to the highest P₂O₅ concentration (0.67 wt%) in the Kumpu RE-pegmatite dyke in Potoskavaara. The high P and elevated U (166.5 ppm) compositions of the RE-enriched Kumpu dyke, would be the result of the protolith mixing of the surrounding host rocks of black schist and mafic volcanites (Figure 24; Hines *et al.* 2023). Nygård *et al.* (2024) suggested the same potential link between LCT-pegmatites, black schists, and mafic volcanites in the Ostrobothnia area. In addition, elevated Be concentrations of Kumpu, and Riienvaara dykes could potentially indicate the presence of cordierite during magma development in

the Potoskavaara (Evensen & London 2002) and in the Kuortane area (Nygård *et al.* 2024). Cordierite binds Be during the melting of pelitic sediments, but under high pressure, it breaks down and releases Be into the melt. If the original melt is too low in Be concentration, it indicates metamorphic conditions outside the stable cordierite zone. Therefore, pegmatites of the Potoskavaara with high Be > 70 ppm concentrations would invalidate the hypothesis of the pegmatite formation being directly formed during anatexis (Hines *et al.* 2023). The formation of zoned pegmatites, however, needs a complex petrogenetic process that could involve multiple melting stages or a combination of anatexis and fractional crystallization (Černý 1991a; Černý 1991b; Simmons & Webber 2008; London 2014).

Table 4. Comparison of the Potoskavaara area in the Kitee-Tohmajärvi pegmatite province with the main Ostrobothnia LCT-deposits of Finland (Alviola 2001, 2003; Mäkitie *et al.* 2001; Martikainen 2012; Ahtola *et al.* 2015; Nygård *et al.* 2023, 2024). RE-minerals are Brl= beryl, Clb = columbite, Cst= cassiterite, Elb= Elbaite, Lpd = lepidolite, Spd = spodumene, Tap= tapiolite, and Trp = triphylite.

Location	Type	RE-enrichment	RE-mineralization	Age (Ga)	Host rock
Potoskavaara	Complex, Beryl	Be, Nb, Ta, Li, Cs, Sn	Brl, Elb, Spd, Lpd, Cst	~1.80	Metasedimentary, metavolcanic
Kaustinen area	Albite-spodumene	Li, Be, Nb	Spd, Clb, Brl	1.79	Metasedimentary, metavolcanic
Kuortane - Alajärvi	Beryl	Be, Nb	Brl, Clb, Trp	1.79–1.80	Metasedimentary
Haapaluoma-Kaatiala	Complex	Be, Nb, Sn, Li, Cs	Spd, Lpd, Elb, Brl	1.79–1.80	Metasedimentary, granodiorite
Seinäjoki	Complex	Sn, Be, Nb, Ta, Li	Cst, Brl, Spd, Tap, Clb	1.79–1.80	Metavolcanic, metasedimentary

6.5 Economic Li-potential

The RE-pegmatites in Potoskavaara have been known for a long time, and the results of this study do not provide new significant evidence regarding the Li potential of the Potoskavaara area. The results show that the most potentially interesting targets for LCT-enrichment are the pegmatite dykes in the Surmasuo, Kumpu, and Selkämpivänrinne, and as an addition to the previous information, also the pegmatite from Riienvaara. However, the pegmatite dyke from Riienvaara appears to represent only a high fractionated dyke and has not been enriched into an economically interesting pegmatite (Selway *et al.*

2005). On the other hand, the pegmatite dyke from Kumpu is contaminated by Mg-rich fluids and is not economically exploitable for this reason.

Further, Selway *et al.* (2005) has stated that the most economic potential of the pegmatite dykes should have concentrations of Li >2 000 ppm, Rb >10 000 ppm, Cs >500 ppm, and Ta >65 ppm, which are not exceeded in Potoskavaara. Additionally, Bradley *et al.* (2017) have stated that the Li₂O concentration should be a minimum of 1 wt% with at least 7 Mt of mineral and with Ta₂O₅ concentration it corresponds to 0.1 wt% and 0.01 Mt of raw material, to be considered economically viable to exploit. The drill-core analysis shows only average Li₂O of 0.71 wt% concentrations in the Surmasuo (Alviola 1974b), which is not sufficient compared to limit values by Bradley *et al.* (2017). So, although the LCT concentrations in Surmasuo, Selkäpäivänrinne, and Kumpu are increased, the pegmatite dykes are not competitive from a European perspective compared to the Kaustinen-Ullava pegmatite province which have average Li₂O concentration of 1.18 wt% in the spodumene pegmatites by Ahtola *et al.* (2015).

There may still be undiscovered LCT-pegmatites in the Potoskavaara area, and exploring the halo effect in surrounding rocks could aid in understanding anatexis and discovery unidentified pegmatites. Successful studies on the impact of the halo effect have been conducted in Kaustinen-Kruunupyy and Seinäjoki-Kuortane (Figure 3), where elevated concentrations of Li, Cs, and Rb were observed in surrounding muscovite-bearing rocks, black schist rocks, and mafic volcanic rocks (Nygård *et al.* 2023; Tiala 2023). Overall and based on the discussion, although the results of this study do not show signs of economic Li-potential, it is clear that more comprehensive studies are required to the full understanding of the Potoskavaara area's formation and lithium potential.

7 Conclusions

1. The peraluminous S-type pegmatite dykes of Potoskavaara area belong to the LCT- family and RMG-group pegmatites in the Kitee-Tohmajärvi pegmatite province. The pegmatite dykes represent heterogeneous and regional zonation, that show clear indications of differences in fertility and fractionation degree in geochemical, mineralogical, and petrographic results.
2. The pegmatite dykes in Potoskavaara area have a decreasing fractionation trend from the RE-enriched pegmatites of Surmasuo >Selkäpäivänrinne >Kumpu >Riienvaara to the potassic pegmatite types of Palomäki >Lamminmaa, to the sodic aplite pegmatite types of Purola >Rajasillannotko, and to the most common pegmatitic leucogranite types of Halla-ahonvuoret >Honkavaara > Kuusela >Kokkokallio >Potoskavaara S.
3. The LCT-pegmatite dykes in Potoskavaara represent fertile pegmatites having the high value of A/CNK >1.1, Mg/Li <10 and Nb/Ta <8, the high Al ratio, low Ca, Fe, and Mg compositions, and variations in the K and Na contents. The RE-enrichment trend in fractionation grade is from Be >Cs >Rb >Nb ≥Ta >Li >Sn, following regional zonation trend. The concentrations of volatile P₂O₅ components correlate positively with increasing fractionation.
4. The source granite of the pegmatite dykes in the Potoskavaara area is likely the Kitee granite. Internal and regional zonation indicates multiple melting stages or a combination of increased fractional crystallization and anatexis. In addition, the elemental concentrations, mineralization, volatiles and alteration events of the pegmatite dykes suggest that magma differentiation occurred under late-stage hydrothermal conditions. Hydrothermal alteration complicates the interpretation, as the original mineral composition may have changed.
5. The most Li-potential pegmatites in the Potoskavaara region are concentrated in northern part around the Surmasuo area, where the most favorable lithologies and most complex structural features for the magma pathways are located. Better regional structure understanding and studies on the impact of the sedimentary halo during anatexis on the surrounding rocks could help identify undiscovered LCT-pegmatite dykes in the Kitee-Tohmajärvi pegmatite province.

Acknowledgements

I would like to express my deepest gratitude to my supervisors Professor Esa Heilimo from University of Turku, and MSc Jaro Kuikka from GTK, for their guidance, insightful comments, and continuous support throughout the entire research process. I would also like to thank GTK for providing this research topic, as well as for the opportunity to work and spend memorable summers in Kitee and Tohmajärvi during the field seasons of 2021 and 2022. Lastly, I would like to thank my family, friends, and the Geohouse staff for their support, understanding, and encouragement throughout my master's thesis and geology studies.

References

- Ahtola, T., Kuusela, J., Käpyaho, A. & Kontoniemi, O. (2015). Overview of lithium pegmatite exploration in the Kaustinen area in 2003–2012. *Geological Survey of Finland, Report of Investigation 220*, 28 p.
- ALS (2024). Geochemistry. Schedule of services & fees, 52 p. 10/2024.
<<https://www.alsglobal.com/en/geochemistry/geochemistry-fee-schedules>>
- Alviola, R. (1974a). Pegmatiittitutkimukset Kiteen Papinniemen alueella kesällä 1973. Geological Survey of Finland, Archive report M19/4213/-74/1/80, 9 p.
- Alviola, R. (1974b). Selostus pegmatiittitutkimuksista Kiteen-Tohmajärven alueella vuosina 1972–1973. *Geological Survey of Finland, Archive report M19/4232/-74/1/8*, 11 p.
- Alviola, R. (2001). Ullavan Längän litiumpegmatiitin mineraaliset tuotteet. Geological Survey of Finland, Archive report M19/2341/2001/85, 26 p.
- Alviola, R. (2003). Pegmatiittien malmipotentialista Suomessa. *Geological Survey of Finland, Archive report M 101-03/1/85*, 7 p.
- Alviola, R. (2012). Distribution of rare element pegmatites in Finland. In: Kukkonen *et al.* (eds): Lithosphere 2012. Seventh symposium on the structure, composition and evolution of the Lithosphere in Finland, Espoo, November 6–8, 2012, programme and extended abstracts. *Institute of Seismology, University of Helsinki, Helsinki, Report S-56*. 1–4.
- Anderson, M. O., Lentz, D. R., McFarlane, C. R. & Falck, H. (2013). A geological, geochemical and textural study of an LCT pegmatite: Implications for the magmatic versus metasomatic origin of Nb-Ta mineralization in the Moose II pegmatite, Northwest Territories, Canada. *Journal of Geosciences* 58: 4, 299–320.
- Baldwin, J.R. & von Knorring, O. (1983). Compositional range of Mn-garnet in zoned granitic pegmatites. *Canadian Mineralogist* 21, 683–688.
- Bradley, D., McCauley, A. & Stillings, L. (2017). Mineral-deposit model for lithium-cesium-tantalum pegmatites. *U.S. Geological Survey, Scientific Investigations, Report 2010-5070-O*, 48 p.
- Breaks, F.W. & Tindle, A.G. (1997). Rare-metal exploration potential of the Separation Lake area: An emerging target for Bikita-type mineralization in the Superior Province of Ontario. *Ontario Geological Survey, Open File Report 5966*, 27 p.
- Breaks, F.W., Selway, J.B. & Tindle, A.G. (2003). Fertile peraluminous granites and related rare-element mineralization in pegmatites, Superior Province, northwest and northeast Ontario: Operation Treasure Hunt. *Ontario Geological Survey, Open File Report 6099*, 179 p.
- Černý, P. & Ercit, T. (1985). Some recent advances in the mineralogy and geochemistry of Nb and Ta in rare-element granitic pegmatites. *Bulletin de Minéralogie* 108: 3, 499–532.
- Černý, P., Meintzer, E. & Anderson, J. (1985). Extreme fractionation in rare-element granitic pegmatites; selected examples of data and mechanisms. *The Canadian Mineralogist* 23: 3, 381–421.
- Černý, P. & Meintzer, R.E. (1988). Fertile granites in the Archean and Proterozoic fields of rare element pegmatites: Crustal environment, geochemistry and petrogenetic relationships. In

Recent Advances in the Geology of Granite-related Mineral Deposits. *Canadian Institute of Mining and Metallurgy, Special Publication 39*, 170–206.

- Černý, P. (1989b). Exploration Strategy and Methods for Pegmatite Deposits of Tantalum. In Möller, P., Černý, P. & Saupé, F. (eds): Lanthanides, tantalum and niobium: mineralogy, geochemistry, characteristics of primary ore deposits, prospecting, processing and applications proceedings of a workshop in Berlin, November 1986. *The Society for Geology Applied to Mineral Deposits, special publication 7*, 274–302.
- Černý, P. (1991a). Rare-element granitic pegmatites. Part I: Anatomy and internal evolution of pegmatite deposits. *Geoscience Canada* 18, 49–67.
- Černý, P. (1991b). Rare-element granitic pegmatites. Part II: Regional to global environments and petrogenesis. *Geoscience Canada* 18, 68–81.
- Černý, P. & Ercit, T. (2005). The classification of granitic pegmatites revisited. *The Canadian Mineralogist* 43, 2005–2026.
- Chappel, B.W. & White, A.J. (2001). Two contrasting granite types: 25 years later. *Australian Journal of Earth Sciences* 48: 4, 489–499.
- Deveaud, S., Gumiaux, C., Gloaguen, E. & Branquet, Y. (2013). Spatial statistical analysis applied to rare-element LCT-type pegmatite fields: An original approach to constrain faults-pegmatites-granites relationships. *Journal of Geosciences* 58, 163–182.
- European Commission (2023). Study on the critical raw materials for the EU 2023: final report. Publications office of the European Union. 158 p. [page visited 12/2024]. <<https://data.europa.eu/doi/10.2873/725585>>
- Evensen, J. M. & London, D. (2002). Experimental silicate mineral/melt partition coefficients for beryllium and the crustal Be cycle from migmatite to pegmatite. *Geochimica et Cosmochimica Acta* 66: 12, 2239–2265.
- Frost, B., Barnes, C., Collins, W., Arculus, R., Ellis, D. & Frost, C. (2001). A geochemical classification for granitic rocks. *Journal of Petrology* 42: 11, 2033–2048.
- GTK (2024). Bedrock map of Finland – DigiKP. Digital map database. Espoo: Geological Survey of Finland. [page visited 9–12/2024, 1/2025]. <<https://gtkdata.gtk.fi/mdae/index.html>>
- Hölttä, P. & Heilimo, E. (2017). Metamorphic map of Finland. In: Nironen, M. (ed.) Bedrock of Finland at the scale 1:1 000 000 – Major stratigraphic units, metamorphism and tectonic evolution. *Geological Survey of Finland, Special paper 60*, 77–128.
- Hölttä, P., Heilimo, E., Huhma, H., Juopperi, H., Kontinen, A., Konnunaho, J., Lauri, L., Mikkola, P., Paavola, J. & Sorjonen-Ward, P. (2012a). Archaean complexes of the Karelia Province in Finland. *Geological Survey of Finland, Special Paper 54*, 9–20.
- Hölttä, P., Heilimo, E., Huhma, H., Kontinen, A., Mertanen, S., Mikkola, P., Paavola, J., Peltonen, P., Semprich, J., Slabunov, A. & Sorjonen-Ward, P., (2012b). The Archaean of the Karelia Province in Finland. Edited by Pentti Hölttä. *Geological Survey of Finland, Special Paper 54* 21–73.
- Jahns R.H. & Burnham C.W. (1969). Experimental studies of pegmatite genesis: I. A model for the derivation and crystallization of granitic pegmatites. *Economic Geology* 64: 8, 43–864.

- Janoušek, V., Farrow, C.M. & Erban, V. (2006). Interpretation of Whole-rock Geochemical Data in Igneous Geochemistry: Introducing Geochemical Data Toolkit (GCDkit). *Journal of Petrology* 47: 6, 1255–1259.
- Keliber (2023). Technical report summary: Keliber lithium project, Finland, Report Number 592138. 238 p. [page visited 12/2024]
<https://minedocs.com/26/Keliber_Lithium_Project_TRS_12312022.pdf>
- Korsman, K., Niemelä, R. & Wasenius, P. (1988). Multistage evolution of the Proterozoic crust in the Savo schist belt, eastern Finland. *Geological survey of Finland, Bulletin* 343, 89–96.
- Kuikka, J., Hulkki, H., Lintinen, P., Kinnunen, M., Nenonen, J., Taivalkoski, A. & Valasti, P. (2023). Geological Survey of Finland, Kiteen-Tohmajärven alueen Li-potentiaalitutkimukset 2019–2022. *Geological Survey of Finland, Archive report* 32/2023, 87 p.
- Kurhila, M., Andersen, T. & Rämö, T. (2010). Diverse sources of crustal granitic magma: Lu–Hf isotope data on zircon in three Paleoproterozoic leucogranites of southern Finland. *Lithos* 115: 1–4, 263–271.
- Kurhila, M., Mänttari, I., Vaasjoki, M., Rämö, O. T. & Nironen, M. (2011). U–Pb geochronological constraints of the late Svecofennian leucogranites of southern Finland. *Precambrian Research* 190: 1–4, 1–24.
- Kähkönen, Y. (2005). Svecofennian supracrustal rocks. In Lehtinen, M., Nurmi, P.A., Rämö, O.T. (eds.): *Precambrian geology of Finland – Key to evolution of the Fennoscandian shield. Developments in Precambrian Geology* 14. Amsterdam: Elsevier, 343–405.
- London, D. (2005). Granitic pegmatites: an assessment of current concepts and directions for the future. *Lithos* 80, 1:4, 281–303.
- Laajoki, K. (2005). Karelian supracrustal rocks. In: Lehtinen, M., Nurmi, P.A., Rämö, O.T. (eds.): *Precambrian Geology of Finland – Key to evolution of the Fennoscandian shield. Developments in Precambrian Geology* 14. Amsterdam: Elsevier, 281–341.
- Lehtinen, M., Nurmi, P.A. & Rämö, O.T., (Eds.) (2005). *Precambrian Geology of Finland – Key to the evolution of the Fennoscandian shield. Developments in Precambrian Geology* 14. Amsterdam: Elsevier. 736 p.
- London, D. (2008). *Pegmatites*. The Canadian Mineralogist, Special Publication 10. Canada. 347 p.
- Luukas, J., Kousa, J., Nironen M., Vuollo, J. & Nironen, M. (2017). In: Nironen, M. Bedrock of Finland at the scale 1:1 000 000 - Major stratigraphic units, metamorphism and tectonic evolution Edited by Mikko Nironen, *Geological Survey of Finland, Special Paper* 60, 9 – 40.
- Luukkonen, E. & Lukkarinen, H. (1986). Explanation to the stratigraphic map of Middle Finland. *Geological Survey of Finland, Report of investigation* 74, 5–36.
- Martikainen, A. J. (2012). Kaustisen ja Ullavan litiumpegmatiittien alueelliset geokemialliset piirteet ja lähdegranitoidit. Helsingin yliopisto, geotieteiden ja maantieteen laitos. 77 p. [in Finnish unpublished MSc thesis]

- Middlemost, E. A. (1985). Naming materials in the magma/igneous rock system. *Earth-sciences reviews* 37: 3–4, 215–224.
- Müller, A., Keyser, W., Simmons, W. B., Webber, K., Wise, M., Beurlen, H., Garate-Olave, I., Roda-Robles, E. & Galliski, M. Á. (2021). Quartz chemistry of granitic pegmatites: Implications for classification, genesis and exploration. *Chemical Geology* 584: 120507, 17 p.
- Müller, A., Simmons, W., Beurlen, H., Thomas, R., Ihlen, P. M., Wise, M., Roda-Robles, E., Neiva, A. & Zagorsky, V. (2022). A proposed new mineralogical classification system for granitic pegmatites—Part I: History and the need for a new classification. *The Canadian Mineralogist* 60: 2, 203–227.
- Mäkitie, H. (ed.) (2001). Svecofennian granitic pegmatites (1.86-1.79 Ga) and quartz monzonite (1.87 Ga), and their metamorphic environment in the Seinäjoki region, western Finland. *Geological Survey of Finland, Special Paper* 30, 1–93.
- Möller, P., Černý, P. & Saupé, F. (1986) Lanthanides, tantalum, and niobium: mineralogy, geochemistry, characteristics of primary ore deposits, prospecting, processing, and applications. proceedings of a workshop in Berlin, November 1986. *The Society for Geology Applied to Mineral Deposits, special publication* 7, 391 p.
- National Land Survey of Finland (2024). Topographic Database open licence. [page visited 9/2024].
<<https://asiointi.maanmittauslaitos.fi/karttapaikka/tiedostopalvelu/maastotietokanta?lang=fi>>
- Nironen, M. (2017). Bedrock of Finland at the scale 1:1 000 000 - Major stratigraphic units, metamorphism and tectonic evolution. *Geological Survey of Finland, Special Paper* 60, 4–129.
- Nykänen, O. (1968). Kallioperäkartan selitys, Tohmajärvi. Summary: Explanation to the map of rocks of Tohmajärvi. *Suomen geologinen kartta, 1:100 000. Kallioperäkartan selitykset*, 4232–4234 Tohmajärvi. Geological Survey of Finland, 5–68.
- Nykänen, O. (1971). On the Karelides in the Tohmajärvi area Eastern Finland. *Bulletin of the Geological Society of Finland* 43: 1, 93–108.
- Nykänen, O. (1975). Kerimäen ja Kiteen kartta-alueen kallioperä. Summary: Precambrian rocks of the Kerimäki and Kitee map-sheet areas. *Suomen geologinen kartta, 1:100 000. Kallioperäkartan selitykset*, 4213 Kerimäki, 4231 Kitee. Geological Survey of Finland, 24 p.
- Nykänen, O. (1983). Punkaharjun ja Parikkalan kartta-alueiden kallioperä. Summary: Pre-Quaternary rocks of the Punkaharju and Parikkala map-sheet areas. *Suomen geologinen kartta 1:100 000, Kallioperäkarttojen selitykset* 4124+4142, Punkaharju ja 4123+4114 Parikkala. Geological Survey of Finland, 81 p.
- Nygård, H., Hulkki, H., Jokinen, J., Kuusela, J., Leskelä, T. & Thurman, N. (2023). Investigation of Dragbacken lithium pegmatite occurrences, Kruunupyy, Ostrobothnia, western Finland. *Geological Survey of Finland, Open file research report* 27/2023, 37 p.
- Nygård, H., Hulkki, H., Kinnunen, M., Kuusela, J., Niskanen, M., Romppanen, S. & Wik, H. (2024). LCT-pegmatiittitutkimukset Etelä-Pohjanmaalla 2021–2023. *Geological Survey of Finland, Open file research report* 12/2024, 40 p.

- Pearce J. A., Harris B.W. & Tindle A.G. (1984). Trace element discrimination diagrams for the tectonic interpretation of granitic rocks. *Journal of Petrology* 25: 4, 956–983.
- Rasilainen K., Eilu P., Ahtola T., Halkaaho T., Kärkkänen N., Kuusela J., Lintinen P. & Törmänen T. (2018). Quantitative assessment of undiscovered resources in lithium–caesium–tantalum pegmatite hosted deposits in Finland. *Geological Survey of Finland, Bulletin* 406, 1–172.
- Shand, S. J. (1943). *Eruptive Rocks. Their Genesis, Composition, Classification, and Their Relation to Ore-Deposits with a Chapter on Meteorite*. John Wiley & Sons, New York. 444 p.
- Selway, J. B., Breaks, F. W. & Tindle, A. G. (2005). A review of rare-element (Li-Cs-Ta) pegmatite exploration techniques for the Superior Province, Canada, and large worldwide tantalum deposits. *Exploration and Mining Geology* 14: 1–4, 1–30.
- Shaw, D. M. (1968). A review of K-Rb fractionation trends by covariance analysis. *Geochimica et Cosmochimica Acta* 32: 6, 573–601.
- Silva, D., Groat, L., Martins, T. & Linnen, R. (2023). Structural controls on the origin and emplacement of lithium-bearing pegmatites. *The Canadian journal of mineralogy and petrology* 61: 2300045, 11 p.
- Simmons, W. (2005). A look at pegmatite classifications. In Proceedings of the crystallization processes in granitic pegmatites. *International meeting Abstracts-23rd-29th May*. New Orleans. 12 p.
- Simmons, W. & Webber, K. (2008). Pegmatite genesis: State of the art. *European Journal of Mineralogy* 20: 4, 421–438.
- Steiner, B. (2019). Tools and workflows for grassroots Li–Cs–Ta (LCT) pegmatite exploration. *Minerals* 9: 8, 499 p.
- Sun S.S. & McDonough W. (1989). Chemical and isotopic systematics of oceanic basalts: implications for mantle composition and processes. *Geological Society of London, special publication* 42: 1, 313–345.
- Taylor, S. R. & McLennan, S. M. (1985). The Continental Crust, Its Composition and Evolution. *The Journal of Geology* 94: 4, 57–72.
- Tiala, A. (2023). Geokemisk och petrografisk variation av glimmerskiffer i förhållande till pegmatiter i Österbottens skifferbälte, Seinäjoki-och Kuortaneregionen, Finland. Åbo Akademi, Turku. 71 p. [in Swedish unpublished MSc thesis]
- Wise, M. A., Müller, A. & Simmons, W. B. (2021). A proposed new mineralogical classification system for granitic pegmatites. *The Canadian Mineralogist* 60: 2, 229–248.

Appendixes

Appendix 1. Coordinates of the observations

Coordinates are in ETRS-TM35FIN system

Sample ID	Location	North	East
KTPA-2022-92.1	Kumpu	6892196	672465
KTPA-2022-93.1	Kuusela	6891621	670569
KTPA-2022-94.1	Halla-ahonvuoret	6888594	670669
KTPA-2022-95.1	Surmasuo	6892888	673545
KTPA-2022-95.3	Surmasuo	6892888	673545
KTPA-2022-95.2	Surmasuo	6892888	673545
KTPA-2022-96.1	Riienvaara	6894152	674786
KTPA-2022-97.1	Honkavaara	6891008	673340
KTPA-2022-98.1	Kokkokallio	6889566	675020
KTPA-2022-99.1	Lamminmaa	6889110	677643
KTPA-2022-101.1	Potoskavaara	6889909	672328
KTPA-2022-102.1	Palomäki	6889979	669487
KTPA-2022-103.1	Selkäpäivänrinne	6892113	671395
KTPA-2022-104.1	Purola N	6892554	674349
KTPA-2022-105.1	Rajasillannotko	6890252	673450

Appendix 2. Geochemical analysis results

The analysis method for the analytes SiO₂, Al₂O₃, Fe₂O₃, CaO, Na₂O, K₂O, Cr₂O₃, TiO₂, MnO, P₂O₅, SrO, BaO, and LOI (Loss on Ignition) is ME-ICP06. For other elements, the method used is ME-MS98L and for Zr is ME-MS85.

Units	%	%	%	%	%	%	%	%	%	%	%	%	%	%	%	%	ppm	ppm	ppm
Sample ID	SiO ₂	Al ₂ O ₃	Fe ₂ O ₃	CaO	MgO	Na ₂ O	K ₂ O	Cr ₂ O ₃	TiO ₂	MnO	P ₂ O ₅	SrO	BaO	LOI	Total	Li ₂ O	Ag	Al	As
KTPA-2022-92.1	64	21.9	0.84	0.5	0.32	8.49	1.35	0.002	0.06	0.23	0.67	<0.01	<0.01	1.27	99.63	0.094732	12	7 9115.4	147
KTPA-2022-93.1	71.4	15.3	0.25	0.23	0.03	3.75	7.07	<0.002	0.02	0.01	0.16	<0.01	<0.01	0.14	98.36	0.0111956	5	7 9115.4	<4
KTPA-2022-94.1	74.2	14.9	1.36	0.43	0.13	4.48	3.02	0.002	0.01	0.35	0.23	<0.01	<0.01	0.75	99.86	0.0096885	<5	10 2929.4	<4
KTPA-2022-95.1	71.5	24.6	0.26	0.01	0.02	0.21	0.03	0.006	<0.01	0.03	0.03	<0.01	<0.01	0.61	97.31	5.3825	10	9 7637.4	7
KTPA-2022-95.3	79.3	13	0.54	0.4	0.05	6.85	0.24	0.002	0.01	0.04	0.34	<0.01	<0.01	0.21	100.98	0.0137792	<5	7 5675.6	9
KTPA-2022-95.2	73.0	16.6	0.25	0.39	0.02	7.6	0.99	0.002	0.02	0.01	0.35	<0.01	<0.01	0.64	99.87	0.058131	9	11 5894.8	10
KTPA-2022-96.1	72.6	15.75	0.46	0.35	0.01	7.79	0.53	0.002	0.02	0.16	0.19	<0.01	<0.01	0.42	98.28	0.0040907	6	8 0967.6	<4
KTPA-2022-97.1	76.6	13.8	0.31	0.79	0.03	5.76	1.5	<0.002	0.02	0.01	0.05	<0.01	<0.01	0.36	99.23	0.0081814	<5	7 8850.8	208
KTPA-2022-98.1	70.7	16.2	0.21	0.04	0.01	2.48	10.2	<0.002	0.02	<0.01	0.13	<0.01	0.01	0.28	100.28	0.0099038	5	13 0183.2	60
KTPA-2022-99.1	73.4	15.15	0.24	0.76	0.02	5.69	2.42	<0.002	0.02	<0.01	0.1	<0.01	<0.01	0.33	98.13	0.0034448	10	6 8796	137
KTPA-2022-101.1	73.2	14.95	0.56	0.63	0.15	4.21	2.99	<0.002	0.04	0.01	0.09	<0.01	<0.01	0.54	97.37	0.0124874	<5	8 7847.2	6
KTPA-2022-102.1	74.7	14.95	0.24	0.38	0.02	5.2	4.03	0.002	0.03	0.01	0.2	<0.01	<0.01	0.45	100.21	0.0012918	<5	8 3349	5
KTPA-2022-103.1	68.9	19.45	0.28	0.36	0.03	9.16	0.72	<0.002	0.02	0.01	0.8	<0.01	<0.01	0.84	100.57	0.142098	<5	7 3029.6	5
KTPA-2022-104.1	72.6	18.45	0.57	0.24	0.07	2.87	3.71	0.004	0.03	0.01	0.24	<0.01	0.01	1.91	100.71	0.0124874	<5	8 5730.4	6
KTPA-2022-105.1	73.6	14.3	0.79	0.24	0.08	4.24	4.32	0.003	0.03	0.11	0.19	<0.01	<0.01	0.42	98.32	0.0040907	11	8 0173.8	101

Units	ppm	ppm	ppm	%	ppm	ppm	ppm	ppm	ppm	ppm	ppm	ppm	%	ppm	ppm	ppm	ppm	ppm	%
Sample ID	Ba	Be	Bi	Ca	Cd	Ce	Co	Cs	Cu	Dy	Er	Eu	Fe	Ga	Gd	Ge	Ho	In	K
KTPA-2022-92.1	37	380	0.3	0.3	1.5	3.8	0.7	155.5	20	0.61	0.12	0.03	0.65	40.7	0.38	5.6	0.06	<0.03	1.6
KTPA-2022-93.1	23	3.3	0.3	0.2	<0.8	1.3	0.7	6.1	<20	0.51	0.37	0.05	0.22	8.5	0.18	2.0	0.1	<0.3	5.7
KTPA-2022-94.1	42	10.0	1.8	0.3	<0.8	1.7	0.6	11.0	<20	0.71	0.35	0.06	0.98	23.9	0.34	2.7	0.11	<0.3	2.39
KTPA-2022-95.1	7	2.4	0.2	<0.1	0.8	0.4	1.2	25.0	<20	<0.03	0.02	<0.03	0.21	27.2	<0.03	12.4	<0.01	<0.3	<0.05
KTPA-2022-95.3	4	9.0	0.5	0.3	<0.8	1.8	0.5	6.7	<20	0.59	0.2	<0.03	0.43	13.6	0.3	3.8	0.11	<0.3	0.24
KTPA-2022-95.2	8	23.7	0.9	0.3	<0.8	0.4	0.6	24.3	<20	0.04	0.02	<0.03	0.24	21.0	0.03	4.5	<0.01	<0.3	0.82
KTPA-2022-96.1	5	133	0.1	0.3	<0.8	1.2	1.1	5.1	<20	0.32	0.07	0.05	0.38	17.0	0.21	5.6	0.04	<0.3	0.45
KTPA-2022-97.1	7	7.8	0.4	0.6	<0.8	1.1	<0.5	4.0	<20	0.15	0.06	0.04	0.27	9.6	0.06	3.1	0.04	<0.3	1.29
KTPA-2022-98.1	120	1.1	0.2	<0.1	<0.8	4	0.6	11.2	<20	0.92	0.56	0.09	0.19	7.8	0.38	2.0	0.16	<0.3	8.52
KTPA-2022-99.1	15	8.5	1.1	0.6	1.3	1.5	0.7	8.6	20	0.14	0.05	0.07	0.23	12.6	0.06	2.6	0.03	<0.3	2.07
KTPA-2022-101.1	33	4.6	1	0.4	<0.8	2.8	0.7	4.1	<20	0.43	0.38	0.11	0.45	13.6	0.13	1.2	0.11	<0.3	2.55
KTPA-2022-102.1	11	5.8	1.8	0.3	<0.8	1.4	0.5	21.4	<20	0.24	0.15	<0.03	0.21	15.1	0.11	4.9	0.06	<0.3	3.35
KTPA-2022-103.1	16	12.5	0.1	0.2	<0.8	0.6	0.7	50.2	<20	0.22	0.02	<0.03	0.22	19.5	0.13	6.3	0.02	<0.3	5700
KTPA-2022-104.1	69	60.9	0.4	0.2	<0.8	1.5	0.7	7.3	<20	0.1	0.05	0.06	0.45	25.4	0.14	3.2	0.02	<0.3	2.92
KTPA-2022-105.1	15	5.2	0.5	0.2	1.9	1.7	0.6	9.0	<20	0.52	0.39	<0.03	0.63	10.0	0.13	2.8	0.1	<0.3	3.55

Units	ppm	ppm	ppm	%	ppm	ppm	ppm	ppm	ppm	ppm	ppm	ppm	ppm	ppm	ppm	ppm	ppm	ppm	ppm	ppm
Sample ID	La	Li	Lu	Mg	Mn	Mo	Nb	Nd	Ni	Pb	Pr	Rb	Re	Sb	Se	Sm	Sn	Sr	Ta	Tb
KTPA-2022-92.1	2.03	440	0.05	0.16	2020	2	160	1.19	10	45	0.41	411	<0.01	12.1	7	0.59	46	20	21.2	0.13
KTPA-2022-93.1	0.7	52	0.14	0.10	60	2	1	0.51	30	51.3	0.15	302	<0.01	0.3	5	0.14	5	20	0.28	0.07
KTPA-2022-94.1	0.77	45	0.06	0.06	2870	2	15.6	0.89	<10	19.1	0.22	210	<0.01	<0.3	<3	0.41	18	20	3.22	0.13
KTPA-2022-95.1	0.29	>25 000	<0.05	0.01	300	2	4.3	0.24	10	0.8	0.05	14.6	<0.01	0.8	6	<0.04	459	<20	8.18	<0.01
KTPA-2022-95.3	0.82	64	<0.05	0.02	300	2	2.9	0.73	<10	11.3	0.22	20.0	<0.01	0.4	3	0.29	3	<20	1.02	0.13
KTPA-2022-95.2	0.26	270	<0.05	<0.01	100	2	9.5	0.08	20	20.4	<0.03	168.0	<0.01	0.7	<3	0.06	18	20	6.64	<0.01
KTPA-2022-96.1	0.44	19	<0.05	<0.01	1400	2	12.8	0.96	40	9.7	0.19	64.2	<0.01	0.3	3	0.28	10	<20	10.75	0.06
KTPA-2022-97.1	0.66	38	<0.05	0.01	80	<2	1.4	0.45	10	25.6	0.16	68.2	<0.01	<0.3	5	0.18	3	20	0.28	0.01
KTPA-2022-98.1	2.03	46	0.15	<0.01	30	2	<0.8	1.58	10	61.3	0.39	365	0.01	0.3	<3	0.34	4	40	0.27	0.11
KTPA-2022-99.1	0.88	16	<0.05	0.01	40	2	4.1	0.54	20	27.8	0.14	104	<0.01	0.4	6	0.14	8	20	1.26	0.02
KTPA-2022-101.1	1.82	58	0.07	0.08	70	<2	4.2	0.88	10	34.0	0.26	103	<0.01	<0.3	<3	0.2	6	50	0.59	0.05
KTPA-2022-102.1	0.82	6	0.07	0.01	70	2	3.1	0.35	<10	31.9	0.16	222	<0.01	0.3	5	<0.04	15	<20	0.79	0.02
KTPA-2022-103.1	0.36	660	<0.05	0.02	100	2	59.7	0.18	10	15.8	0.08	167	<0.01	0.3	3	0.24	1320	<20	141	0.05
KTPA-2022-104.1	0.77	58	<0.05	0.03	110	2	22.8	0.94	20	14.8	0.25	303	<0.01	<0.3	<3	0.24	33	40	12.45	0.02
KTPA-2022-105.1	0.78	19	0.19	0.04	980	2	3.2	0.68	20	31.1	0.20	198	<0.01	<0.3	4	0.15	8	<20	0.49	0.05

Units	ppm	ppm	ppm	%	ppn	ppm	ppm	ppm	ppm	ppm	ppm	ppm	ppm	ppm	ppm
Sample ID	Tb	Te	Th	Ti	Tl	Tm	U	V	W	Y	Yb	Zn	Zr	Hf	
KTPA-2022-92.1	0.13	1.2	1.8	0.02	2.92	0.05	166.5	<1	2.4	3.3	0.38	100	221	20	
KTPA-2022-93.1	0.07	0.7	0.2	<0.005	1.91	0.1	7.0	<1	0.3	4.3	0.75	20	29	10	
KTPA-2022-94.1	0.13	0.8	0.9	0.01	0.91	0.06	7.9	<1	3.6	5.1	0.43	20	30	10	
KTPA-2022-95.1	<0.01	1.1	<0.1	<0.005	0.09	<0.01	0.5	<1	0.4	0.2	<0.02	20	5	10	
KTPA-2022-95.3	0.13	0.6	0.1	0.01	0.12	0.04	6.5	<1	0.4	4.3	0.37	50	32	10	
KTPA-2022-95.2	<0.01	<0.5	0.1	<0.005	0.99	<0.01	2.0	<1	1.4	0.2	<0.02	30	15	10	
KTPA-2022-96.1	0.06	0.8	0.5	<0.005	0.25	0.02	1.4	<1	0.9	2.3	0.06	30	23	10	
KTPA-2022-97.1	0.01	0.6	0.1	<0.005	0.42	0.01	10.6	<1	0.4	0.8	0.17	10	12	10	
KTPA-2022-98.1	0.11	0.8	0.6	<0.005	2.2	0.13	3.5	<1	<0.3	5.9	0.93	20	13	10	
KTPA-2022-99.1	0.02	1.0	<0.1	<0.005	0.58	0.01	3.7	<1	1.0	0.9	0.09	20	5	10	
KTPA-2022-101.1	0.05	0.5	0.4	0.01	0.54	0.09	2.0	<1	4.1	3.8	0.56	20	11	<10	
KTPA-2022-102.1	0.02	0.9	0.3	<0.005	1.67	0.03	5.8	<1	1.0	1.8	0.34	10	11	10	
KTPA-2022-103.1	0.05	0.6	0.4	<0.005	1.1	0.01	3.5	<1	1.2	1.1	0.07	30	9	10	
KTPA-2022-104.1	0.02	0.6	0.1	0.01	1.52	<0.01	2.5	<1	2.9	0.9	0.04	40	7	10	
KTPA-2022-105.1	0.05	0.8	0.3	0.01	1.1	0.11	18.9	<1	0.5	4.9	1.21	40	29	10	